Fermi National Accelerator Laboratory

FERMILAB-FN-599

Beauty for Beginners

Dan Green

Fermi National Accelerator Laboratory
P.O. Box 500, Batavia, Illinois 60510

December 1992

Operated by Universities Research Association Inc. under Contract No. DE-AC02-76CHO3000 with the United States Department of Energy

Disclaimer

BEAUTY FOR BEGINNERS

November 1992

Dan Green
Fermi National Accelerator Laboratory
Batavia, IL

"There is no excellent beauty that hath not some strangeness in the proportion"

Francis Bacon

TABLE OF CONTENTS

5. "Box" Diagrams and SM Calculations

- 5.1 M_{12} and B_d, B_s
- 5.2 $(\Delta M / M)_K$
- 5.3 $\Delta M / \Gamma$ for K, D, B
- 5.4 M_Z/M_W to $O(\alpha_W)$
- 5.5 FCNC in $B \to \mu\mu$, $K \to \mu\mu$ and the GIM Mechanism
- 5.6 Γ_{12} in the SM, ε for B_d, K
- 5.7 $\varepsilon' / \varepsilon$ and EM Penguins

6. Summary

Abstract

This is the text of a series of lectures given to Fermilab post docs and students. The plan of the lectures is to begin with a discussion on electroweak decays (Section 1) . First, we discuss the decays of the vector gauge bosons which are of order α_W and following that the decays of leptons with virtual intermediate gauge bosons which are of order $\alpha_W{}^2$. Then an attempt is made to look very briefly at the decays of light mesons and baryons. Following that there is a brief discussion of the Cabbibo-Kobayashi-Maskawa (CKM) matrix, flavor changing neutral currents, FCNC, and the GIM mechanism to suppress flavor changing neutral currents. Finally, Section 1 ends with a discussion of semileptonic decays of heavy quark mesons.

In Section 2, the topic of nonleptonic weak decays of heavy quark mesons is taken up. First, there is a discussion of spectator, annihilation, and exchange graphs. Following that, one assumes that the spectator amplitudes dominate and various conclusions drawn from that dominance are examined in nonleptonic B and D decays. Finally, a discussion of penguins and loops in rare decays in higher order is taken up to end Section 2.

Section 3 is devoted to a discussion of the phenomenology necessary to discuss CP violation. First, the mass and decay matrices are defined, followed by a discussion of the eigenvalue problem. The eigenvalue problem solution leads to a definition of the ε parameter. This parameter indicates CP violation in the mass matrix. The implication of CP violation and mixing for the time evolution of a two state system and the CP violation asymmetry then round out Section 3.

Section 4 is a discussion of CP violation and mixing in detail. We begin with the time evolution of the states and the CKM phases. Following that the unitary triangle is defined. Then follows a discussion of kaon decays. Section 4 concludes with an explication of what information can be gained from time integrated data from lepton pairs, from semileptonic K decay asymmetry, from mixing data, and finally from CP violation asymmetry.

Section 5 consists of a descripton of the box diagram and Standard Model, SM, calculations for the parameters which have been defined and discussed in the previous Sections. We begin with a discussion of the mass difference and higher order effects in the gauge bosons due to top quark loops. Following that we have an estimate of flavor changing neutral current decays. Then the B system and the GIM mechanism are revisited. There is a discussion of the decay matrix calculation in the Standard Model and an estimate of the size of the ε parameter for the B and K systems. Following that, the mixing parameter x is estimated for the D and B systems. Finally, there is a brief discussion of the ε' parameter and electromagnetic penguins in the kaon system.

The references which are given in this volume of lecture notes are extremely limited and indicate an idiosyncratic choice of some of the references used by the author. There are many review articles on B physics; an extensive literature exists which is accessible in the bibliography found in those articles.

1. INTRODUCTION TO EW DECAYS

1.1 W, Z Decays, $O(\alpha_W)$, FCNC, and GIM

In thinking about decay processes, it is perhaps best to begin with the simplest possible decay mechanisms. For that reason, we begin with first order electroweak processes which are the decays of the gauge bosons themselves. Let us begin with the charged gauge bosons, the W particles. They couple to lepton and quark pairs and, since they are responsible for the charged current interaction, they couple to charged pairs; for example, the electron neutrino, ($e\nu_e$) the muon neutrino ($\mu\nu_\mu$), and the τ neutrino ($\tau\nu_\tau$) pairs. They also couple to quark pairs and they do so in a fashion which we will be explicating throughout these lectures. The decay diagram for a W^+ is shown in Fig. 1.1.1. For now, we list in Eqs. 1.1.1 only those decays which are favored in the Cabbibo-Kobayashi-Maskawa (CKM) coupling scheme. That scheme we will explain later.

$$\begin{aligned} W^+ &\rightarrow \begin{matrix} u & c \\ d & s \end{matrix} \quad \begin{matrix} e^+ & \mu^+ & \tau^+ \\ \nu_e & \nu_\mu & \nu_\tau \end{matrix} \\ B\left(W^+ \rightarrow \mu^+ \nu_\mu\right) &\sim 1/9 \end{aligned} \qquad 1.1.1$$

One then counts the final state degrees of freedom in order to estimate the branching ratio into these different decay modes. We have to remember that there are three color degrees of freedom which means that, for example, the branching ratio of a W boson into a muon and neutrino we would predict to be roughly one ninth. And indeed, looking at the Particle Data Group tables, that is the observed branching ratio.

What about the Lorentz structure of the decays? Well, suffice it to say, a summary of many years of study leads us to believe that a V-A pattern is the structure of the weak interactions. The interaction Lagrangian for that theory is given below:

$$\begin{aligned} L_I &\sim \overline{\Psi}\gamma_\lambda(1-\gamma_5)\Psi W^\lambda \\ &\sim g_W J_\lambda W^\lambda \\ &\sim g_W \overline{u}_e \gamma_\lambda (1-\gamma_5) u_\nu W^\lambda \,. \end{aligned} \qquad 1.1.2$$

The V-A theory for leptons implies that quarks are left-handed with respect to helicity as are leptons, whereas antiquarks and antileptons are right-handed. That means one can draw the favored helicity orientation in a W leptonic decay as shown in Fig. 1.1.2. The W boson is a vector. In a two body decay the electron and antineutrino come out on opposite sides in order to conserve momentum. Looking at Fig. 1.1.2, one sees that spin is simultaneously conserved.

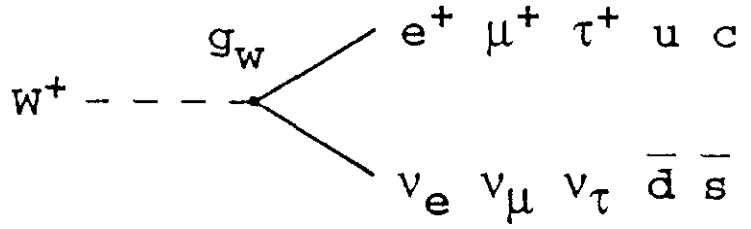

Fig. 1.1.1 First order EW decay diagram for W to quark and lepton pairs.

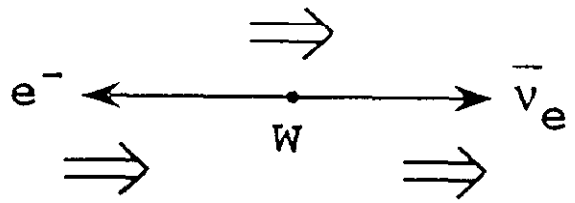

Fig. 1.1.2 (V-A) helicity structure for $W^- \rightarrow e^- \bar{\nu}_e$ decay.

What about the absolute rate and the coupling constants? As one can see from Fig. 1.1.1, this is a first order process and one can therefore expect that the decay rate is proportional to the first power of the weak fine structure constant, α_W. Since there is only one other mass scale in the problem, which is the mass of the boson itself, from dimensional arguments the width of the W boson should be proportional to α_W times the mass of the W boson.

$$\begin{aligned} &\alpha_W \equiv g_W{}^2 / 4\pi \sim 1/30 \\ &\Gamma_W \sim \alpha_W M_W \end{aligned} \qquad 1.1.3$$

The W boson weighs about 100 GeV. Therefore, the width should be of order 3 GeV which is what is observed as one can see in looking at the book of Particle Data Properties.

What about the decays of the neutral EW gauge boson, Z, which is responsible for the neutral current interaction? For the W boson we've simply put up all the CKM allowed charged current combinations and said that they were all universally and equally coupled to the W through an EW coupling constant g_W. For the neutral gauge bosons something more subtle must be going on. For example, if one looks at Fig. 1.1.3 and allows coupling of the Z to any neutral quark antiquark combination, then one allows for the existence of a flavor changing neutral current (FCNC) decay. In Fig. 1.1.3 the decay is kaon goes to muon pairs. We know experimentally that this decay is very rare. Therefore, we cannot allow Z to couple to all possible combinations of neutral quark antiquark pairs in analogy to what we did for the W boson.

What we do know is that the quarks are produced strongly. Therefore, they are strong eigenstates. Since the weak interactions violate many of the strong interaction selection rules, there is no need that the weak eigenstates be congruent to the strong eigenstates.

$$\begin{aligned} &\begin{pmatrix} d' \\ s' \end{pmatrix} = \begin{pmatrix} \cos\theta & \sin\theta \\ -\sin\theta & \cos\theta \end{pmatrix} \begin{pmatrix} d \\ s \end{pmatrix} \\ &D' \equiv VD \\ &\sin\theta \sim 0.2 \end{aligned} \qquad 1.1.4$$

In fact, we can allow an arbitrary rotation of the negatively charged quarks due to the mismatch between strong and weak eigenstates. The coupling of the Z boson to the up, down, charm and strange quarks is then as shown in Fig. 1.1.4. Given the Cabbibo rotation shown in Eqs. 1.1.4, the neutral current amplitude for the Z is;

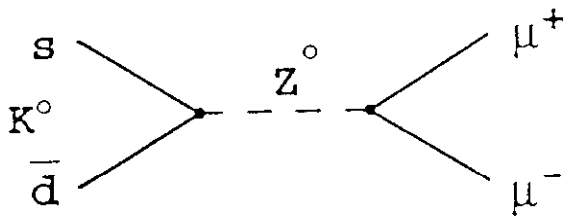

Fig. 1.1.3 Possible $K^0 \to \mu^+\mu^-$ FCNC decay diagram with Z^0 intermediate state.

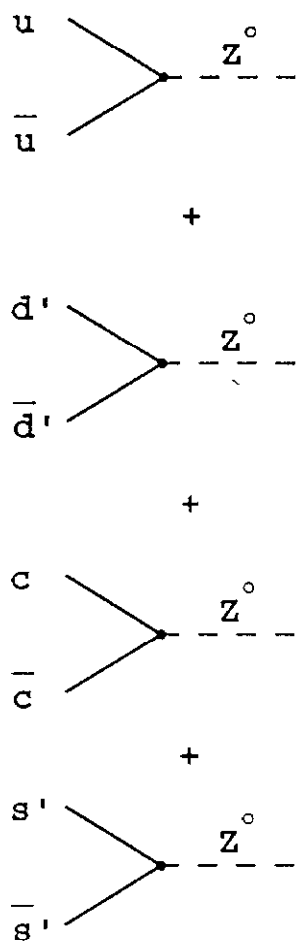

Fig. 1.1.4 $Z \to q\bar{q}$ couplings and the GIM mechanism for cancellation of FCNC.

$$
\begin{aligned}
a_{nc} \sim\ & u\bar{u} + c\bar{c} \\
& + (d\bar{d})\cos^2\theta + (s\bar{s})\sin^2\theta \\
& + (s\bar{d} + \bar{s}d)\sin\theta\cos\theta \\
& + (d\bar{d})\sin^2\theta + (s\bar{s})\cos^2\theta \\
& - (s\bar{d} + \bar{s}d)\sin\theta\cos\theta\,.
\end{aligned}
\qquad 1.1.5
$$

Note that the existence of two doublets (up and down, charm and strange) automatically cancels out the flavor changing neutral current to this order in the amplitudes.

$$
\begin{aligned}
a_{nc} &\sim u\bar{u} + c\bar{c} + d\bar{d} + s\bar{s} \\
&\sim \delta q\bar{q}'
\end{aligned}
\qquad 1.1.6
$$

This was, in fact, part of the theoretical motivation for predicating the existence of charm. The charm quark was required to cancel the flavor changing neutral currents which were not observed, for example, in K_L decay into two muons. Therefore, one can assume that Z decays only to quark antiquark pairs of exactly the same flavor and color. This absence of flavor changing neutral currents to first order is called the GIM mechanism.

Note though that what one has left (Eqs. 1.1.6) is a universal equal strength coupling of Z to the quark antiquark pairs. It is clear that requiring that the transformation matrix be unitary insures both universality and the absence of flavor changing neutral currents. Therefore, we expect that if there are more generations of quarks, then the unitarity of the matrix connecting the weak and strong eigenstates insures the absence of FCNC. We will see later that this first order cancellation of FCNC fails in higher orders. However, FCNC decays are still suppressed and therefore, will remain rare decays.

1.2 Decays of Leptons, $O(\alpha_W{}^2)$

Having considered the simplest possibilities, the first order decays of W and Z electroweak gauge bosons, let's go on to the next simplest electroweak decays. Those are the decays of leptons with virtual intermediate gauge bosons. These decays are second order, but there are few strong interaction effects, at least for the lightest leptons. The electron is straight forward since it is stable. The muon is a "heavy electron" and can decay leptonically into an electron and a neutrino antineutrino pair. The second order electroweak diagram for this decay is given in Fig. 1.2.1. The existence of the intermediate W and the $1/\left(q^2 + M_W^2\right)$ behavior of the W propagator in the amplitude means that, on dimensional grounds, one expects a decay width which goes as the fifth power of the mass of the decaying particle.

$$\Gamma \sim \alpha_W{}^2 \left(\frac{M}{M_W} \right)^4 M \qquad 1.2.1$$

This is an extremely important scaling property which we will be using throughout this note. It works over many orders of magnitude in the scaling of decay rates.

What about the implication of the Lorentz V-A structure that we have already talked about? This is a three body decay and there is a preferred orientation which is forced upon the decay by the V-A helicity structure, as shown in Fig. 1.2.2. The electron is favored to come out recoiling against the neutrino antineutrino pair. That pair has its spins paired so that the muon spin is aligned to the electron spin. This orientation implies that the electron carries roughly the maximum available energy.

As we'll see, the coupling constant for this decay is determined from a measurement of the decay rate. This effective coupling constant is called the Fermi coupling constant, which has dimensions.

$$G = 1.2 \text{ x } 10^{-5} \ (GeV)^{-2} \qquad 1.2.2$$

A similar coupling is also measured in nuclear beta decays. However, we will not discuss them at all. Suffice it to say that the muon and nuclear beta decays are completely consistent with one another and imply the universal coupling of quarks and leptons as mentioned already. That is, of course, not the whole story. The effective Fermi theory is a low energy approximation to the electroweak theory. The weak interaction is related to the electromagnetic interaction. The synthesis of those two forces implies that the electroweak fine structure constant is proportional to the Fermi coupling constant.

$$\begin{aligned} g_W{}^2 / 8M_W{}^2 &= G / \sqrt{2} \\ g_W \sin\theta_W &= e \\ \pi\alpha_W / \sqrt{2} M_W{}^2 &= G \end{aligned} \qquad 1.2.3$$

What is seen in Eqs. 1.2.3 is the relationship between the fundamental electroweak coupling constant, g_W, and the Fermi coupling constant, G. It's also true that the electroweak coupling constant is proportional to, and comparable to, the electromagnetic charge. In what follows, we will use the effective weak interaction Fermi constant, G, and the electroweak fine structure constant, α_W, interchangeably.

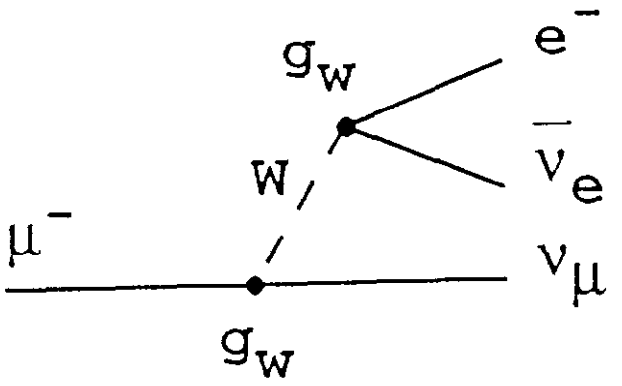

Fig. 1.2.1 Second order EW decay diagram for $\mu^- \rightarrow e^- \bar{\nu}_e \nu_\mu$.

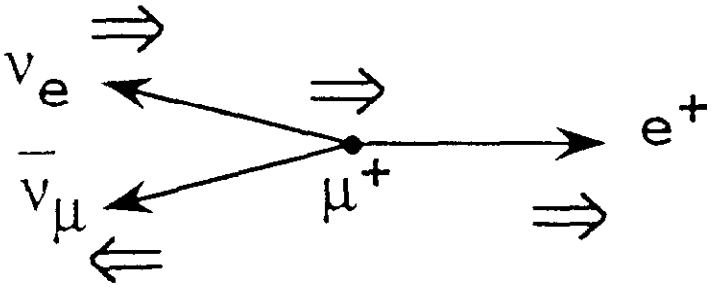

Fig. 1.2.2 (V-A) helicity structure for the 3 body decay, $\mu^+ \rightarrow e^+ \nu_e \bar{\nu}_\mu$.

It is worthwhile to look more deeply into the muon decay rate because it will be the basis of the study of many other semileptonic rates such as those of heavier leptons and quarks. The differential decay rate is defined by kinematics and by the V-A dynamics to which we've already alluded.

$$
\begin{aligned}
d\Gamma &\sim \left(d\vec{P}_e / E_e\right)\left(\frac{1}{M_\mu}\right)\left\{\alpha_W{}^2[x(3-2x)]\right\} \\
x &= P_e{}^* / \left(M_\mu / 2\right) \\
d\Gamma &\sim 4\pi P_e dP_e G^2 M_\mu{}^3[x(3-2x)] \\
&\sim G^2 M_\mu{}^5 x^2(3-2x)dx
\end{aligned}
\qquad 1.2.4
$$

The phase space factor is factored out along with the coupling constant and the dependence on x, where x is the fraction of the maximum possible electron momentum in the center of mass. The x dependence is imposed by the dynamics of the V-A theory. Recall that an x of 1 is the favored alignment, as we saw in drawing a graph of the helicity structure for this decay. Both the scaling of the decay width with the fifth power of the q value in the decay and the high x peaking imposed by the Lorentz structure of electroweak dynamics are evident in Eq. 1.2.4.

The observed width for the muon is 3 x 10^{-19} GeV or, what is perhaps easier to remember, a lifetime of 2.2 microseconds.

$$
\begin{aligned}
\Gamma_\mu &\sim G^2 M_\mu{}^5 \sim \left[\alpha_W{}^2\left(\frac{M_\mu}{M_W}\right)^4\right] M_\mu \\
\Gamma_\mu &= \frac{G^2 M_\mu{}^5}{192\pi^3}, \ \tau_\mu = 2.2\ \mu\text{sec}
\end{aligned}
\qquad 1.2.5
$$

The dimensional scaling argument leads you to a decay rate estimate which is close. One takes the exact calculation as one way to measure the Fermi coupling constant G. As mentioned before, this value of G is cross checked with the value extracted from nuclear beta decay.

What about τ decays? Since the τ is another sequential heavy lepton, we expect to be able to understand its behavior in the same way that we understood muon decays. The simplest second order electroweak decay diagram that one can draw is given in Fig. 1.2.3. This diagram is just Fig. 1.1.1 folded back on itself to concatenate two first order diagrams in order to get a second order diagram. First let's ask about the branching ratios. Naive color counting and the CKM allowed possible charged currents lead you to expect a branching ratio into muons of one fifth.

$$\tau^+ \to \begin{matrix} u & e^+ & \mu^+ \\ \bar{d} & \nu_e & \nu_\mu \end{matrix} = 3:1:1 \qquad 1.2.6$$

The data on the branching ratios for τ is given in Table 1.1. Indeed, the leptonic branching ratios are roughly 20%, whereas the hadronic branching ratios make up the remainder. The hadronic decay modes appear to be dominated by the vector ρ in the final state. Simple hadronic diagrams for the decay of the virtual W are given in Fig. 1.2.4. Numerically one finds that the leptonic decay rate for τ agrees very well with the muon decay rate scaled up as the fifth power of the lepton mass.

$$\Gamma\left(\tau^- \to e^- \bar{\nu}_e \nu_\tau\right) \sim \left(\frac{M_\tau}{M_\mu}\right)^5 \Gamma_\mu \qquad 1.2.7$$

As seen in Table 1.1, the assumption of universal lepton coupling and of simple color counting for the branching ratios seems to be well satisfied. The quark antiquark decays of the virtual W cause us now to have to think about the strong interactions. For example, it looks as if the vector W^+ is preferentially coupled to the vector ρ^+ in the $u\bar{d}$ decay of the virtual W^+. This means that the assumption that the weak charged current is dominated by meson poles is perhaps plausible. It would seem as if the decays of the leptons, the muon and the τ, can be simply related to knowledge of W and Z decays. One imagines that any heavier sequential leptons will follow a similar path and therefore, that one will have some rough understanding of the branching fractions, the kinematics, and the dynamics of sequential heavy leptons.

1.3 $q\bar{q}$, qqq Decays, $O\left(\alpha_W{}^2\right)$

We give now an extremely brief and cursory discussion of the decays of light mesons and baryons. This is, in fact, an entire subject unto itself. What we will try to do is to extract those salient features which are needed for the discussion of the decays of heavy flavors, in particular, the b quark. By light hadrons we mean those consisting of up, down or strange quarks.

First let's consider the lightest meson, the pion. It has a purely leptonic decay. Recall the helicity assignments imposed by the V-A interactions. For example, quarks are left-handed. However, one needs to know that this is only true in the limit of massless quarks. In fact, the helicity is roughly equal to beta, which is the velocity possessed by the quark divided by the speed of light.

$$\underset{\pi \to e\nu}{< \vec{\sigma} \bullet \vec{P} >} = \pm\beta \qquad 1.3.1$$

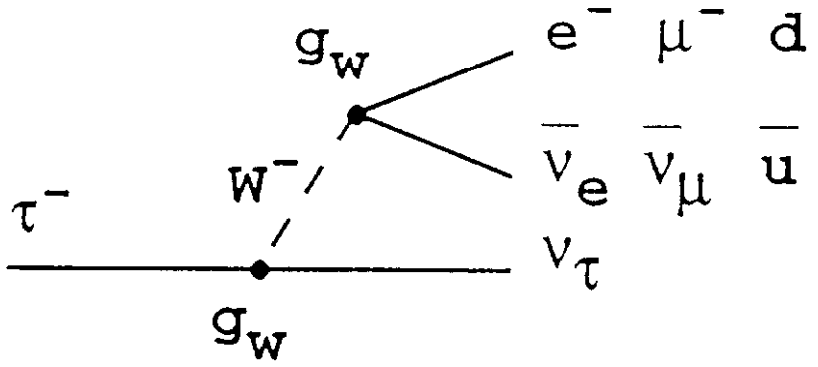

Fig. 1.2.3 Second order EW decay diagram for $\tau^- \rightarrow \nu_\tau W^-$ where W^- can virtually decay into quark or lepton pairs.

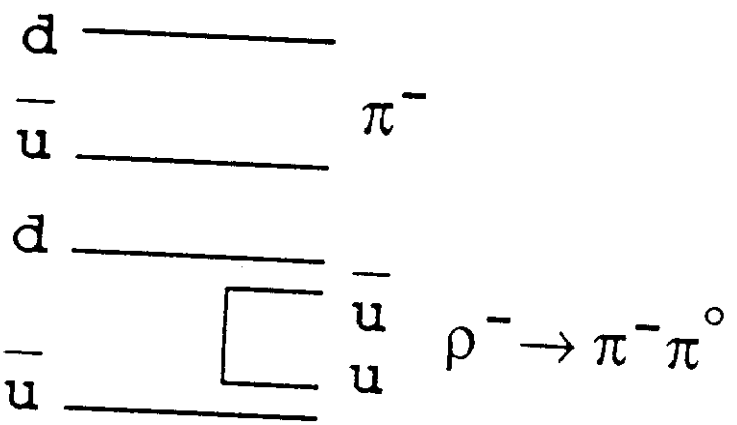

Fig. 1.2.4 Quark diagrams for hadronic final states in virtual $W^- \rightarrow d\bar{u}$ decays.

TABLE 1.1

τ DECAY BRANCHING RATIOS

DECAY MODE	BR (%)
$\mu \nu \bar{\nu}$	17.8
$e \nu \bar{\nu}$	17.7
$\pi^- \nu$	11.0
$\rho^- \nu$	22.7
$3\pi\nu$ (A_1)	14.6

As one can see from looking at Fig. 1.3.1, in distinction to W decay, the high velocity pion decay to electron is disfavored. In fact, the pion decays into muons and not electrons. This is the reason why Fermilab has muon neutrino beams and not electron neutrino beams. Sometimes theoretical ideas have profound "practical" implications.

Let us turn now to the semileptonic strange decays.

$$s \to u\ell^- \bar{\nu} \qquad 1.3.2$$

The basic diagram for this decay is given in Fig. 1.3.2. One expects the same sort of branching fractions as for the τ since the diagrams are essentially the same. However, one expects that the absolute rate is suppressed by CKM vertex factors. Looking at Eqs. 1.1.4, the rate relative to say muon decay, all else being equal, would be reduced by a factor of about 25. We will assume that the strange particle "spectator" decay shown in Fig. 1.3.2 is the dominant diagram for the semileptonic decays of mesons and baryons. We will discuss the possible reasons for this dominance later. In this note we will only look at semileptonic decay rates of light mesons and baryons. A compendium is given in Table 1.2. What is extremely gratifying to see is that the semileptonic rates are all of the order of a few times 10^{-18} GeV for both mesons and baryons. This leads us to believe that, indeed, the spectator mechanism, for which the decay rate is independent of the details of the binding dynamics, has some validity. In particular, the M^5 scaling with the Cabbibo vertex factor as indicated in Fig. 1.3.2, is quite plausible. Strange particle decay rates of the order of 10^{-18} GeV are expected if one scales the decay rates of leptons.

In general, the nonleptonic decays of light mesons and baryons have a rather higher rate than would be implied by the factor shown in Fig. 1.3.2. This "nonleptonic enhancement" is not very well understood theoretically. We expect that it will be of less importance as the mass scales for the mesons and baryons increase. Therefore, we will basically evade the problem of the nonleptonic enhancements for light mesons and baryons and only consider it cursorily in looking at D decays. The enhancement can be somewhat understood as the effects of QCD. One knows that the QCD coupling constant "runs." Thus, QCD effects should be large when the mass scale is low. Therefore, one can hope to reduce the problem by going to heavy flavors where the mass scale is large enough to drive the QCD coupling constant down.

There is a topic which we will need in evaluating some of the higher level diagrams in heavy flavor decays which is the purely leptonic decays of pseudoscalar mesons. In particular, the pion and the kaon leptonic decay rates have been measured whereas the B and the D leptonic decay rates have yet to be measured. The diagram is shown in Fig. 1.3.3. One expects that QCD effects

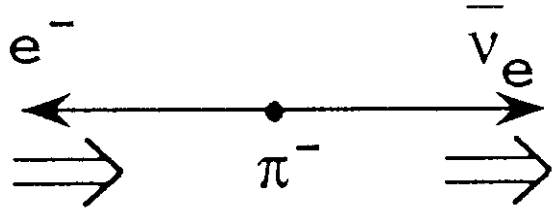

Fig. 1.3.1 (V-A) helicity structure for the disfavored decay $\pi^- \to e^-\overline{\nu}_e$.

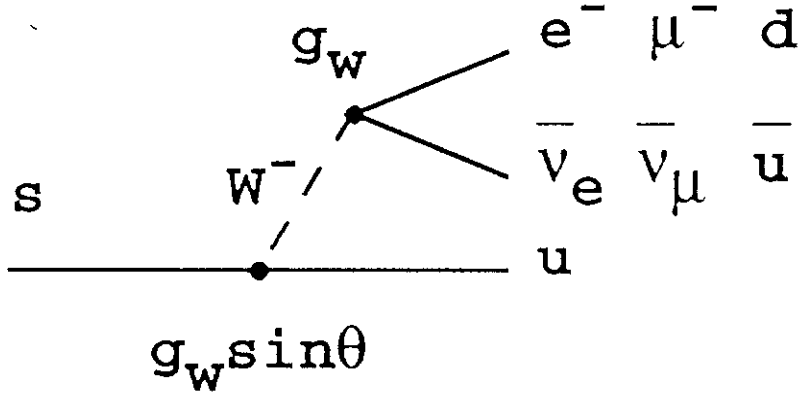

Fig. 1.3.2 Second order EW decay diagram for $s \to uW^-$ where W^- can virtually decay into quark or lepton pairs. Note the $V_{su} \sim \sin\theta$ CKM vertex factor in $s \to uW^-$.

TABLE 1.2

STRANGE QUARK SEMILEPTONIC DECAY RATES

DECAY	Γ x 10^{18} GeV
$K^+ \rightarrow \pi^0 \ell^+ \nu$	4.2
$K_L \rightarrow \pi^{\pm} \ell^{\mp} \nu$	8.3
$\Lambda \rightarrow p \ell^- \overline{\nu}$	2.5
$\Sigma^- \rightarrow n \ell^- \overline{\nu}$	6.5
$\Xi^- \rightarrow \Lambda^0 \ell^- \overline{\nu}$	4.1
$\Omega^- \rightarrow \Xi^0 e^- \overline{\nu}_e$	45.0

$$\Gamma_\mu \left(\frac{m_s = 300 \text{ MeV}}{M_\mu = 105 \ MeV} \right)^5 \left(\theta = \frac{1}{5} \right)^2$$

$= 2.3 \times 10^{-18}$ GeV

may be large. Therefore, one cannot expect to be able to use the simple fundamental diagram but have recourse to a phenomenological coupling constant. The amplitude is given below.

$$\begin{aligned} a &\sim \frac{G}{\sqrt{2}} < o\left|J_\mu^h\right|h > \left[\bar{u}_\ell \gamma_\mu (1-\gamma_5) u_\nu\right] \\ &\sim \frac{G}{\sqrt{2}} f_p q_\mu V_{if} \left[\bar{u}_\ell \gamma_\mu (1-\gamma_5) u_\nu\right] \end{aligned} \qquad 1.3.3$$

The strong interactions are all subsumed into the pseudoscalar coupling constant f_p. The decay rate is proportional to the pseudoscalar mass, as it must be, and also proportional to the square of the muon mass. This is the helicity suppression factor which we already saw in Fig. 1.3.1. Pseudoscalar meson decays into purely leptonic final states are helicity disfavored.

$$\begin{aligned} \Gamma &\sim \left[\frac{G^2}{8\pi} {f_p}^2 {V_{if}}^2 {M_\mu}^2\right] M \\ \frac{\Gamma}{M} &\sim {\alpha_W}^2 \left(\frac{f_p M_\mu V_{if}}{{M_W}^2}\right)^2 \end{aligned} \qquad 1.3.4$$

The observed coupling constant extracted from the pion leptonic decay rate is roughly f_π = 138 MeV. The kaon pseudoscalar coupling constant is roughly the same as the pion coupling constant. As one can see from what we've done so far, the decay rate into purely leptonic final states goes as the mass of the parent, whereas the decay rate into semileptonic final states goes as the fifth power of the parent mass. Therefore, it is extremely difficult to measure the pseudoscalar coupling constant of the D and B. One needs recourse, then, to a model to estimate the pseudoscalar coupling constant. It will be shown that the coupling constant is important to some of the elements of heavy quark theory. The simplest ansatz is to assume a universal value for the pseudoscalar coupling constant but it is hard to attach an error to that assumption. In what follows we will usually assume that the B and D have pseudoscalar couplings which are equal to those of the pion.

1.4 CKM Matrix

As mentioned before, the strong eigenstates created at production are not the same as the weak eigenstates and, therefore, the strong eigenstates are mixed in weak decays. The unitary transformation describing that mixing has already been given for the case of two generations.

$$(u,c) V_{if} \begin{pmatrix} d \\ s \end{pmatrix}, \; V_{if} = \begin{pmatrix} \cos\theta & \sin\theta \\ -\sin\theta & \cos\theta \end{pmatrix} \qquad 1.4.1$$

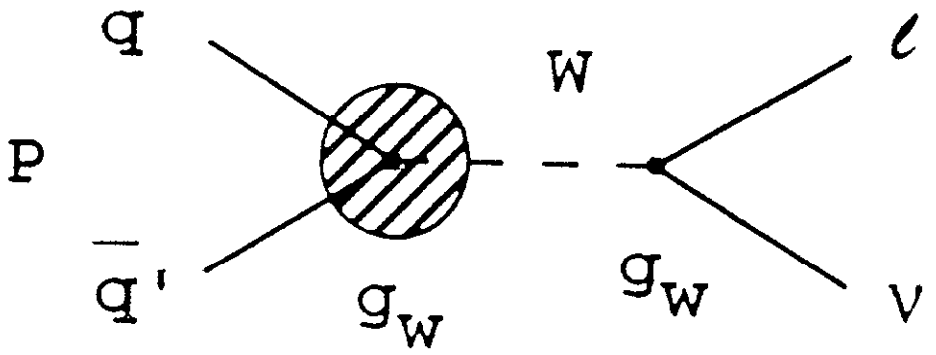

Fig. 1.3.3 Second order EW decay diagram for purely leptonic pseudoscalar meson decays, $P \to \ell\nu$.

For the case of three generations, the simplest unitary matrix has three angles and one phase. This is particularly fortunate because one needs a complex phase in order to accommodate CP violation within the Standard Model. This is far from explaining CP violation within the Standard Model but at least it allows for its existence. The CKM matrix itself is almost diagonal, which means that the mixing is not particularly large. This fact allows us to make a parameterization of the CKM matrix which is particularly intuitive.

$$V = \begin{pmatrix} V_{ud} & V_{us} & V_{ub} \\ V_{cd} & V_{cs} & V_{cb} \\ V_{td} & V_{ts} & V_{tb} \end{pmatrix}$$

$$\sim \begin{pmatrix} 1 & \theta & \theta^3 re^{-i\delta} \\ -\theta & 1 & \theta^2 \\ \theta^3\left(1-re^{i\delta}\right) & -\theta^2 & 1 \end{pmatrix} \begin{pmatrix} u \\ c \\ t \end{pmatrix} \qquad 1.4.2$$

$$\begin{pmatrix} d & s & b \end{pmatrix}$$

The two by two submatrix of Eq. 1.4.1 is expanded using the fact that the angle θ is small. The other elements will be explained and the values of those parameters given in the explanations which follow. The definition of the CKM matrix is given below.

$$J_\mu = U_{up} V\ \gamma_u\left(1-\gamma_5\right)U_{down} \qquad 1.4.3$$

Recall that the CKM matrix, V, is unitary in order to suppress FCNC using the GIM mechanism of paired doublets of quarks.

1.5 Semileptonic $Q\bar{q}$ Decays

The quark level diagrams for semileptonic electroweak decays of charm and beauty are given in Figs. 1.5.1a and b respectively. By simple color counting, one expects a branching fraction into electron and neutrino of the c quark of one fifth, whereas for the b quark, the branching fraction should be one ninth. Some representative branching fractions for B and D semileptonic decays are shown in Table 1.3. One notes that for the D^+, the inclusive electronic decay branching fraction is roughly 20%, which agrees with expectations. For the B decays there is a universal coupling in that the semielectronic and semimuonic decay rates are equal. The 12% branching fraction is in accord with our branching fraction estimate of one ninth.

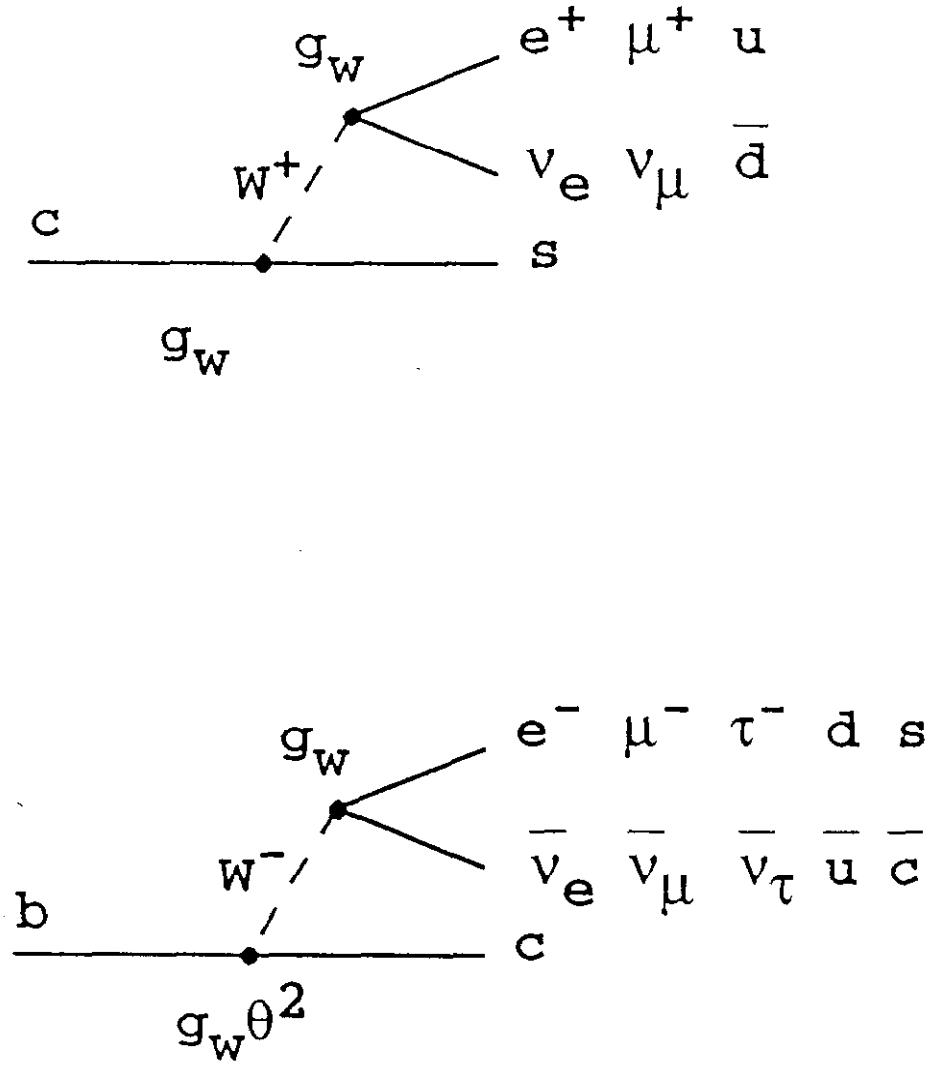

Fig. 1.5.1 Second order EW decay diagram for $Q \rightarrow qW$. Only the CKM favored W decay modes are shown.

a. $c \rightarrow sW^+$ where W^+ can virtually decay into quark or lepton pairs.

b. $b \rightarrow cW^-$ where W^- can virtually decay into quark or lepton pairs.

TABLE 1.3

B AND D SEMILEPTONIC
EXCLUSIVE AND INCLUSIVE
DECAY BRANCHING FRACTIONS

PARENT	FINAL STATE	BR (%)
D^+	$e^+ X$	19.2
	$K^* e^+ \nu$	2.5
D^0	$e^+ X$	7.7
	$K^- e^+ \nu$	3.4
B	$e \nu X$	12.1
	$\mu \nu X$	11.0
B^0	$D^- e\nu$	0.9
	$D^{*-} e\nu$	4.9

$$B(b \to c\, e\nu) \sim 1/9$$
$$B(c \to s\, e\nu) \sim 1/5 \qquad 1.5.1$$

The relationship of the branching fractions for exclusive and inclusive decays lead us to believe that simple poles contribute substantially to the decay dynamics. Therefore, a pole dominance model might be expected to have some validity. For example, in D^+ semileptonic inclusive decays, the K^* are prominent in the exclusive final state $K^*e\nu$. In the case of the D^0, the branching ratio into inclusive semileptonic states appears to be reduced from our expectation. This could be a nonleptonic enhancement as will be discussed later. Suffice it to say that the branching fraction into electrons for D^0 is suppressed by about a factor of two relative to that for D^+.

Again, for the B decays the pole dominance appears to be a useful concept. For example, the branching fraction of B^0 into D^*-eν is roughly 5%, which is a substantial fraction of the expected 11% inclusive branching fraction.

The momentum spectrum for semileptonic B decays is shown in Fig. 1.5.2. Recalling the helicity structure for muon decay, one can see that this spectrum is a typical three body leptonic decay spectrum in the V-A theory. The lepton would like to come out in a quasi two body alignment. This fact can be utilized in a "flavor tag" using the transverse momentum of the muon, P_T, in semileptonic decays. In the figure one sees the end point for the Cabbibo favored decay, the sequential $c \to s\ell\nu$ decay, and the Cabbibo disfavored decay $b \to u\ell\nu$. Again, this latter mode is also a typical beta decay three body spectrum. The expected decay rates for semileptonic decays are given from a simple extrapolation of the M^5 scaling which we've discussed previously and the CKM matrix elements in the transition. Note a convention of upper case M for external particles, and lower case m for unobserved quarks.

$$\Gamma(Q \to q\ell\nu) = \frac{G^2 m_Q{}^5}{192\pi^3}\left|V_{Qq}\right|^2$$
$$= \left[\alpha_W{}^2 \left(m_Q / M_W\right)^4 \left|V_{Qq}\right|^2 / 384\pi\right] m_Q \qquad 1.5.2$$

A compilation of decay rates for semileptonic decays is given in Table 1.4. The masses of the quarks are taken from the quarkonium spectroscopy. The muon rates and the τ rates we've already discussed. Scaling over six orders of magnitude is quite adequate. For kaon semileptonic decays, with a matrix element θ, the agreement is also quite adequate as we've previously discussed. For semileptonic up quark decays, we've used the n lifetime and the $\pi^\pm$ semileptonic decay rate. The q value there is only 2 MeV, so the extrapolation is large. However, it should be noted that we're scanning from B to n roughly fifteen orders of magnitude. In fact, a correct

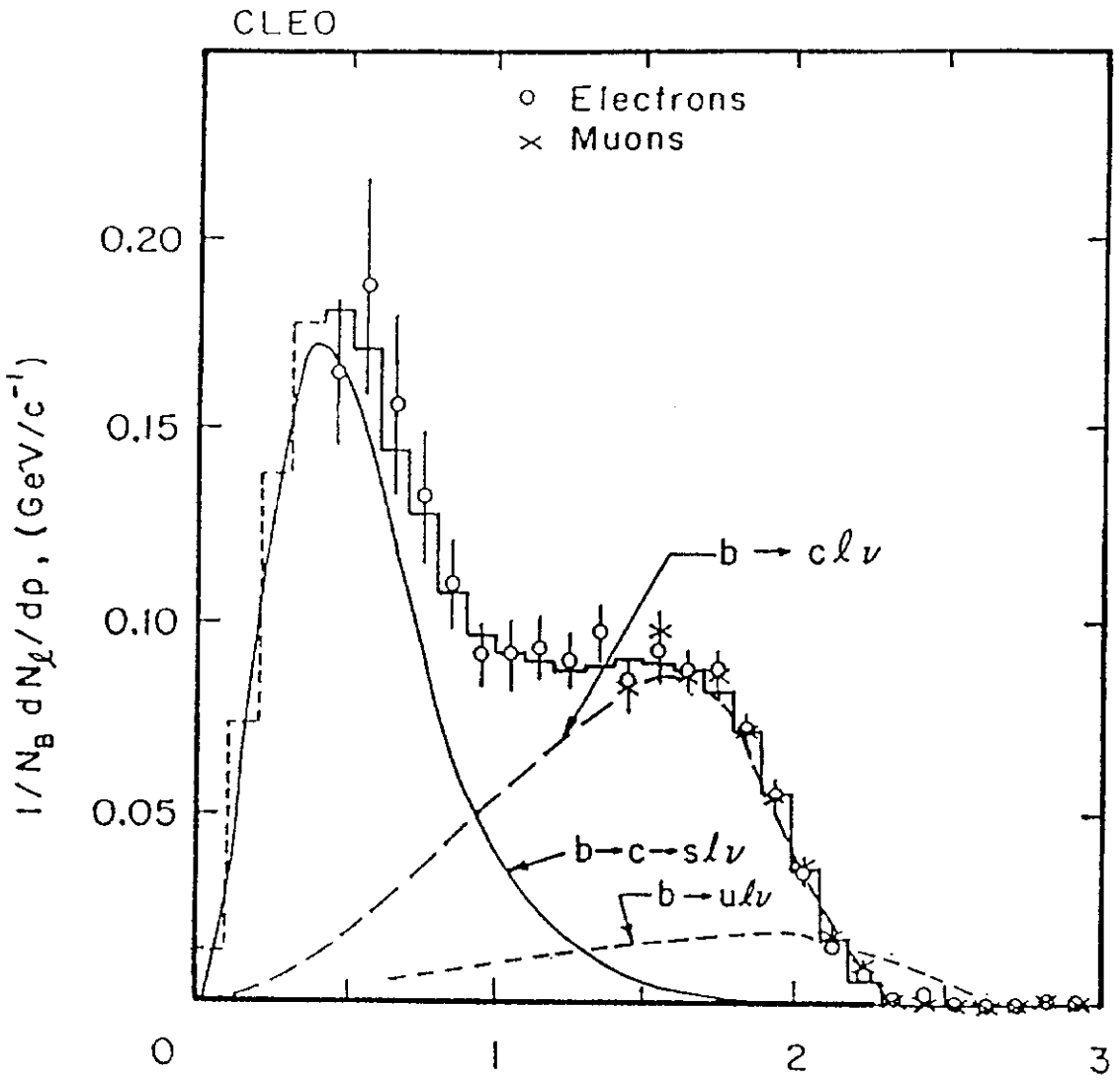

Fig. 1.5.2 Momentum spectrum for $b \to qlv$. Recall the V-A alignment implied in Fig. 1.2.2. Expected shapes for $b \to clv$, $c \to slv$, and $b \to ulv$ are shown.

treatment of the neutron is in perfect agreement with the B decay and the CKM matrix element. The data from Table 1.4 is plotted in Fig. 1.5.3 so as to show the M^5 power law scaling and the good agreement over many decades in decay rate.

For D inclusive semileptonic decays, the agreement in rate with full strength matrix elements of the CKM matrix is very good. This would indicate that any disagreement in semileptonic branching ratio most likely has to do with disagreements in hadronic rates and not semileptonic rates. For B semileptonic decays, the decay rate is essentially the same as that of the D, while the quark is more than three times heavier. Therefore, one needs to slow the B decay rates down by a rather small matrix element. Using θ^2 for the V_{bc} CKM matrix element, the agreement is good. In summary, looking at Table 1.4, and extrapolating over 15 orders of magnitude in semileptonic rates, both the leptons (the μ and the τ) and the up, strange, charm and bottom quarks are in good agreement with V-A spectator diagram dominance. In fact, these decay rates determine the CKM matrix elements. A more detailed description of the D and B matrix elements using pole dominance and form factors is given in Ref. 3.

For exclusive semileptonic decays of B mesons there are many predictions for decays to both charmed and charmless final states. Reference 3 provides an explication. This model certainly appears to work in some detail in explaining semileptonic decays. Due to the fact that the naive treatment given here works reasonably well, we do not go into details for semileptonic decays but defer to the references.

TABLE 1.4

SEMILEPTONIC DECAY RATES FOR LEPTONS AND HADRONS WITH $M^5|V_{Qq}|^2$ SCALING FACTORS

DECAY	Γ^{exp} x 10^{13} GeV	M (GeV)	M^5 Scaling x 10^{13} GeV	V_{Qq}	$M^5\|V_{Qq}\|^2$ Scaling
$\mu^- \rightarrow e^-\bar{\nu}_e\nu_\mu$	3 x 10^{-6}	0.105	$\equiv$ 3 x 10^{-6}	1	$\equiv$ 3 x 10^{-6}
$\tau^- \rightarrow e^-\bar{\nu}_e\nu_\tau$	3.95	1.78	4.2	1	4.2
$n \rightarrow pe^-\bar{\nu}_e$	7.4 x 10^{-15}	$2P^* = 0.0024$	1.8 x 10^{-14}	1	1.8 x 10^{-14}
$\pi^+ \rightarrow \pi^0 e^+\nu_e$	2.6 x 10^{-12}	$2P^* = 0.0082$	8.6 x 10^{-12}	1	8.6 x 10^{-12}
$K^+ \rightarrow \pi^0\ell^+\nu$	4 x 10^{-5}	~ 0.3	5.7 x 10^{-4}	$\theta \equiv 0.2$	2.3 x 10^{-5}
$D^+ \rightarrow X^0\ell^+\nu$	2.4	~ 1.5	1.78	1	1.78
$D^0 \rightarrow X^-\ell^+\nu$	2.4	~ 1.5	1.78	1	1.78
$B \rightarrow X\ell\nu$	1.3	~ 5.0	734	θ^2	1.18

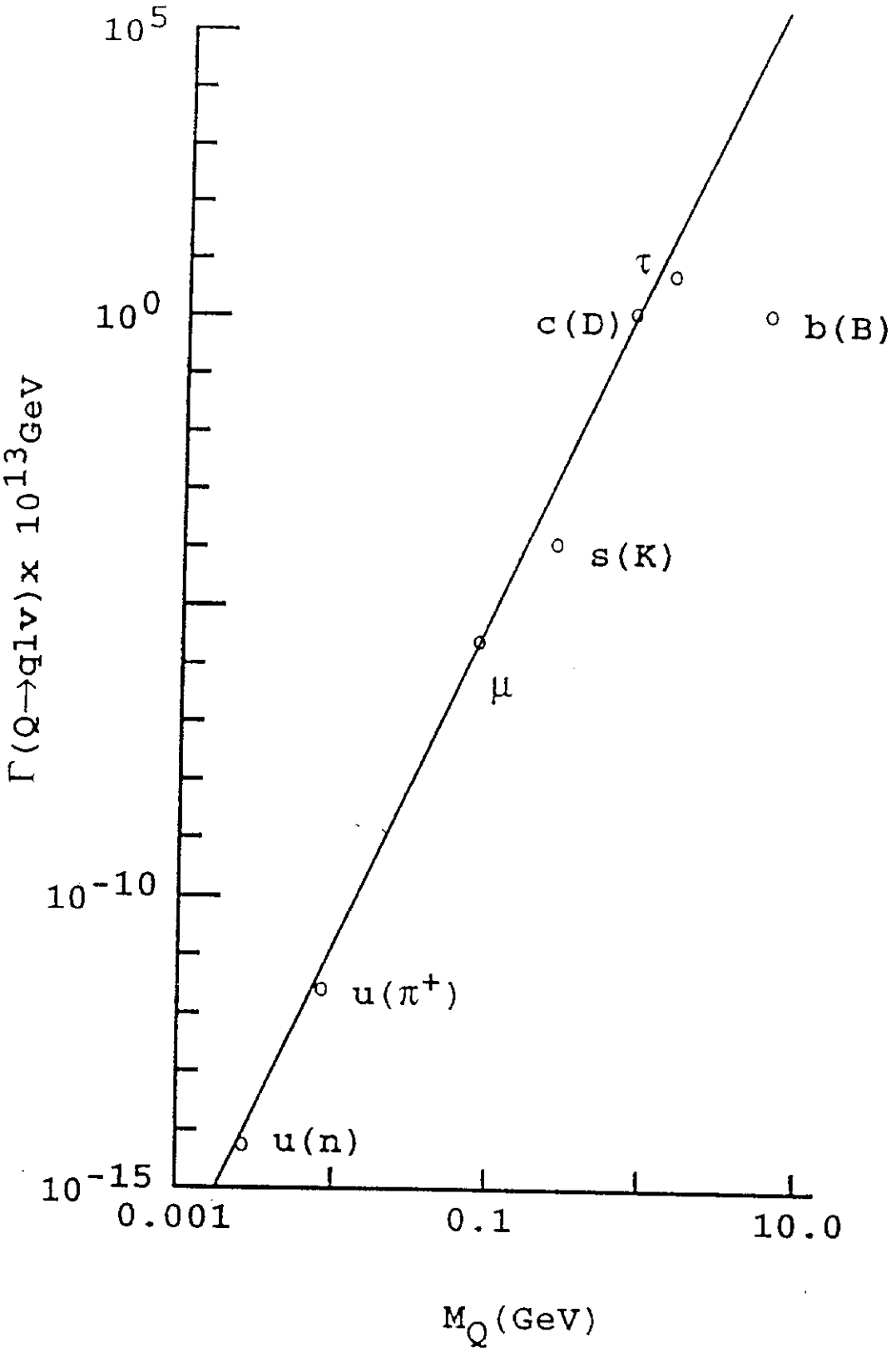

Fig. 1.5.3 Semileptonic decay rates as a function of quark or lepton mass or twice the maximum c.m. momentum. The u quark points come from n and $\pi^{\pm}$ data. The s, c, and b points come from K, D, and B data, respectively.

2. NON-LEPTONIC B DECAYS

In Section 1 we looked at the decays of leptons and the semileptonic decays of hadrons. We found that the decays were explicable in terms of the fundamental interactions mediated by the vector gauge bosons. However, by drawing simple spectator graphs, we found out that there was a nonleptonic enhancement which was substantial. For example, the square root of the ratio of the decay rates for a $\Lambda \to p\pi^-$ compared to the rate $\Lambda \to pe^-\nu$ is a factor of 28. Basically, that means that the amplitude for nonleptonic decay (where if you wish the virtual W goes into a pion) is 28 times larger than the amplitude where the virtual W (in the spectator diagram context) goes into an eν pair. Obviously, the spectator model for quark decays is suspect in the case of light quarks (up, down, and strange). Therefore, in order to build up some experience with nonleptonic decays, we jump immediately to the charm quark sector and examine the situation. We previously argued that we would be in better shape if the QCD effects which might be large were driven down by going to higher mass scales. We begin Section 2 with a classification of possible diagrams which can contribute to nonleptonic decays, other than spectator diagrams.

2.1 Spectator, Annihilation, Exchange Graphs

Three possible diagrams contributing to nonleptonic decays are shown in Fig.2.1.1. They are called respectively spectator, exchange, and annihilation graphs. The names are obviously related to the topological properties of the graphs. We've already looked at the spectator diagram. We are aware that the three body decay dynamics along with the virtual W propagator gives us a decay rate which scales as the fifth power of the heavy quark mass. What about the exchange diagram? For pseudoscalar mesons the exchange diagram is disfavored by helicity because it is essentially the same as the diagram for $\pi \to e\nu$. For Fig. 2.1.1 one has, for example, $D^0 \to s\bar{d}$. As also indicated in Fig. 2.1.1, this suppression can be evaded by exchanging a virtual vector gluon. However, it costs you a power of the strong coupling constant.

The third type of diagram is called the annihilation diagram. A Cabbibo favored graph for D_S annihilation into pion pairs is shown as the third graph in Fig. 2.1.1. Again this is an helicity disfavored graph because it is essentially a two body graph. Therefore, it will require gluonic effects to enhance it. What can we say about the relative ratio, for example, of annihilation and spectator graphs? Clearly for the annihilation graph, the partial decay rate depends on the wave function at the origin. The probability density has a dimensionality of one over length cubed which means that the ratio of the annihilation rate to the spectator rate must go like the wave function at the origin squared over the mass of the system cubed.

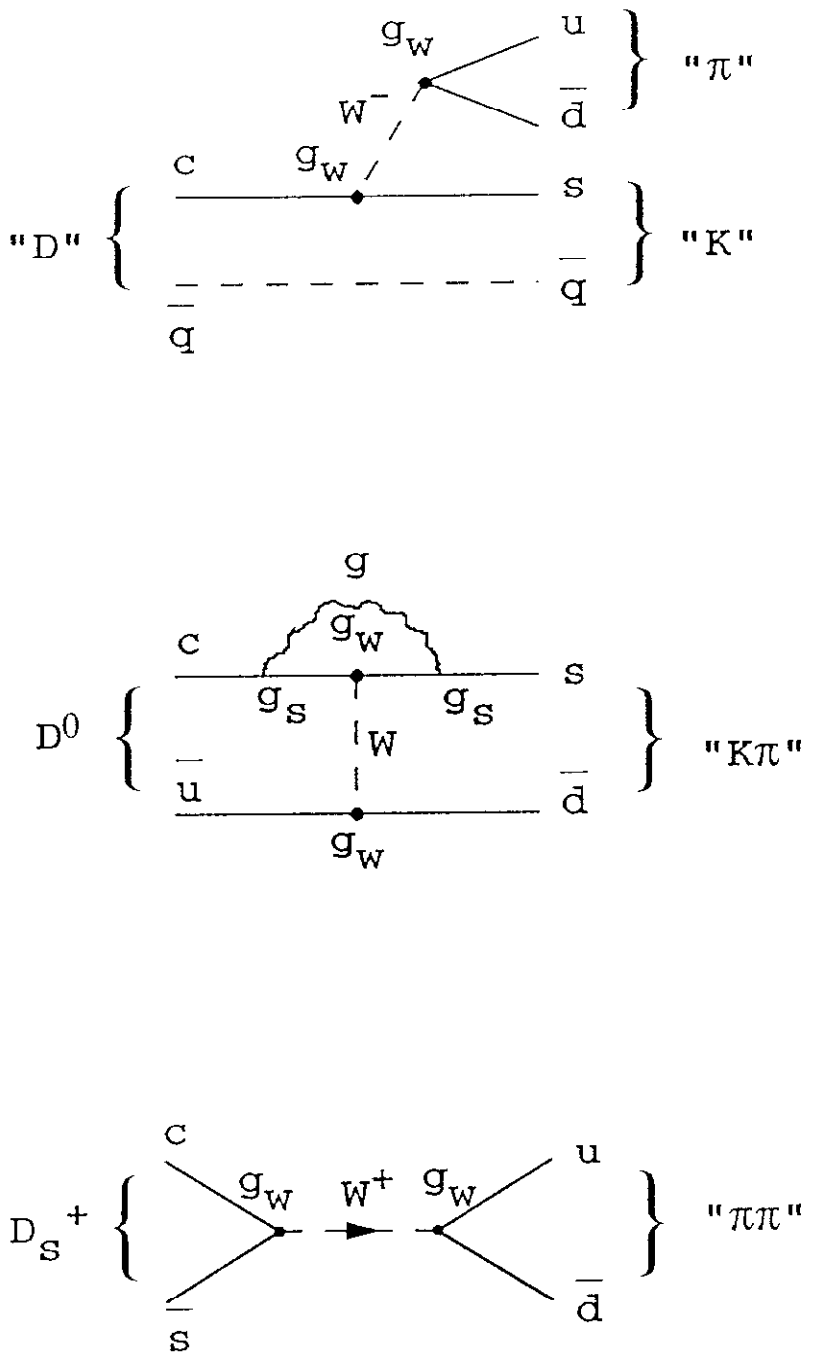

Fig. 2.1.1 Spectator, exchange, and annihilation decay diagrams for charmed meson decays.

$$\Gamma_A \sim m^2 |\Psi(o)|^2$$
$$\frac{\Gamma_A}{\Gamma_S} \sim \frac{|\Psi(o)|^2}{m^3} \qquad 2.1.1$$

The wave function at the origin has a characteristic size which is set by the mass of the system. That mass and the coupling constant are the only scales in the problem. It should be familiar from atomic physics that the Bohr radius is related to the coupling constant for the mass of the electron, assuming QCD is analogous;

$$|\Psi(o)|^2 = \alpha_s^3 / \pi \lambda\!\!\!^{-3} \,,\; a_o = \lambda\!\!\!^{-} / \alpha_s, \lambda\!\!\!^{-} = \hbar / m$$
$$\frac{\Gamma_A}{\Gamma_S} \sim \alpha_s^3 \left(m_q / m_Q\right)^3 \qquad 2.1.2$$

This means that in the case of a heavy and light $Q\bar{q}$ meson state with strong QCD binding, the ratio of the annihilation to the spectator amplitude will go roughly as the cube of the light to heavy quark mass ratio and as the cube of the coupling constant. Clearly, as the mass of heavy quark goes up, the annihilation graph will become less and less important. Therefore, it is as asserted that any enhancement due to annihilation will die off for higher mass states. This occurs effectively because the lighter quark is in orbit around the heavy quark. Thus, the wave function at the origin does not increase as the mass of the heavy system increases. By the way, this argument also shows that the annihilation diagram will indeed be important for light mesons where the mass ratio is effectively one and where the strong coupling constant is also large at those low mass scales. This appears to be validated in the sense that we know we have a nonleptonic enhancement, say for Λ decays, of a factor of about a thousand in rate, whereas the difference between D^+ and D^0 lifetimes is only a factor of two.

Therefore, we expect that we will be able to simply assume spectator dominance in studying B decays. Recall that in a pure spectator model the semileptonic decay rate would be the same, for example, for all charmed particles and, indeed, this is what one observes for the D^+ and D^0. However, there is a factor of two difference between the total decay rate for D^+ and D^0 which leads us to believe that there are other quark diagrams which are important in the nonleptonic decays. There is indeed a nonleptonic enhancement although it is sharply reduced from what is seen in strange particle decays.

2.2 Spectator Amplitudes

From now on we will assume, based on the arguments given above, that for B and D decays only spectator amplitudes are important. However, one should note that there are two topologically different spectator diagrams which we will call "exterior" and "interior." These diagrams are shown in Fig. 2.2.1a and b. Note that in the exterior diagram the colorless virtual W is allowed to decay into three possible $u\bar{d}$ color singlet final states. In contrast, in the interior diagram, in order to form colorless final states, only one of three possible virtual W decays is allowed. Therefore, the interior diagram is suppressed by a factor of one over the number of colors N_C with respect to the exterior diagram. However, as shown in Fig. 2.2.1c, the interior diagram can avoid the color suppression factor by the initial exchange of a gluon. The color suppression factor is evaded at the cost of a factor of the strong coupling constant in the amplitude. However, this gluon can be quite soft. Therefore, $\alpha_s\left(q^2\right)$ for that gluon may "run" to large values.

Let us practice by first looking at nonleptonic D decays. The reason to start with D decays is that much more precise data are available at present in the charm quark systems than in the b quark. First let us write down a phenomenological Lagrangian for the system. In this case one uses the fact that the second order decay with an intermediate W boson effectively happens at a single space time point with an effective coupling constant, G, that has dimensions. This is the effective four fermion interaction. For the purposes of studying D decays, it is perfectly sufficient to use an effective interaction.

$$\begin{aligned} H_I &= \frac{G}{\sqrt{2}} J_\mu J^\mu \\ &= \frac{G}{\sqrt{2}} V_{cs} V_{ud}^* (\bar{s}c)_L (\bar{u}d)_L \\ H_I &= \frac{G}{\sqrt{2}} V_{cs} V_{ud}^* \left[a_+ O_+ + a_- O_-\right] \\ O_\pm &= (\bar{s}c)_L (\bar{u}d)_L \pm (\bar{s}d)_L (\bar{u}c)_L \end{aligned} \qquad 2.2.1$$

Note that in these equations one has written down the currents for the active quarks in the decays and rearranged them into two operators corresponding to exterior and interior diagrams. The operators O_+, O_- can be read off from the quark level diagrams given in Fig. 2.2.1a and b. One then allows for phenomenological parameters involving QCD and gluon emission and fits the D decays for those parameters, a_+ and a_-. Without QCD corrections, $a_+ = a_- = 1$.

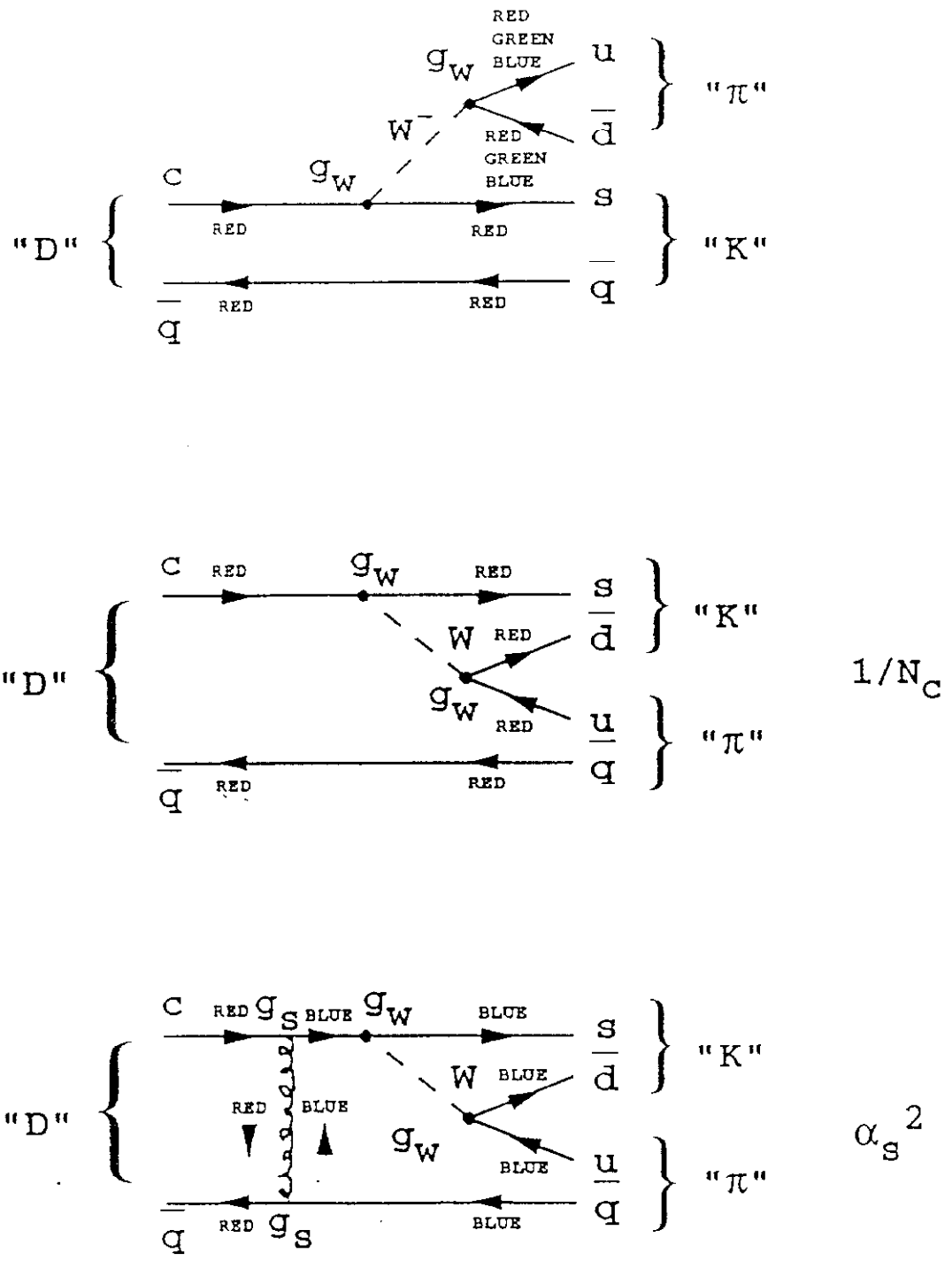

Fig. 2.2.1 Spectator diagrams for charmed meson decays.

a. "Exterior" decay diagram.

b. "Interior" decay diagram with color factor 1/Nc made explicit.

c. "Interior" decay diagram with gluon emission evading the color factor at a cost of $\alpha_s^2(q^2)$.

$$\Gamma = \left(2\,a_+^{\,2} + a_-^{\,2}\right)\Gamma_0,\ \Gamma_0 = \text{ Semileptonic Rate}$$

$$H_I = \frac{G}{\sqrt{2}} V_{cs} V_{ud}^{*} \left[\left(\frac{a_+ + a_-}{2} \right) (\bar{s}c)_L (\bar{u}d)_L + \left(\frac{a_+ - a_-}{2} \right) (\bar{s}d)_L (\bar{u}c)_L \right] \qquad 2.2.2$$

$$\equiv \frac{G}{\sqrt{2}} V_{cs} V_{ud}^{*} \left[a_1 (\bar{s}c)_L (\bar{u}d)_L + a_2 (\bar{s}d)_L (\bar{u}c)_L \right]$$

$$H_I^{\,\prime} \equiv \frac{G}{\sqrt{2}} V_{cs} V_{ud}^{*} \left[a_1^{\,\prime} (\bar{s}c)(\bar{u}d) + a_2^{\,\prime} (\bar{s}d)(\bar{u}c) \right]$$

One should note that given this phenomenological form, the D^+ and D^0 widths need no longer be the same because topologically D^+ and D^0 have different "exterior" and "interior" topologies. In fact, one can imagine interference between the interior and exterior graphs and, therefore, a relative suppression of the D^0 with respect to D^+. Using simple color counting, one gets an estimate for the two phenomenological matrix elements that are fit for, given the values for a_+ and a_- that are calculated in QCD.

$$\text{No QCD: } a_+ = a_- = 1,\ a_1 = 1,\ a_2 = 0$$

$$2a_1^{\,\prime} = (1+\varepsilon)a_+ + (1-\varepsilon)a_- = \text{"}Exterior\text{"}$$

$$2a_2^{\,\prime} = (1+\varepsilon)a_+ - (1-\varepsilon)a_- = \text{"}Interior\text{"} \qquad 2.2.3$$

$$\text{QCD: } \varepsilon \sim 1/N_C \sim 1/3,\ a_+ \sim 0.7,\ a_- \sim 2.0$$

$$a_1 \sim 1.3,\ a_2 \sim -0.6$$

$$a_1^{\,\prime} \sim 1.1,\ a_2^{\,\prime} \sim -0.2$$

In performing the fit, as done in, for example, Ref. 3, one has the amplitude for the decay D goes to Kπ.

$$A(D \to K\pi) \sim \left\langle K \middle| J_\mu \middle| D \right\rangle \left\langle \pi \middle| J^\mu \middle| o \right\rangle$$

$$\sim \left\langle K \middle| J_\mu \middle| D \right\rangle f_\pi q^\mu \qquad 2.2.4$$

$$\sim \frac{h_1 f_\pi}{\left(1 - \dfrac{q^2}{M_{D_s}^{\,2}}\right)}$$

The amplitude is assumed to factorize, and in the factorization, one needs the pion decay constant and some assumption as to the form factor for the D transition. The assumption which is made is that the form factors are pole dominated. As mentioned before, there is some noncompelling evidence for the dominance of poles in D semileptonic decays.

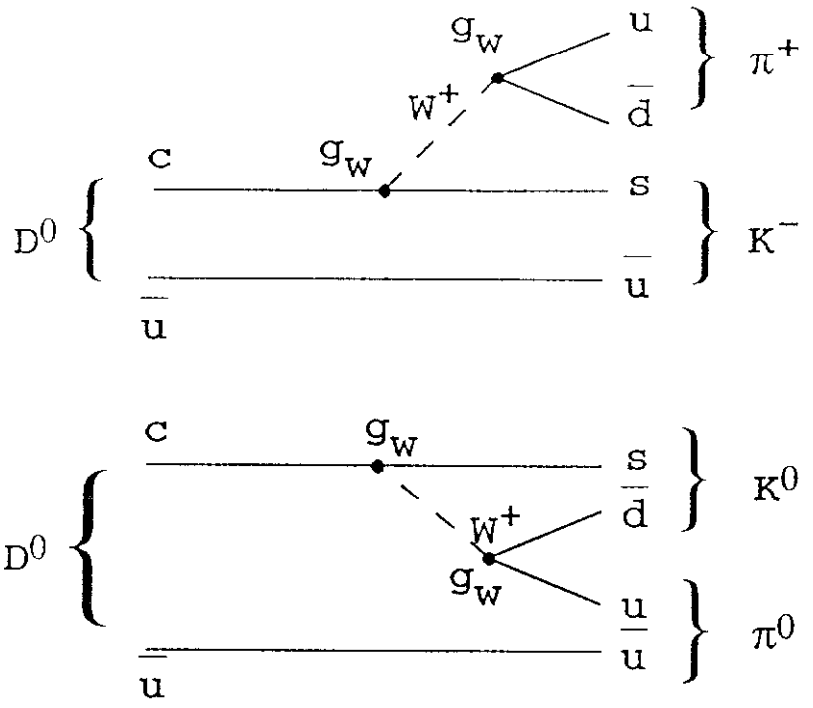

Fig. 2.3.1 Spectator diagram for D^0 decays.

a. "Exterior" $D^0 \to K^-\pi^+$ diagram.

b. "Interior" $D^0 \to K^0\pi^0$ diagram.

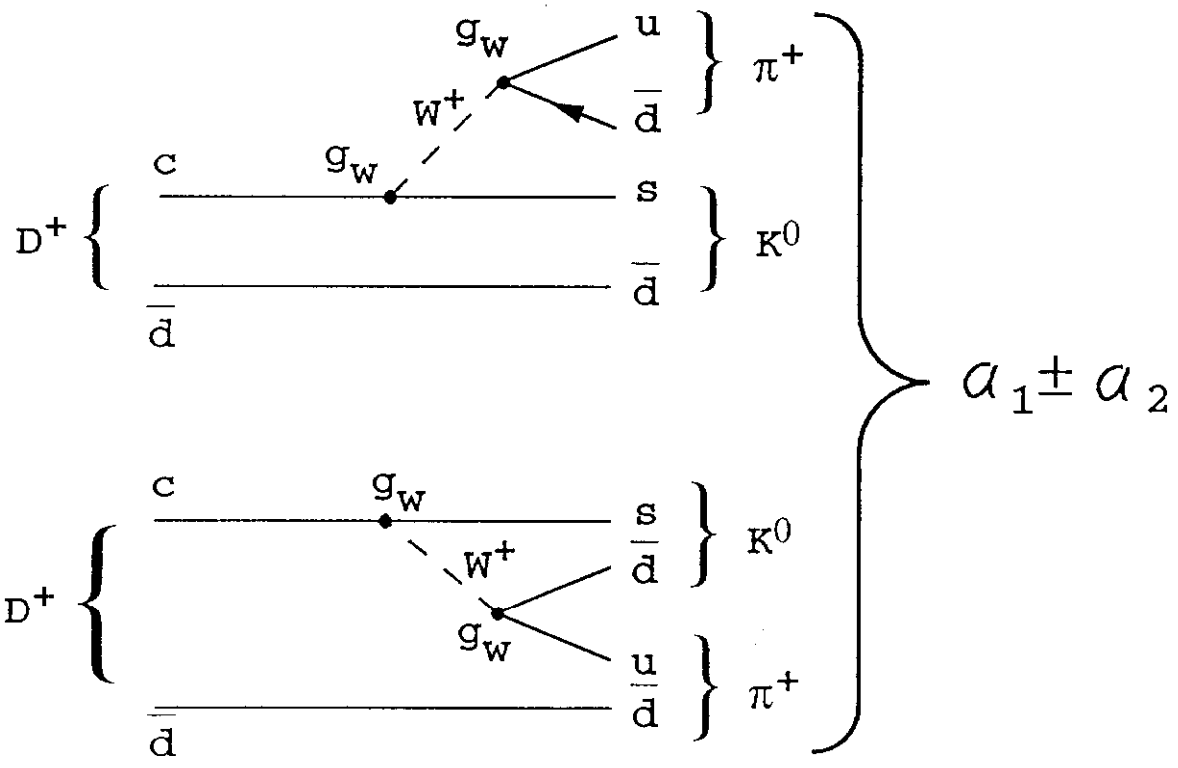

Fig. 2.3.2 Spectator diagram for D^+ decays.

a. "Exterior" $D^+ \to K^0\pi^+$ diagram.

b. "Interior" $D^+ \to K^0\pi^+$ diagram.

2.3 Nonleptonic D Decays

The formulas shown in Section 2.2 have been used in Ref. 3 to fit all of the observed nonleptonic D decay modes to two parameters, the amplitude for the interior graph and the amplitude for the exterior spectator graph. For example, in Fig. 2.3.1, one sees the spectator diagrams for D^0 decays into $K^-\pi^+$ which is an exterior diagram and into $K^o\pi^o$ which is an interior diagram. In contrast, the spectator diagrams for D^+ decays are shown in Fig. 2.3.2. There is an exterior diagram for D^+ to $K^o\pi^+$ and a topologically different interior diagram for D^+ to the same final state. This means that one has the possibility for D^+ interference within the spectator model.

As mentioned before, the possible interference which one can see in Fig. 2.3.2 means that it is plausible that the spectator decay rates for D^+ and D^0 can be different. The results of a fit for the parameters a_1 and a_2 in nonleptonic D decays are shown in Fig. 2.3.3. The fact that these two numbers are a reasonable representation of all the data tells us that the spectator model with the factorization assumption given in Eq. 2.2.4 is a reasonable phenomenological representation of the data. Note that both the matrix elements and the CKM elements, V_{cs} and V_{cd}, are fit. An input which is necessary is the pseudoscalar decay constant. Basically, one assumes that all the decay constants are the same. This is certainly very nice phenomenology in that one can explain within its context all D decays in terms of spectator diagrams and two numbers.

2.4 Nonleptonic B Decays

The nonleptonic spectator diagrams for B decays are essentially exactly the same as those for charm decays except that the virtual W can decay into a $u\bar{d}$ or a $c\bar{s}$ pair since both are Cabbibo favored and there is enough mass in this case to make the $c\bar{s}$ pair kinematically allowed. We again ignore exchange and annihilation graphs on the basis that the nonleptonic enhancement in D decays is already small and that we expect a scaling as the cube of the mass of the heavy system. The interior spectator diagram, where the W goes to a $c\bar{s}$ pair, is shown in Fig. 2.4.1. One interesting feature of this particular diagram is that both the B and the $\overline{B}$ can feed the final state ΨK_s. What's interesting about that final state is the possibility that B and $\overline{B}$ effectively mix by going through the common intermediate states or that they can interfere giving a rise to CP violation or asymmetry in the exclusive decay $B_d \rightarrow \Psi K_s$. Since the same final state is fed by both B and $\overline{B}$, it is possible that there is such a CP violating interference effect.

The center of mass momentum for such a two body final state is easy to calculate and comes out to be;

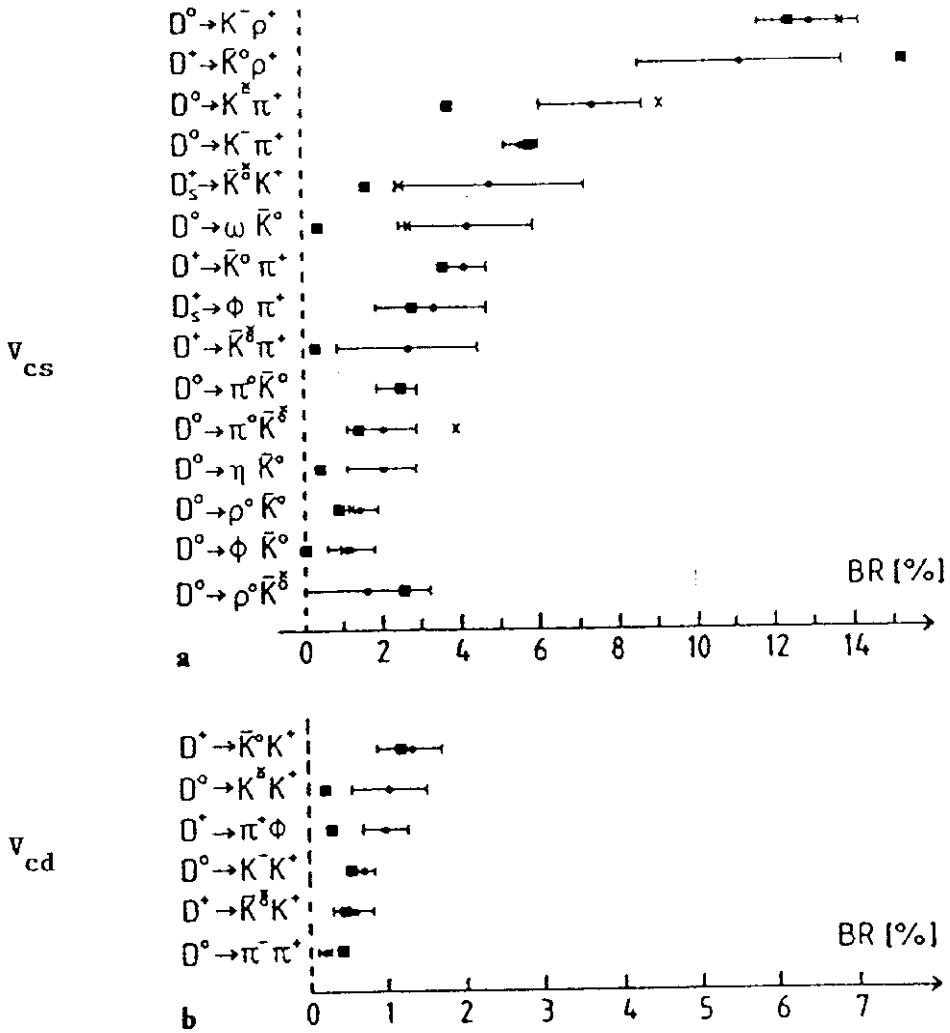

Fig. 2.3.3 Nonleptonic D decays; data and the fit using the BWS model for allowed (V_{cs}) and suppressed (V_{cd}) decays.

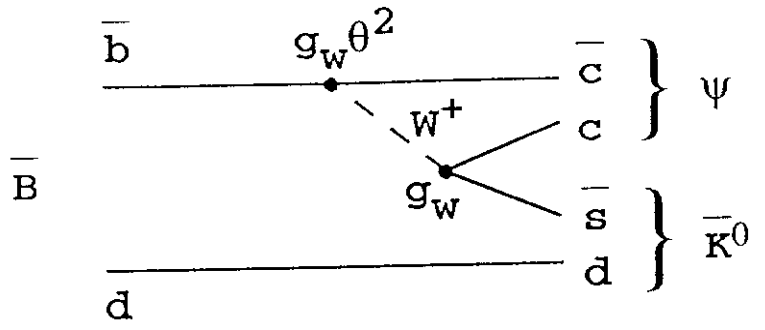

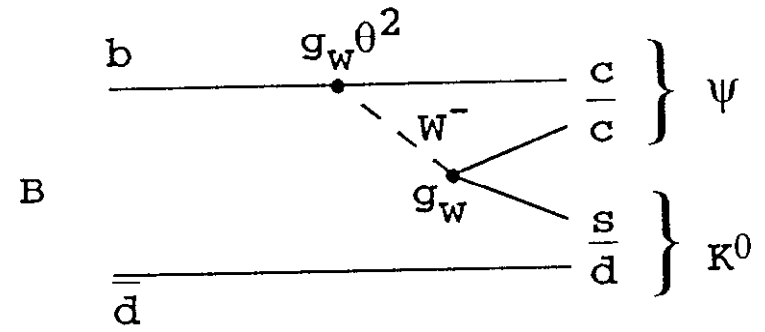

$B_d \rightarrow \psi K_s$

$\bar{B}_d \rightarrow \psi K_s$

Fig. 2.4.1 "Interior" spectator diagrams for $b \rightarrow cW^- \rightarrow c(\bar{c}s)$.

a. $\bar{B} \rightarrow \Psi \bar{K}^0$

b. $B \rightarrow \Psi K^0$

$$P^*(B \to \Psi K) = 1.68\ GeV \simeq \left[M_B{}^2 - M_\Psi{}^2\right]/2M_B \quad . \tag{2.4.1}$$

Data from e^+e^-colliders on the momentum distribution of inclusive ψ decays are shown in Fig. 2.4.2. Note that the existence of high momentum in the inclusive spectrum indicates that there may be a large fraction of exclusive two body like final states in the ψ inclusive data. Again, pole dominance leads us to believe that the $s\bar{d}$, going along with the ψ, will be dominated by K and K* poles. In fact, data from e^+e^-colliders indicates that the inclusive branching ratio into ψ plus anything is about 1% for B^0 and, of that 1%, about 37% is due to ΨK^*. So, in fact, the two body pole dominance seems to also be a phenomenological fact of life in the B system. Again, in Ref. 3, a fit to all nonleptonic B decays was done. For example, in Fig. 2.4.3 one has spectator diagrams for B_d into $D^+\pi^-$ and B_d into $D^0\pi^0$ which have exterior and interior graphs respectively. The results of such a fit are shown in Fig. 2.4.4. As with the D decays, the entire nonleptonic data set can be represented by two numbers, a_1 and a_2.

In fact, there is perhaps slightly more information than that when one compares the results of the fits for B and D decays.

$$\begin{aligned} D: &\quad a_1' \sim 1.3 \quad a_2' \sim -0.55 \\ B: &\quad a_1' \sim 0.9 \quad a_2' \sim -0.2 \end{aligned} \tag{2.4.2}$$

Note that the D decays have a larger absolute value of a_2 than the B decays for the best fit. This in some sense is plausible because the amplitudes can be QCD evolved from the D to the B mass scales. In fact, the naive estimate via color counting can be thought of as the expectation for infinitely massive quarks. Comparing Eq. 2.2.3 and 2.4.2 one can see that the B decay fit values are not terribly far from the asymptotic theoretical estimates. Therefore, as far as the nonleptonic decays go, one appears to have a situation where spectator diagrams dominate. This conclusion follows from looking, in the progression from strange to charm to beauty decays, at the size of the nonleptonic enhancement. Futhermore, one has a phenomenological theory with only a few parameters which gives an "adequate" representation of the data.

2.5 Penguins, Loops, and Rare Decays

First, let us consider some of the decays which are rare but are not of higher order. The purely leptonic D and B decays have yet to be measured. The limit, for example, for the $D^+ \to \mu^+\nu$ branching fraction is 7 x 10^{-4}. One recalls that the purely leptonic decays go like the first power of the mass of the heavy quark, whereas the semileptonic rate goes as the fifth power.

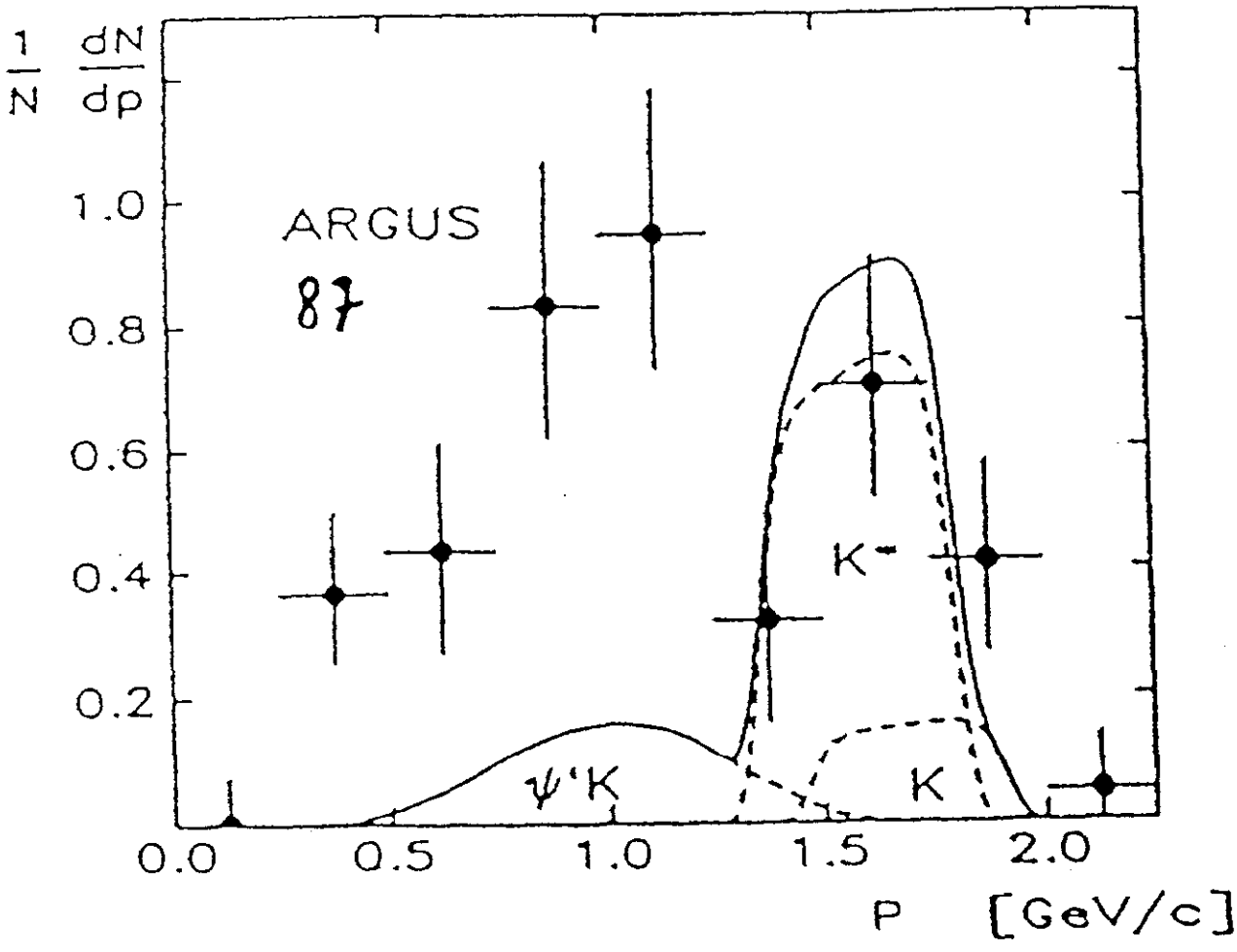

Fig. 2.4.2 Ψ momentum distribution in inclusive $B \to \Psi X$ decays. The spectrum shows a "2 body" like component.

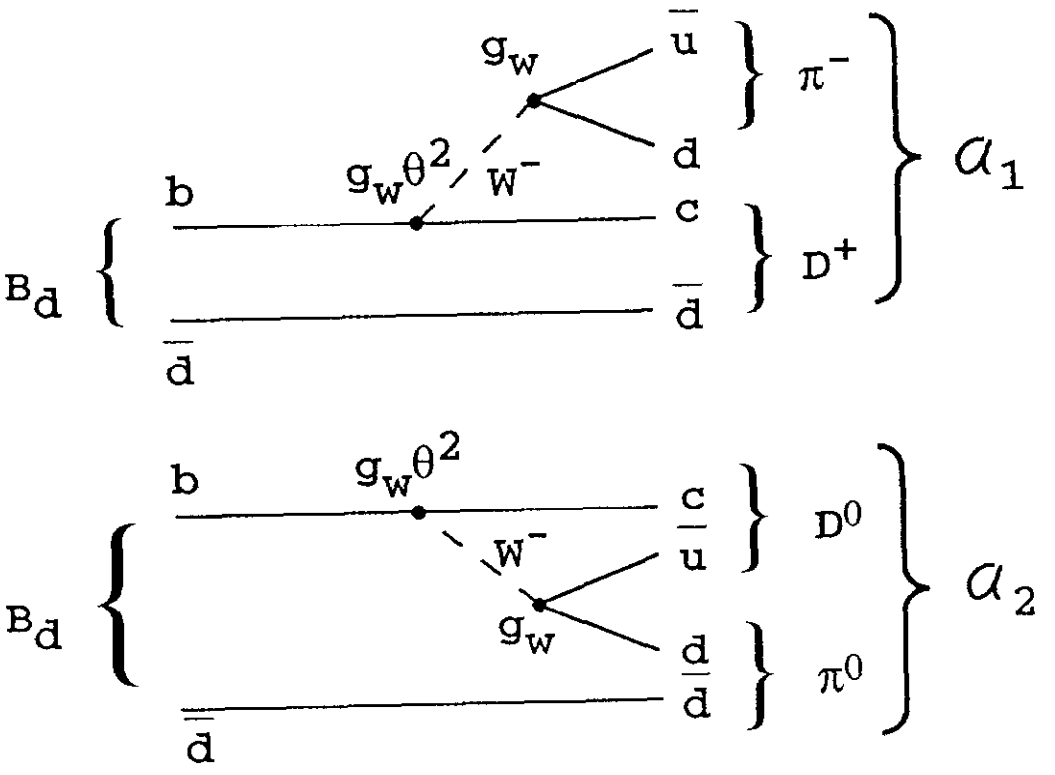

Fig. 2.4.3. Spectator diagram for B_d decays into Dπ.

a. "Exterior" decay $B_d \to D^+\pi^-$.

b. "Interior" decay $B_d \to D^0\pi^0$.

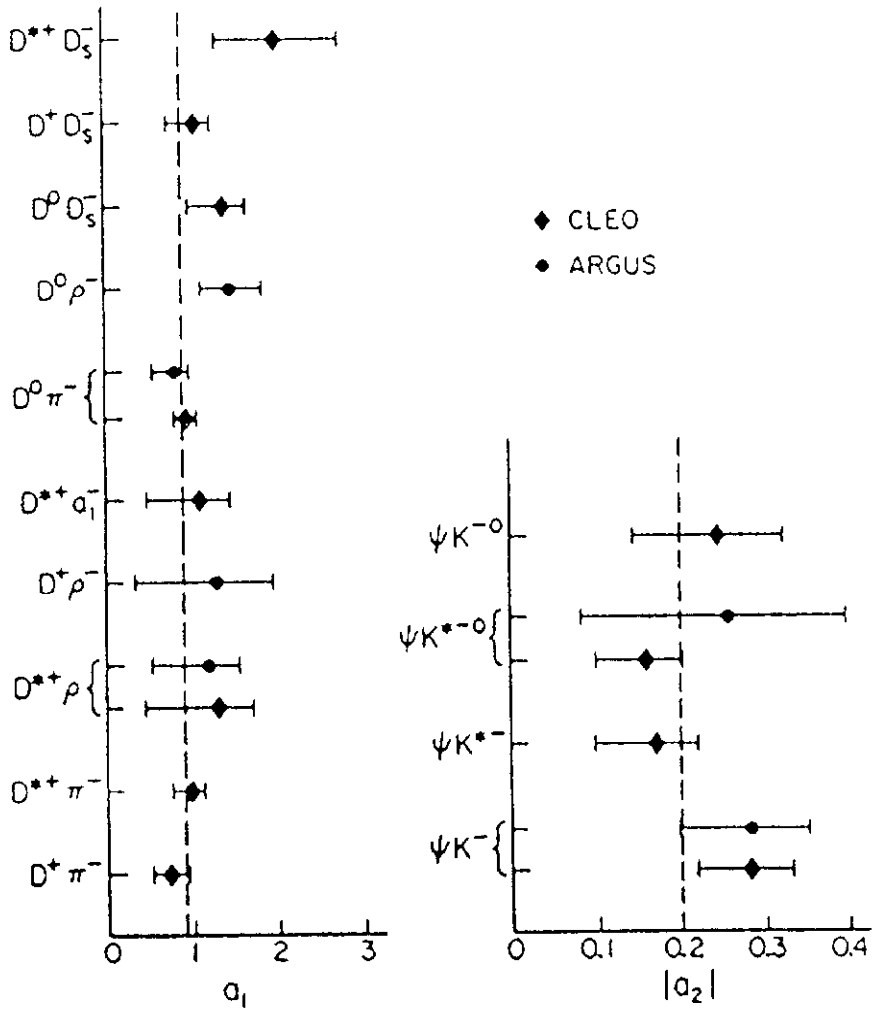

Fig. 2.4.4 Parameters a_1, a_2 for nonleptonic B decays; data and the fit using the BWS model.

Therefore, it will be extremely hard to observe the purely leptonic decays and extract the decay constants. This is unfortunate because those decay constants are important phenomenological inputs. In particular, there are higher order diagrams which are used in the Standard Model to estimate the mass and decay matrices relating to mixing and CP violation which depend on f_B and f_D.

Another class of rare decays are the Cabbibo unfavored charmed decays. For example, the branching ratio for $D^0 \to K^- e^+ \nu$ is 3.4%, whereas the branching fraction into $\pi^- e^+ \nu$ is 0.39%. The absolute decay rate tells us that the CKM matrix element V_{cs} is at full strength or roughly equal to 1, whereas the matrix element V_{cd} is roughly equal to θ or one fifth. Measurements of this type define V_{cd}. Therefore, $V_{ud}, V_{us}, V_{cd}, V_{cs}$ follow from n, K, "$D \to \pi$" and "$D \to K$" decays respectively. The B decay rate yields V_{cb}, so that 5 of the CKM matrix elements are now defined.

There is another category of decays having to do with higher order diagrams for processes which are forbidden in lowest order, for example, flavor changing neutral current, FCNC, processes. We've already discussed how the GIM mechanism kills FCNC in lowest order. In order to begin this study, we go back to Feynman's treatment of higher order effects in the propagator. The photon loop diagram used in that study is shown in Fig. 2.5.1. This virtual photon is reabsorbed by the electron and it causes a modification to the simple electron propagator. The vertex and propagator factors for Fig. 2.5.1 can easily be written.

$$\alpha \int \frac{dq^4}{\not{p} - M_o} \left[\gamma_\mu \left(\frac{1}{\not{p} - \not{q} - M_o} \right) \gamma_\mu \left(\frac{1}{q^2} \right) \right] \frac{1}{\not{p} - M_o} \qquad 2.5.1$$

One can expand the revised propagator assuming a modified mass term and compare that to the expression given in Eq. 2.5.1. The idea is that the virtual loop causes a change in the fermion self energy and thus, in the mass.

$$\frac{1}{(\not{p} - M_0 - \delta M)} = \frac{1}{\not{p} - M_o} + \frac{1}{\not{p} - M_0} \delta M \frac{1}{\not{p} - M_0} + \ldots$$

$$\delta M = \alpha \int \frac{dq^4}{q^2} \left[\gamma_\mu \left(\frac{1}{\not{p} - \not{q} - M_0} \right) \gamma_\mu \right] \qquad 2.5.2$$

One can see that the mass shift for the electron is proportional to the fine structure constant, and an integral over all the internal loop momentum. Now in Feynman's treatment, one attempts to do the loop integral and requires that the external electron lines be on shell. In the limit of large

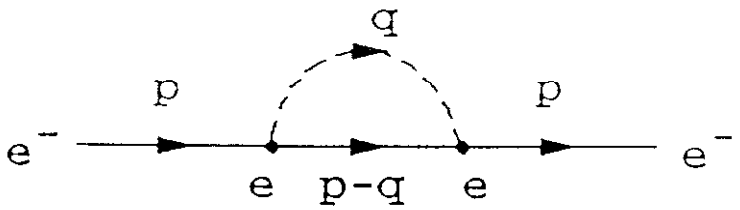

Fig. 2.5.1 Photon loop diagram used in the study of the behavior of the electron propagator in higher order QED.

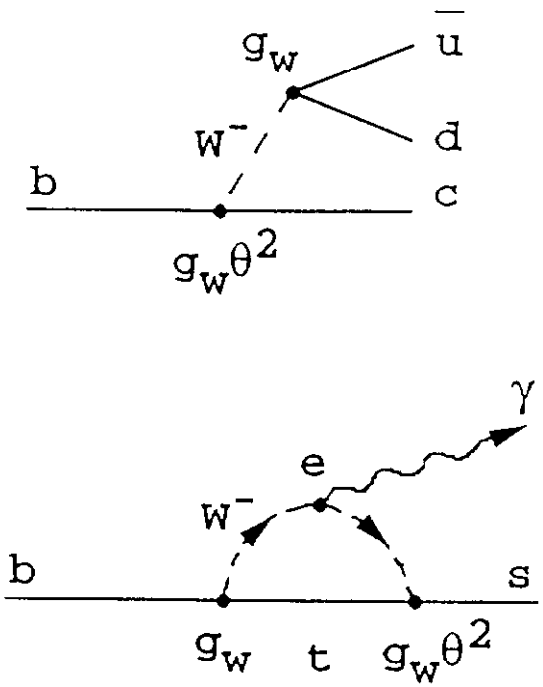

Fig. 2.5.2 Comparison of spectator decays for normal and rare "penguin" processes.

a. $b \to c(\bar{u}d)$.

b. $b \to W^- t \to s\gamma$.

q^2, the integral will give trouble. It turns out to be logarithmically divergent. It is then modified by a cutoff factor, with a cutoff parameter λ, which gives one a mass shift as shown below.

$$\begin{aligned} &\delta M \to \alpha \int \frac{q^3 dq}{q^4}\left[2M_0\right] \\ &-\left[\lambda^2/\left(q^2-\lambda^2\right)\right] \\ &\frac{\delta M}{M_0} = 3\alpha\left[3\ell n\left(M_0/\lambda\right)^2 + 3/4\right] \end{aligned} \qquad 2.5.3$$

It is typical of this sort of diagram that one has a mass shift which depends linearly on the coupling and logarithmically on the square of the mass of the system. An application of such a loop term occurs in looking at rare B decays in flavor changing neutral currents. What one compares is the standard spectator decay to an internal W loop which allows the external decay $b \to s\gamma$, or a FCNC in higher order. These diagrams are shown in Fig. 2.5.2.

Given the discussion of the propagator loop for electrons, it's clear that having a large value of the internal quark mass, and in this case the top is available, will help enhance the FCNC amplitude. The question is whether the enhancement is large enough to be useful. One can read off the amplitude factors and compare the two diagrams given in Fig. 2.5.2. One makes an estimate of the CKM matrix elements and finds out that even though the top is not strongly coupled to the s, one is fortunate in that the b decay itself is quite slow. Recall that the B lifetime has a θ^4 factor in it. This is the factor which we already saw in comparing the semileptonic decay rates of all the different quark systems. The fact that the main spectator diagram is so slow means that the FCNC is more nearly comparable to the main decay and is, in fact, not particularly rare. This is a general property of the B system in comparison to the K or D systems; "rare" decays are not "rare."

$$\begin{aligned} \frac{\Gamma(b \to s\gamma)}{\Gamma(b \to c\bar{u}d)} &\sim \alpha\left[\frac{V_{tb}{}^2 V_{ts}{}^2 \ell n\left(\frac{m_t}{M_w}\right)^4}{V_{cb}{}^2 V_{ud}^2}\right] \\ &\sim \alpha\left[\left(\frac{m_t}{M_W}\right)^4\right] \end{aligned} \qquad 2.5.4$$

In this case the cutoff parameter λ is supplied by the fact that the heavy quark masses cut off the available internal momentum of the loops. A "real" theoretical estimate, with QCD corrections, is more likely to be that the branching fraction of $b \rightarrow s\gamma$ is 2 x 10^{-3} and that the branching fraction of the B meson to a $K\gamma$ is 1 x 10^{-4}. Still, these are not enormously rare decays and may be measured with a large enough sample of B's. In particular, a simpler signature would be that the photon shown in Fig. 2.5.2b, virtually decay into a pair of muons or electrons. In this case, the FCNC is $B \rightarrow K\mu^+\mu^-$ or $B \rightarrow Ke^+e^-$. Obviously, looking at the diagram, the decay gives information on the CKM matrix elements V_{ts} and V_{td} because the top quark will dominate in the virtual loop. This is a FCNC search which has a spectacularly good signature, although the rates are not terribly compelling.

3. PHENOMENOLOGY FOR CP VIOLATION

The purpose of this Section is to sketch out the phenomenology for two level quantum systems which are in communication, which means that there exist amplitudes connecting the two states. This phenomenology is applicable to neutral mesons containing strange quarks, charm quarks and b quarks. An attempt will be made in this Section to carry through a general phenomenology that only makes approximations appropriate for the s, c, or b mesons as necessary. The reason for adopting this approach is that the approximations appropriate to different systems are, in fact, different. Therefore, an intuition which one has built up in the K system does not trivially carry over to the B system.

3.1 Mass, Decay Matrix

Let us consider the situation where the weak Hamiltonian is a small perturbation on the strong and electromagnetic interactions. This is obviously a good assumption for the systems we're dealing with. This particular phenomenology has been in existence for about 30 years and was first applied to the kaon system. Assuming that the weak Hamiltonian is a perturbation, one can expand the S matrix in powers of the perturbative Hamiltonian.

$$S-1 \equiv T \cong H_W + H_W\left[\frac{1}{E-H_0+i\varepsilon}\right]H_W \qquad 3.1.1$$

The second order perturbation can be sandwiched with a complete set of eigenstates of the unperturbed Hamiltonian H_0. The causal displacement ε can be broken into two pieces, the principle value, which implies off shell transitions, and a δ function which corresponds to on shell decays. This leads to the transition matrix, T, given below.

$$T = H_W + P\sum_n \frac{H_W|n><n|H_W}{M_0-E_n} - i\pi\sum_n \delta(M_0-E_n)H_W|n><n|H_W \qquad 3.1.2$$

A graphical representation of the second order expansion is given in Fig. 3.1.1a. For reference purposes, Fig. 3.1.1b has the Standard Model expansion of the general intermediate states implied by the box diagram. For future reference, the vertex factors and the exchanged particles are given in that Figure. For the on shell final states, the δ function in Eq. 3.1.2 can be replaced by the density of final states, ρ_n. The transition matrix can then be broken into two parts, the mass matrix and the decay matrix.

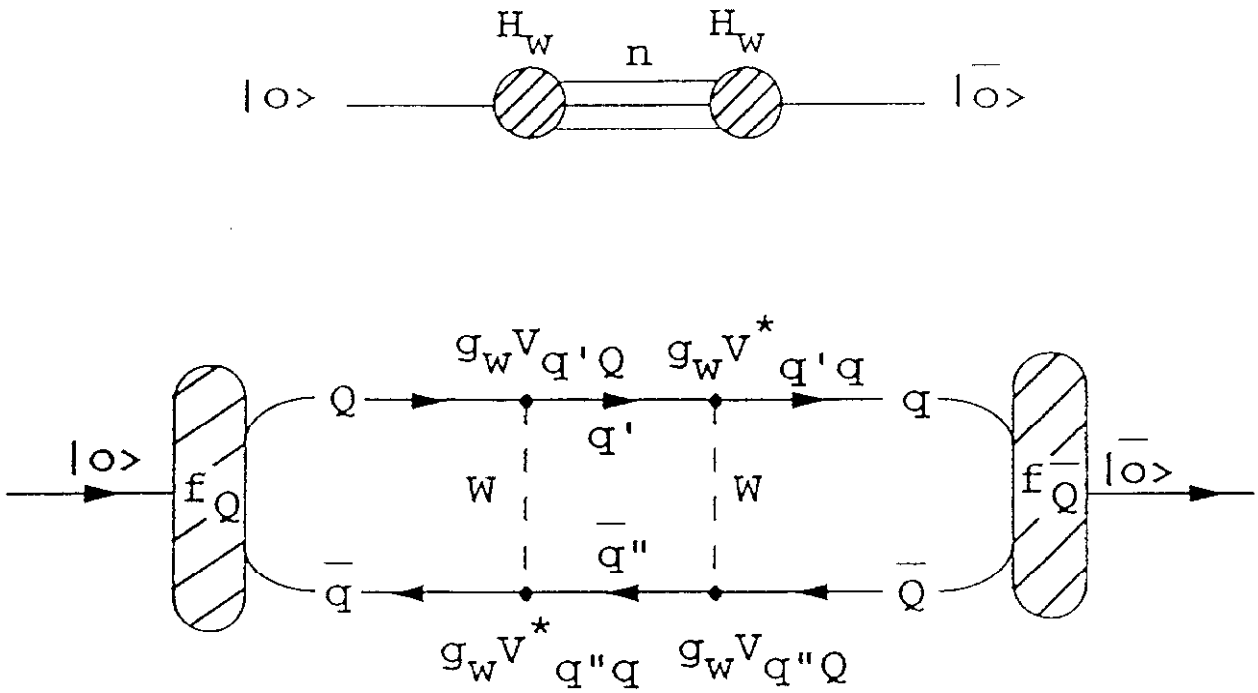

Fig. 3.1.1 Diagrams for $|0> \leftrightarrow |\bar{0}>$ transitions.

a. General second order EW diagram.

b. The "Box Diagram" realization of *a*. with vertex factors shown explicitly.

$$
\begin{aligned}
&T \equiv M - i\Gamma/2 \\
&M = H_W + P\sum_n \frac{H_W|n><n|H_W}{(M_0 - E_n)} \\
&\Gamma = 2\pi\sum_n \rho_n H_W|n><n|H_W
\end{aligned}
\qquad 3.1.3
$$

The mass matrix has terms in first and second order corresponding to virtual transitions between states. The decay matrix has a density of states factor appropriate to on shell decays. Now, in fact, in the perturbation formulas, the transition operator T is the time development operator containing pieces corresponding to level shifts and decays. The definition of the mass and decay matrices is such that the mass matrix corresponds to a phase for the wave function whereas the decay matrix corresponds to a probability density which decays exponentially with time and having a characteristic decay width Γ.

$$
\begin{aligned}
&\partial\psi/\partial t = -iT\psi = -(\Gamma/2 + iM)\psi \\
&|\psi|^2 = e^{-\Gamma t},\ \psi = e^{-(\Gamma/2+iM)t}
\end{aligned}
\qquad 3.1.4
$$

In what follows we'll use as basis states the strong eigenstates, which are assumed to be orthogonal. We'll also assume that the perturbation Hamiltonian obeys CPT invariance which leads to the following relationships:

$$
\begin{aligned}
&|0>, |\overline{0}> \textit{ basis states} \\
&\Gamma_{11} = \Gamma_{22} \equiv \gamma \\
&\Gamma_{12} = \Gamma_{21}^* \\
&M_{11} = M_{22} \equiv M_0 \\
&M_{12} = M_{21}^* \quad .
\end{aligned}
\qquad 3.1.5
$$

Basically, these relationships mean that particle and antiparticle mass and lifetime are the same. That's certainly familiar as a consequence of the CPT theorem. Using as basis states the strong eigenstates, it is straightforward to construct the CP eigenstates of the system. There is a unitary transformation, U_{CP}, which transforms from strong eigenstates to CP eigenstates.

$$
\begin{aligned}
CP|0> &\equiv |\bar{0}> \\
|1>_{CP} &= \frac{1}{\sqrt{2}}\left(|0> + |\bar{0}>\right) \\
|2>_{CP} &= \frac{1}{\sqrt{2}}\left(|0> - |\bar{0}>\right) \\
U_{CP} &= \frac{1}{\sqrt{2}}\begin{pmatrix} 1 & 1 \\ 1 & -1 \end{pmatrix}
\end{aligned}
\qquad 3.1.6
$$

In the strong eigenstate basis, which is a complete set, one can expand any arbitrary wave function. The time development of that wave function in that basis is given below.

$$
\begin{aligned}
\psi &= \begin{pmatrix} |0> \\ |\bar{0}> \end{pmatrix} \\
-\frac{\partial \psi}{\partial t} &= \left[\begin{pmatrix} \gamma & \Gamma_{12} \\ \Gamma_{12}^{*} & \gamma \end{pmatrix}/2 + i\begin{pmatrix} M_0 & M_{12} \\ M_{12}^{*} & M_0 \end{pmatrix}\right]\psi
\end{aligned}
\qquad 3.1.7
$$

Having developed the formulas to this point, it is clear that we now need to solve the eigenvalue problem.

3.2 Eigenvalues and Eigenvectors

In general, the eigenvectors of an operator in quantum mechanics are defined such that the operator operating on the eigenvector returns the eigenvector itself times some number, the eigenvalue. In order for that to be true, the secular equation needs to be satisfied. There are also two invariants in the problem. The trace of the operator (in any representation using a complete set of wave functions) is the sum of the eigenvalues, while the determinant of the operator is the product of the eigenvalues.

$$
\begin{aligned}
O\psi &= \lambda\psi \\
(O - \lambda I)\psi &= 0 \\
|O - \lambda I| &= 0 \\
Tr\,O &= \Sigma\lambda i \\
DET\,O &= \pi\lambda i
\end{aligned}
\qquad 3.2.1
$$

In Eq. 3.2.1, the operator is represented by O, the eigenvector by the wave function ψ, and the eigenvalue by λ. The operator is Hermitian. That requirement assures that the eigenvalues are

real. The eigenvalue equations are a set of linear homogeneous equations. Thus, the secular equation needs to be true if a nontrivial solution exists.

Specializing to the case of the transition matrix and labeling the two eigenvectors and eigenvalues with a subscript j, one finds that the transition matrix eigenvectors propagate diagonally in time with the eigenfrequencies appropriate to the energy eigenvalues.

$$\begin{aligned}(\Gamma/2+iM)\psi_j &= \lambda_j\psi_j \\ \psi_j(t) &= e^{-\lambda_j t}\psi_j(0)\end{aligned} \qquad 3.2.2$$

Note that M and Γ are Hermitian operators but T is not Hermitian because probability is not conserved. Decays exist, and the wave function squared is the probability density which must decay exponentially in time. We will use the fact that the energy eigenvectors evolve diagonally in time when studying the time dependence of a system containing mixtures of the strong eigenstates. The secular equation in the specific case of the transition matrix, written in the strong eigenvector basis, is given below.

$$\begin{vmatrix} A-\lambda_j & p^2 \\ q^2 & A-\lambda_j \end{vmatrix} = 0$$

$$\Gamma/2+iM \equiv \begin{bmatrix} A & p^2 \\ q^2 & A \end{bmatrix} \qquad 3.2.3$$

$$A = \gamma/2+iM_o$$

$$p^2 = \Gamma_{12}/2+iM_{12} \qquad p^2+q^2 = \mathrm{Re}\,\Gamma_{12}+2i\,\mathrm{Re}\,M_{12}$$

$$q^2 = \Gamma_{12}^*/2+iM_{12}^* \qquad p^2-q^2 = i\,\mathrm{Im}\,\Gamma_{12}-2\,\mathrm{Im}\,M_{12}$$

These equations follow from the time development equation given in Eqs. 3.1.7. The solution of the secular equation is straightforward and the eigenvalues are easily determined.

$$\lambda_j = A \pm pq$$

$$\lambda_j = \frac{\gamma}{2} + iM_0 \pm \sqrt{p^2 q^2}$$

$$\lambda_1 - \lambda_2 = 2\sqrt{p^2 q^2}$$

$$\begin{matrix} |1> \\ |2> \end{matrix} = \frac{1}{\sqrt{|p|^2 + |q|^2}} (p|0> \pm q|\bar{0}>) \qquad 3.2.4$$

$$U = \frac{1}{\sqrt{|p|^2 + |q|^2}} \begin{pmatrix} p & q \\ p & -q \end{pmatrix}$$

The eigenvectors in the strong eigenstate basis are given in Eqs. 3.2.4 along with the diagonalizing transformation which goes from the strong eigenstates to the weak eigenstates. Note that the diagonalizing transformation collapses to that appropriate to CP conservation given in Eqs. 3.1.6, if p and q are both real and equal to 1.

$$\begin{aligned} &\text{If } CP, p = q = 1 \\ &\text{Im}\,\Gamma_{12} = \text{Im}\,M_{12} = 0 \\ &(\Gamma_{1,2})_{CP} = \gamma \pm \Gamma_{12} \\ &(M_{1,2})_{CP} = M_o \pm M_{12} \\ &\Delta\Gamma = \Gamma_1 - \Gamma_2 = 2\Gamma_{12} \\ &\Delta M = M_1 - M_2 = 2M_{12} \end{aligned} \qquad 3.2.5$$

Note from Eq. 3.2.3 that in the case where CP is conserved, the imaginary parts of the off diagonal elements of the mass and decay matrix are equal to 0. In that case, the decay rates and masses are such that the difference in decay rates is just the off diagonal element of the decay matrix while the mass difference is, analogously, simply the off diagonal element of the mass matrix. Note, in this case, that the eigenvalues are real for the mass and decay matrices. It is useful to go through the CP conserving case because, as we will see, it is intrinsic to the Standard Model that CP violation is small. Therefore, the approximation that it is vanishing is sometimes quite useful.

3.3 The ε Parameter

If indeed CP violation is a small effect, then p and q are roughly real and equal to 1. One expects that deviations from the values appropriate to CP conservation are small and should be characterized by a small parameter. In the literature, this is the ε parameter which is familiar from

usage in the kaon system. Therefore, let us consider the case where CP violation exists but is in some sense small. In that case Eqs. 3.2.4 for the weak Hamiltonian eigenstates becomes Eqs. 3.3.1.

$$\begin{aligned} |1> \\ |2> \end{aligned} \equiv \frac{1}{\sqrt{1+|\varepsilon|^2}}[(1+\varepsilon)|0> \pm (1-\varepsilon)|\bar{0}>]$$

$$<1|2> = 2\,\mathrm{Re}\,\varepsilon \qquad 3.3.1$$

$$= (|p|^2 - |q|^2)/(|p|^2 + |q|^2)$$

Note that, in this case, the weak eigenstates are not orthogonal whereas in the case of CP conservation they would be. Therefore, it is important to realize that the basis states, the eigenstates, in the presence of CP violation are no longer orthogonal; whereas, by definition, the strong eigenstates are an orthonormal basis set in two dimensions. So far, what we've done involves no approximations. One can now make the approximation that the ε parameter is small.

$$\begin{aligned} \varepsilon &= (p-q)/(p+q) \\ &\sim (p^2 - q^2)/2(\lambda_1 - \lambda_2) \end{aligned} \qquad 3.3.2$$

In that case, there is a simple relationship between the small parameter ε and the imaginary parts of the mass and decay matrices (see Eq. 3.2.3).

$$\varepsilon \sim (i\,\mathrm{Im}\,\Gamma_{12} - 2\,\mathrm{Im}\,M_{12})/2(\lambda_1 - \lambda_2) \qquad 3.3.3$$

We note that CP violation is due to imaginary elements in the mass and decay matrices as we have seen previously. CP violation, therefore, in the weak eigenstates is defined by the ε parameter. Looking at Eqs. 3.3.3, it's clear that the phase of ε depends on the relative size of the mass and decay matrices and on the relative size of the real and imaginary parts of the eigenvalues. We'll see that the answer in the case of the K system is rather different than that for the B system. Using Eqs. 3.3.1 and the defining equations for the eigenvectors, Eq. 3.2.4, one can get an expression for the ratio of q to p in the case where the off diagonal elements of the mass matrix are much larger than the off diagonal elements of the decay matrix.

$$\begin{aligned}\left|\frac{1-\varepsilon}{1+\varepsilon}\right| &= |q/p| \\ &= \left|\sqrt{q^2/p^2}\right| \\ &= \left|\sqrt{\frac{M_{12}^* - i\Gamma_{12}^*/2}{M_{12} - i\Gamma_{12}/2}}\right| \\ &\sim \left|\sqrt{\frac{M_{12}^*}{M_{12}}}\right| \\ &\sim 1\end{aligned} \qquad 3.3.4$$

Note that, in this case, the ratio of q to p is a complex number of modulus one. Looking at Eqs. 3.2.5, one might expect that if the mass matrix elements are larger than the decay matrix elements, then the mass splitting is much larger than the splitting in decay widths. Such a situation might obtain in the case of B mesons where there is lots of phase space available and where different CP eigenstates are typically characterized simply by a pion mass difference. The situation is much different in the kaon system where the CP eigenstates are the two pion and three pion states and the available energy for two pion states is much larger than that available in three pion final states. For example, the sum of the three pion masses is about 0.42 GeV with a kaon parent of only 0.49 GeV. This simple kinematic coincidence is responsible for the fact that the CP eigenstates, K_S and K_L, have decay rates which differ by a factor of 580. In the case of the b quark, one has a system with 5 GeV available which is an order of magnitude larger than the q value available in the kaon system. Hence, one expects that the difference in decay rate between CP odd and even states would be rather small. That being the case, one expects that the mass difference between the CP eigenstates will be much larger than the decay rate difference. This is one of those situations where the K and the B system, although conceptually the same, differ strongly because of the masses and the available q value.

In the case where one neglects the off diagonal decay matrix elements, the ratio q/p is a pure phase and ε, for example, for the b system, is purely imaginary (see Eqs. 3.3.1). If one makes the approximation that Γ_{12} is small with respect to M_{12}, one can expand the q/p ratio and keep the first order term.

$$\begin{aligned} q/p &\sim e^{-i\phi_{12}}\left[1 - \frac{1}{2}\{\mathrm{Im}(\Gamma_{12}/M_{12})\}\right] \\ M_{12} &\equiv |M_{12}| e^{i\phi_{12}}\end{aligned} \qquad 3.3.5$$

Given the next order correction, one can look at ε and see that a consequence of keeping the correction is that ε for the b system picks up a small real part.

$$|q/p| = \left|\frac{1-\varepsilon}{1+\varepsilon}\right| \sim 1 - 2\,\mathrm{Re}\,\varepsilon$$
$$4\,\mathrm{Re}\,\varepsilon \sim [\mathrm{Im}(\Gamma_{12}/M_{12})] \qquad 3.3.6$$

Note again that one needs to be careful. Remember that, for example, for the K system, the phase of ε is 45° and it is in no way a purely imaginary number. That's mirrored in the fact that the mass difference for the kaon system is comparable to the decay rate difference which, as we said, is dramatic for the K_L-K_S system.

3.4 Time Evolution of the States

In this Section, we begin the study of the general time evolution of the two level system in the presence of CP violation. The eigenvalue problem yields eigenvectors and the vacuum eigenstates of the T matrix propagate diagonally and independently. The expression for these eigenstates in terms of the strong eigenstates has been given in Eqs. 3.2.4. The inverse relationship between the eigenstates of the T matrix and the strong eigenstates is given in below.

$$\begin{matrix} |0> \\ |\bar{0}> \end{matrix} = \frac{\sqrt{|p|^2+|q|^2}}{2} \begin{pmatrix} \frac{1}{p} & (|1>+|2>) \\ \frac{1}{q} & (|1>-|2>) \end{pmatrix} \qquad 3.4.1$$

Now suppose, for example, that one produces the state $|0>$ at time, t = 0, 0 in a strong interaction production process. In that case the initial state can be decomposed into weak eigenstates.

$$|\bar{0}(0)> = 0$$
$$|1(0)> = \frac{1}{\sqrt{|p|^2+|p|^2}}(p|0>) \qquad 3.4.2$$
$$|2(0)> = \frac{1}{\sqrt{|p|^2+|p|^2}}(p|0>)$$

By construction we know that the weak eigenstates evolve diagonally, with a time dependence defined by the eigenvectors of the weak Hamiltonian.

$$
\begin{aligned}
|1(t)>&= e^{-\lambda_1 t}|1(0)> \\
|2(t)>&= e^{-\lambda_2 t}|2(0)>
\end{aligned}
\qquad 3.4.3
$$

In order to find the strong eigenstate content of the system at any given time, one uses Eq. 3.4.1.

$$
\begin{aligned}
|0(t)>&= \frac{\sqrt{|p|^2+|q|^2}}{2}\left(\frac{1}{p}\right)(|1(t)>+|2(t)>) \\
|0(t)>&= \frac{1}{2}[e^{-\lambda_1 t}|0>+e^{-\lambda_2 t}|0>] \qquad 3.4.4 \\
|\overline{0}(t)>&= \frac{1}{2}\left[\frac{p}{q}\right][e^{-\lambda_1 t}|0>-e^{-\lambda_2 t}|0>]
\end{aligned}
$$

A schematic representation of the above equations is shown in Fig. 3.4.1 as an aid to visualization. One can follow the path in Fig. 3.4.1 and simply multiply out the indicated factors.

So far, we've not made any drastic approximation. At this point one may specialize to the B system. We will assume that the decay rates of the weak eigenstates are the same so that the difference between decay rates is zero.

$$
\begin{aligned}
&\Delta M \doteq M_1 - M_2, \Delta\Gamma \equiv 0, \Gamma_1 = \Gamma_2 = \Gamma \\
&2M \doteq M_1 + M_2 \sim 2M_0 \\
&|0(t)>= e^{-\left(\frac{\Gamma}{2}+iM\right)t}\cos(\Delta M t/2)|0> \qquad 3.4.5 \\
&|0(t)>= e^{-\left(\frac{\Gamma}{2}+iM\right)t}\left(\frac{p}{q}\right)i\sin(\Delta M t/2)|0>
\end{aligned}
$$

One can easily go through exactly the same exercise for the situation where one has a state $|\overline{0}>$ made at time t = 0 and by this proceed to the general case.

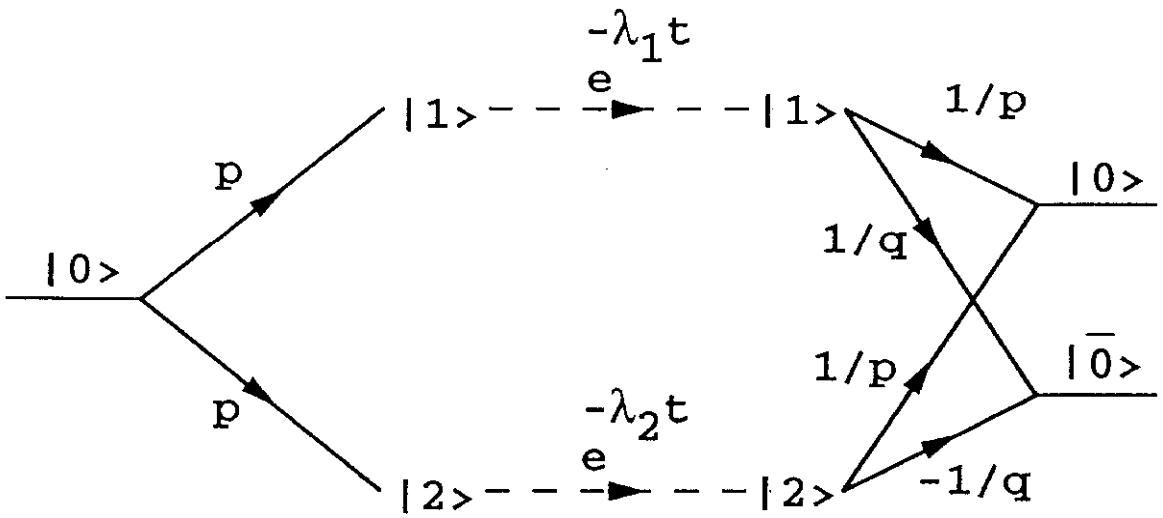

Fig. 3.4.1 Schematic representation of the decomposition of a state, $|0>$, produced at $t = 0$. The state propagates in time as states $|1>$ and $|2>$ and a second decomposition into states $|0>$ and $|\bar{0}>$ at time t is then made.

$$
\begin{aligned}
|0(t)> &= f_+(t)|0> + \left(\frac{q}{p}\right) f_-(t)\left|\overline{0}\right> \\
\left|\overline{0}(t)\right> &= \left(\frac{p}{q}\right) f_-(t)\,|0> + f_+(t)\left|\overline{0}\right> \\
f_+(t) &= e^{-\left(\frac{\Gamma}{2}+iM\right)t}\cos(\Delta M t/2) \\
f_-(t) &= ie^{-\left(\frac{\Gamma}{2}+iM\right)t}\sin(\Delta M t/2)
\end{aligned}
\qquad 3.4.6
$$

Therefore, it is clear that a general property is that the $|0>$ and $\left|\overline{0}\right>$ content of any state oscillates in time due to the fact that the weak eigenstates contain different mixtures of the strong eigenstates $|0>$ and $\left|\overline{0}\right>$. This situation is very analogous to the situation of having linearly and circularly polarized light, decomposing an initially linearly polarized state into circularly polarized states which propagate and therefore mix, and studying the linear polarizations as a function of time. Using the simplest example of the state which is purely $|0>$ at t = 0, one can square the wave functions given in Eqs. 3.4.5 and get an expression for the probability, as a function of time, to observe the state $|0>$ and the state $\left|\overline{0}\right>$ having produced a pure $|0>$ state at t = 0.

$$
\begin{aligned}
\Gamma(t) &= e^{-\Gamma t}(1+\cos\Delta M t)/2 \\
\overline{\Gamma}(t) &= e^{-\Gamma t}\left|\frac{p}{q}\right|^2(1-\cos\Delta M t)/2 \\
\Gamma(t)+\overline{\Gamma}(t) &= e^{-\Gamma t}
\end{aligned}
\qquad 3.4.7
$$

Note that the sum of the probabilities displays a simple exponential decay as might be expected. The probability to see a $\left|\overline{0}\right>$ state as a function of time vanishes at t = 0, builds up and exhibits oscillatory behavior. In contrast, the $|0>$ state has a probability 1 at t = 0, but decays, in time, and exhibits oscillatory behavior. In particular, at characteristic values of the time, there exist zeroes in the probability. Note that the scale for the time is defined by the competition between decay and oscillation. Therefore, in order to simply observe this oscillation of the $|0>$ and $\left|\overline{0}\right>$ states, one needs a mass difference which is comparable to the decay rate, $\Delta M/\Gamma \sim 1$.

The probabilities given in Eqs. 3.4.7 are graphically displayed in Figs. 3.4.2 and 3.4.3. In Fig. 3.4.2, one sees the behavior of the probability to find state $|0>$ as a function of time having produced a state $|0>$ at t = 0. Obviously, that probability has a limit that it be one at t = 0. What is plotted are curves for different values of the characteristic parameter $\frac{\Delta M}{\Gamma}$. One can see that

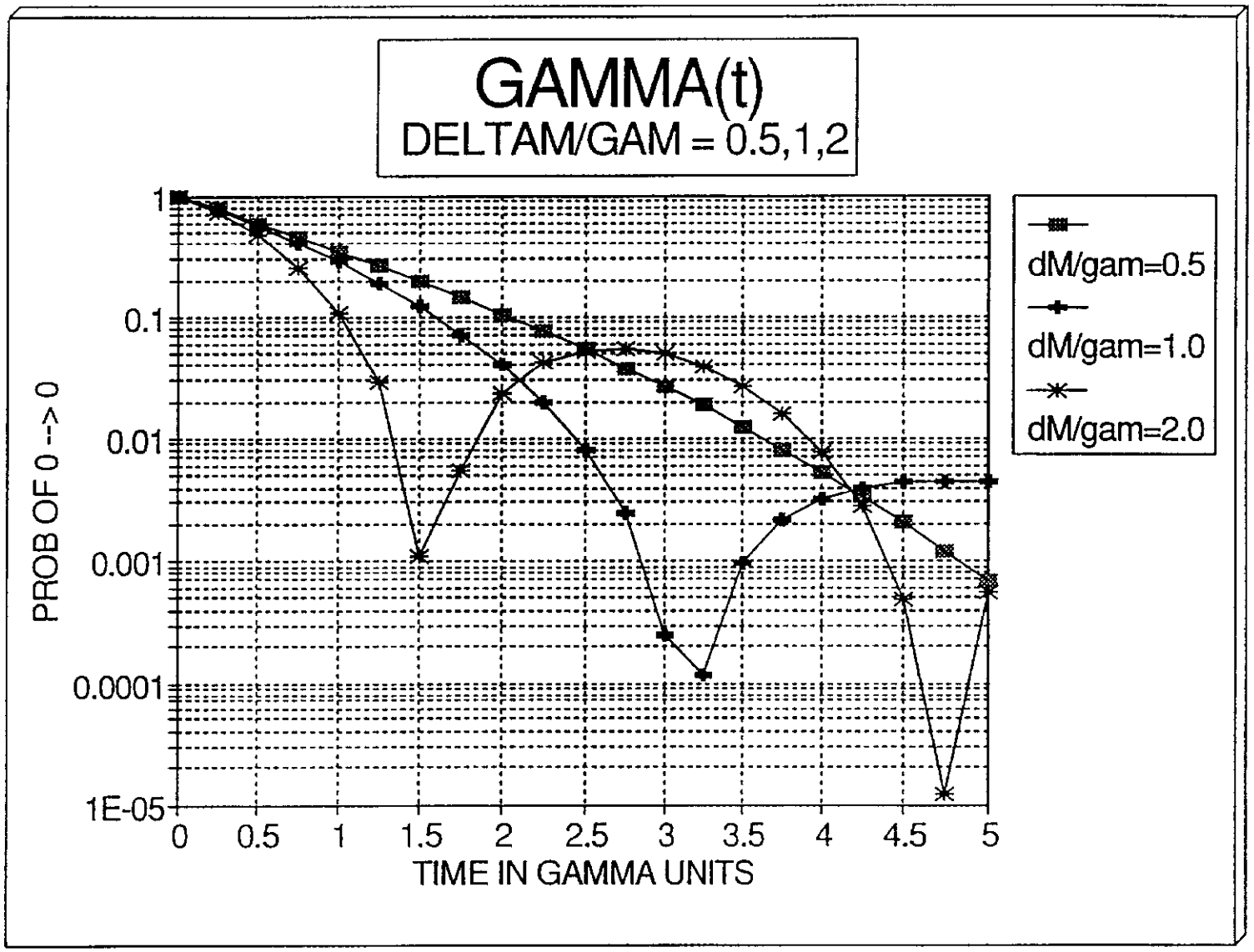

Fig. 3.4.2 $\Gamma(t) \equiv \Gamma[0(t)]$ as a function of time for $\Delta M / \Gamma = 0.5, 1.0, 2.0$.

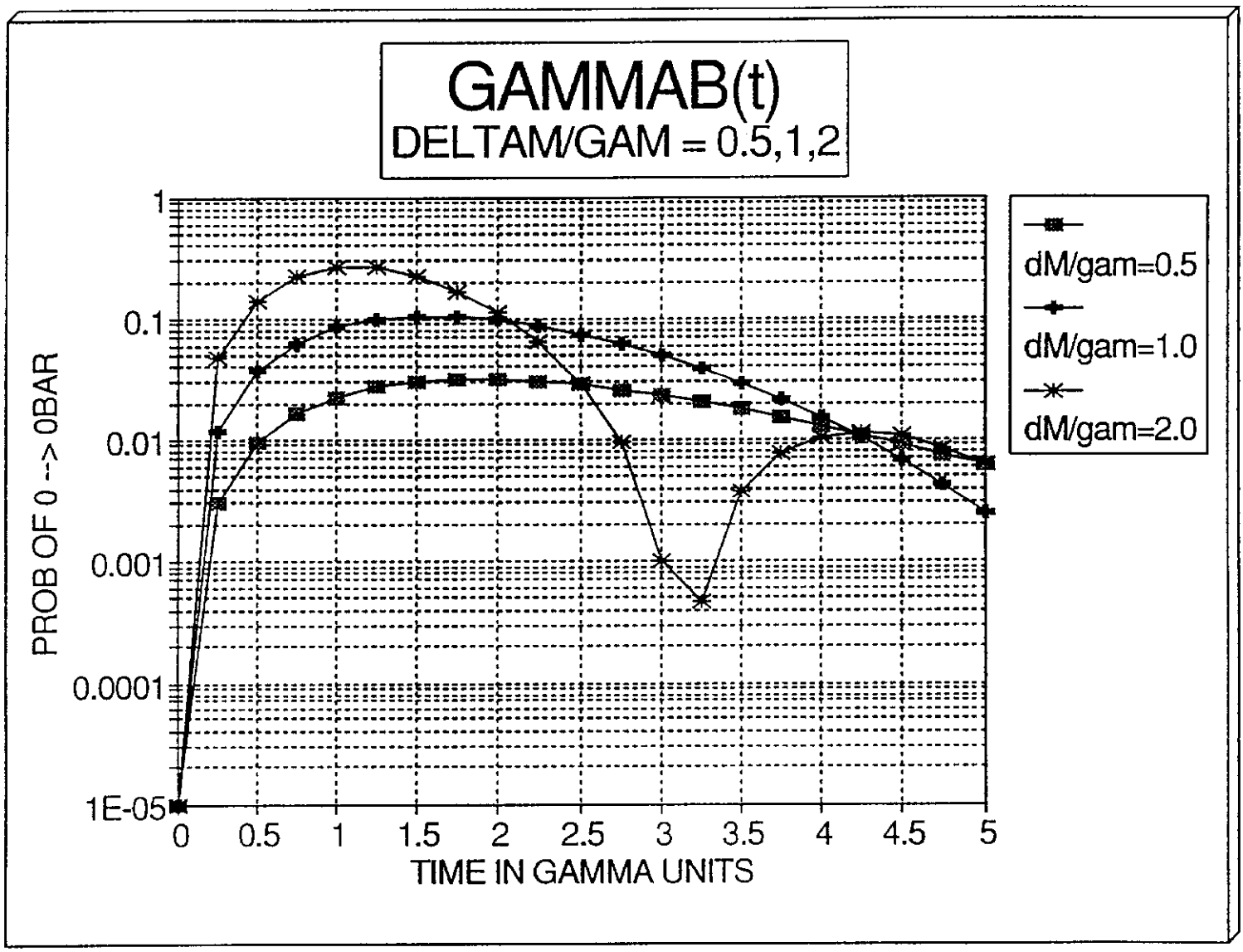

Fig. 3.4.3 $\overline{\Gamma}(t) \equiv \Gamma\left[\bar{0}(t)\right]$ as a function of time for $\Delta M / \Gamma = 0.5, 1.0, 2.0$.

there are changes in the location of the oscillatory zero which occur around the overall exponential decay. For comparison in Fig. 3.4.3, one sees the probability for observing the state $|\bar{0}>$ having produced the state $|0>$ at t = 0. Again, the obvious boundary condition is that this probability vanishes at t = 0. Looking at Fig. 3.4.3, it is clear that the probability rises and then exhibits oscillatory behavior around a decaying exponential. Again, curves for the values of $\frac{\Delta M}{\Gamma}$ of 0.5, 1.0 and 2.0 are shown.

We've gone fairly hurriedly over this Section on the time development of the states. The assumption is that the very similar analysis of K_S and K_L in terms of K^0 and $\overline{K^0}$ is well known to practitioners of particle physics. The major difference, as we said before, is that in the K system the CP eigenstates have large decay width differences. In this Section, by comparison, what has been assumed is that the decay rate differences are small on the scale of the mass differences of the CP eigenstates.

3.5 CP Violation Asymmetry

Having looked at the time development of the states, we are now in a position to advance to looking at the temporal characteristics of CP violating asymmetries. In this Section, we will proceed entirely phenomenologically with no particular guidance as to possible magnitudes or sources of the CP violation. If CP is conserved, then the partial decay rate of a state $|0>$ into final state $|f>$ is equal to the decay rate of the state $|\bar{0}>$ into the conjugate final state $|\bar{f}>$. Therefore, CP violation would be measured by a difference in those decay rates. This argument leads us to a definition of a time dependent asymmetry indicating CP violation.

$$A(t) \equiv \frac{\left\{\Gamma[0(t) \to f] - \Gamma[\bar{0}(t) \to \bar{f}]\right\}}{\left\{\Gamma[0(t) \to f] + \Gamma[\bar{0}(t) \to \bar{f}]\right\}} \qquad 3.5.1$$

Now if both $|f>$ and $|\bar{f}>$ final states can be reached by $|0>$ and $|\bar{0}>$ and if $|f>$ and $|\bar{f}>$ are CP eigenstates, then there is a common final state. The mixing which we have already discussed implies an interference in the final states and, therefore, a CP violating asymmetry. Using Eqs. 3.4.6 for the amplitude of state $|0>$ as a function of time and state $|\bar{0}>$ as a function of time, one can sandwich those with final states $|f>$. The amplitude for the partial decay rate of the state $|0>$, decaying to state $|f>$ as a function of time, is then;

$$< f|0(t) > \equiv e^{-\left(\frac{\Gamma}{2}+iM\right)t}\left[< f|0 > \left(\cos\frac{\Delta Mt}{2}\right)+\frac{q}{p}< f|\bar{0} > i\left(\sin\frac{\Delta Mt}{2}\right)\right]$$

$$\Gamma[0(t)\to f] = e^{-\Gamma t}\,|< f|0 >|^2 \left\{ \begin{array}{l} \cos^2\left(\frac{\Delta \mathrm{M}t}{2}\right)+\left|\frac{q}{p}\frac{< f|\bar{0} >}{< f|0 >}\right|^2 \sin^2\left(\frac{\Delta \mathrm{M}t}{2}\right) \\ -2\,\mathrm{Im}\left(\frac{q}{p}\frac{< f|\bar{0} >}{< f|0 >}\right)\cos\left(\frac{\Delta \mathrm{M}t}{2}\right)\sin\left(\frac{\Delta \mathrm{M}t}{2}\right) \end{array} \right\} \qquad 3.5.2$$

If only one amplitude contributes to the transition, then overall CPT conservation implies the following.

$$\begin{aligned} |< f|0 >| &= |< \bar{f}|\bar{0} >| \\ |< \bar{f}|0 >| &= |< f|\bar{0} >| \end{aligned} \qquad 3.5.3$$

In addition, if the final states themselves are CP eigenstates, then there is a relationship between the transitions to the $|f>$ and $|\bar{f}>$ final states.

$$\begin{aligned} CP|f> &\equiv \pm|\bar{f}> \\ < f|\bar{0} > &= \pm < \bar{f}|\bar{0} > \end{aligned} \qquad 3.5.4$$

Now recall from Section 3.3, in particular Eqs. 3.3.4, that the ratio q/p is a complex number of modulus one for the case of the B system (by assumption). In that case, the following quantity is also a complex number of modulus one.

$$\begin{aligned} \left|\frac{q}{p}\frac{< f|\bar{0} >}{< f|0 >}\right| &= \left|\frac{q}{p}\right|\left|\frac{< f|\bar{0} >}{< f|0 >}\right| = \left|\frac{< f|\bar{0} >}{< f|0 >}\right| \\ &= \frac{|< f|\bar{0} >|}{|< f|0 >|} \\ &= \frac{|< \bar{f}|0>|}{|< f|0 >|} \\ &= 1 \end{aligned} \qquad 3.5.5$$

In this particularly simple limiting case, Eqs. 3.5.2 collapse into a rather simple form.

$$\Gamma[0(t) \to f] = e^{-\Gamma t} |< f|0 >|^2 \left[1 - \mathrm{Im}\left(\frac{q}{p} \frac{< f|\bar{0} >}{< f|0 >} \right) \sin(\Delta M t) \right]$$

$$A(t) = -\mathrm{Im}\left(\frac{q}{p} \frac{< f|\bar{0} >}{< f|0 >} \right) \sin(\Delta M t) \qquad 3.5.6$$

$$\alpha \equiv \left(\frac{q}{p} \frac{< f|\bar{0} >}{< f|0 >} \right)$$

$$\Gamma[0(t) \to f] = e^{-\Gamma t} |< f|0 >|^2 [1 - \mathrm{Im}\, \alpha \sin(\Delta M t)]$$

The asymmetry then has a simple time dependence, with an amplitude defined by the imaginary part of the ratio of decay amplitudes. This simple form again indicates that the existence of imaginary amplitudes drives the CP asymmetry. The situation for decays to CP eigenstates is that the CP violating parameter seen in the asymmetry as a function of time is a pure phase. It has two sources, the mixing, which is indicated in the q to p ratio from the mass matrix, and the decays, indicated in the ratio $< f|\bar{0} > / < f|0 >$ in the decay amplitudes.

A plot of a possible asymmetry is shown in Fig. 3.5.1, which shows the difference in decay rates for the state $|0>$ to final state $|f>$ and state $|\bar{0}>$ to final state $|\bar{f}>$ as a function of time. The plot assumes that the imaginary part of the amplitude is 20% and that the mass difference is 0.5, 1.0, or 2.0 times the common decay rate Γ. Obviously, the maximum modulation of the decaying exponential occurs when the sine goes through 90°. The asymmetry at those angles becomes maximal. Clearly, the asymmetry oscillates sinusoidally with time and has a 0 when ΔMt is equal to 0 or π. This means, of course, that if one made such a measurement, it would allow one to extract the modulus of that asymmetry. Since this is an imaginary amplitude, it obviously gives us a measurement of a CP violating parameter.

In the next Section, we will discuss our expectations for the magnitudes of potential CP violating parameters. Suffice it to say that in exclusive final states in B decays, the CP asymmetry can reach large values (tens of percent). In particular, the decay that was discussed in Section 2, $B_d \to \Psi K_S$ is topologically accessible to both B_d and $\overline{B}_d$. Thus, one has a CP eigenstate for the final state which is accessible to both B_d and $\overline{B}_d$. Therefore, one can potentially generate a CP violating asymmetry. In fact, the estimated asymmetry is at the 20% level.

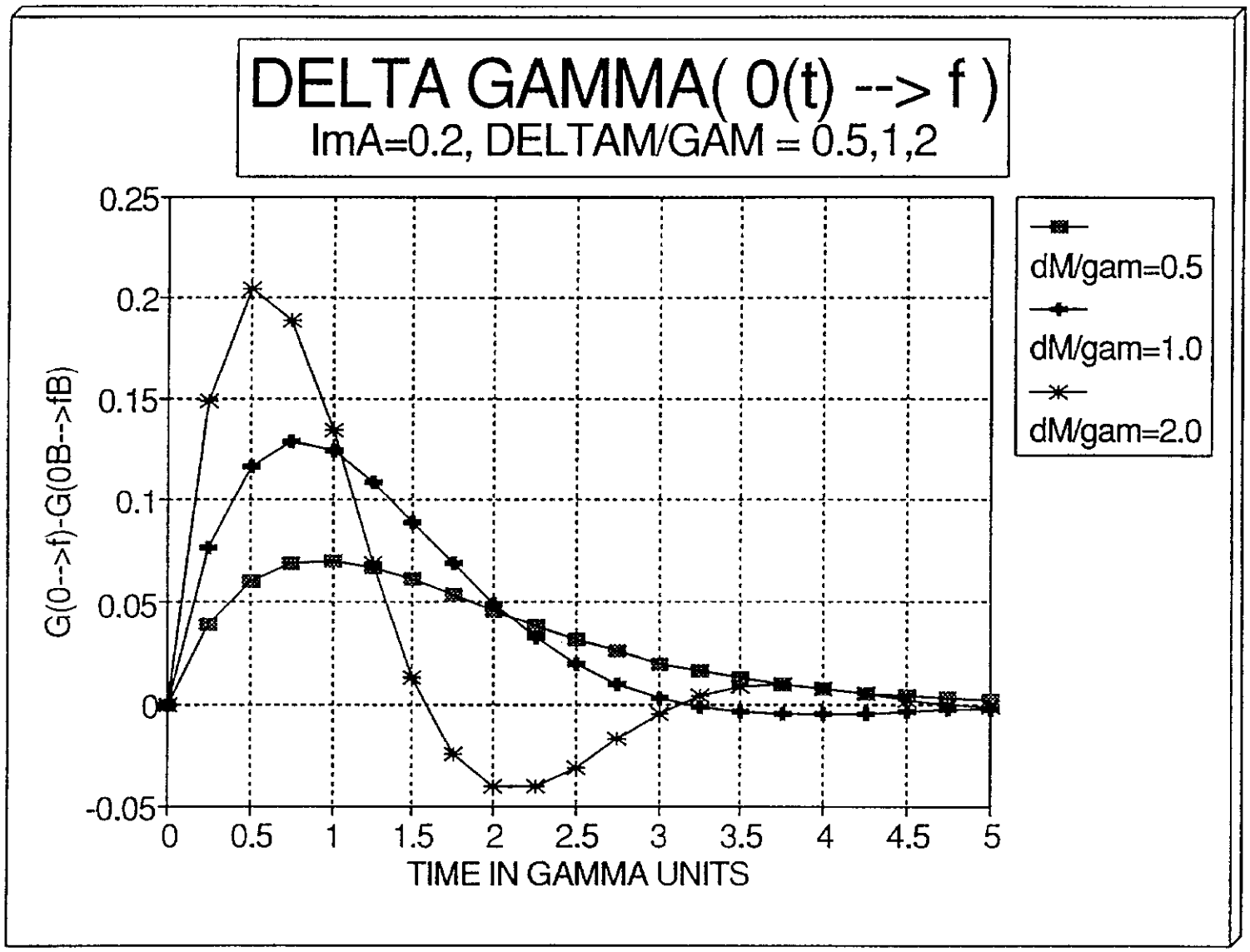

Fig. 3.5.1 Decay rate difference, $\Gamma[0(t) \to f] - \Gamma[\bar{0}(t) \to \bar{f}]$ as a function of Γt for $\Delta M / \Gamma$ = 0.5, 1.0, and 2.0. Imα is 0.2.

4. CP VIOLATION AND MIXING

In this Section we attempt to go beyond the purely phenomenological description of CP violation in the B system and connect asymmetry parameters and the like to more fundamental quantities such as CKM matrix elements.

4.1 Time Evolution and CKM Phases

For now, in this Section, let us assume that the off diagonal elements of the mass matrix which are responsible for mixing the $|0>$ and $|\overline{0}>$ states are driven by the box diagrams which have been shown in Fig. 3.1.1b. Let us further assume, and we will establish this later, that the heaviest quark in the internal box loop is the one which dominates the amplitude. Let us also use the approximate values of the CKM matrix given in Eqs. 1.4.2. In explaining or predicting the results of a CP violating asymmetry experiment, what we are interested in is the phase of various mass and decay matrix elements. It will be sufficient to use the assumptions just given to read off the phase of the mass matrix elements.

$$M_{12} \sim \left(V_{tb}V_{tq}^{*}\right)^{2}$$
$$\frac{q}{p} \sim \sqrt{\frac{M_{12}^{*}}{M_{12}}} \qquad 4.1.1$$

Recall that the M_{12} element is that matrix element which, in the strong eigenstate basis, connects the $|0>$ and $|\overline{0}>$ states. Therefore, it is effectively a $\Delta B = 2$ transition. Since those do not occur in the Standard Model to lowest order, we require two transitions. The simplest diagram that is possible is just the box diagram which has been given in Fig. 3.1.1. Given the CKM parameters described before and written down, one can trivially read the q/p ratio for the two neutral B mesons, the B_d and the B_s.

$$\left(\frac{q}{p}\right)_{Bd} = \frac{V_{td}}{V_{td}^{*}} = e^{2i\phi td}$$
$$\left(\frac{q}{p}\right)_{Bs} = \frac{V_{ts}}{V_{ts}^{*}} = 1 \qquad 4.1.2$$

Clearly, the B_d has a phase given by the td element of the CKM matrix while the B_s has a q/p parameter given by the ts element of the CKM matrix. Since that latter element is real, q/p for

the B_S is a real number. We said before, in the discussion of ε for the B system, that q/p for B_d is a complex number of modulus one. Comparing with Eqs. 3.3.6, it is clear that Eqs. 4.1.2 are consistent with the expectation that ε is purely imaginary parameter for the B system.

What about the phase for the final states? The transition is b goes to q + virtual W which is determined by the vertex factor V_{bq}. This vertex factor can also be read off our representation of the CKM matrix. For b to c transitions this parameter is one, whereas for b to u transitions, it is a complex number of modulus one.

$$\begin{aligned} \frac{<f|\bar{0}>}{<f|0>} &= V_{bq}^{*} / V_{bq} \\ &= 1, b \to c \\ &= e^{2i\delta}, b \to u, \phi_{bu} = -\delta \end{aligned} \qquad 4.1.3$$

Therefore, from our previous discussion of asymmetries, it is clear that the experimental measurement of an asymmetry is, in fact, a direct measurement of the phase of a CKM matrix element which is a more fundamental quantity.

4.2 The "Unitary Triangle"

One recalls from Section 1 that the CKM matrix was constructed to be a unitary matrix so as to have a universal strength electroweak interaction and to suppress FCNC. Let us first define unitarity for the CKM matrix.

$$\begin{aligned} V^{-1} &\equiv V^{+} \\ VV^{-1} &= 1 = VV^{+} = V^{+}V \end{aligned} \qquad 4.2.1$$

A unitarity matrix is one whose inverse is its Hermitian adjoint. One can write the unitarity relations down in matrix form for any given representation. In particular, the representation of V in the strong eigenstate basis for rows and columns was done in Section 1, and is conventional.

$$\begin{aligned} \sum_k V_{k\mu}^{*} V_{k\nu} &= \delta_{\mu\nu} \\ V_{ud}^{*} V_{ub} + V_{cd}^{*} V_{cb} + V_{td}^{*} V_{tb} &= 0 \\ V_{ub} - \theta(\theta^2) + V_{td}^{*} &= 0 \end{aligned} \qquad 4.2.2$$

In Eq. 4.2.2, a special case of the unitarity condition was explicitly written out using two columns, b and d. The numerical result of that special case of the unitarity condition can be read

off using our representation of the CKM matrix given in Eq. 1.4.2. This particular choice was made because, in the Standard Model, one has only one complex phase, δ. The matrix elements V_{ub} and V_{td} are the only ones which have significant imaginary parts. Written out explicitly, one sees that there is a "unitary triangle" in the sense that one has three vectors which form a closed triangle of non-zero area.

$$\begin{aligned} V_{ub} + V_{td}^{*} &= \theta^3 \\ |V_{ub}|e^{-i\delta} + |V_{td}|e^{-i\phi_{td}} &= \theta^3 \end{aligned} \qquad 4.2.3$$

This closed vector triangle in shown in Fig. 4.2.1. Also indicated in Fig. 4.2.1 are experimetal ways in which one might measure the matrix elements. For example, b semileptonic decays give information about V_{qb} as we discussed in Section 2. The box diagram for $B-\overline{B}$ mixing, with the assumed dominance of the heaviest quark in the internal loop, means that $B-\overline{B}$ mixing informs on the V_{td} matrix element. This assertion will be discussed in great detail in Section 5.

As discussed in Section 4.1, and in Section 3, a measurement of a CP violating parameter is directly related, in the Standard Model, to the CKM matrix elements. For example, one can imagine a "complete" set of measurements of decay asymmetries for B_d where the transition is b goes to c and B_S where the transition is also b to c. Rare decay asymmetry measurements of B_d and B_S would have the underlying spectator transition b goes to u. Reading off from Eqs. 4.1.2 and 4.1.3 one can simply find, by inspection, the phase of the CP violating asymmetry parameter in the four decays of interest.

$$\begin{aligned} &B_d(b \to c),\ 2\phi_{td} \\ &B_s(b \to c),\ 0 \\ &B_d(b \to u),\ 2(\phi_{td} + \delta) \\ &B_s(b \to u),\ 2\delta \end{aligned} \qquad 4.2.4$$

For B_d decays one has a complex phase, whereas for allowed B_S decays, since the direct CKM matrix elements are not complex, one has no asymmetry. In any case, this complete set of four measurements depends on only two parameters, the phase of V_{td} and the phase of V_{bu}, defined to be δ. The magnitudes of V_{td} and V_{bu} are assumed to be separately determined by mixing and measuring rare decays respectively. Therefore, one can expect that if one could perform such a set of measurements, one would both specify the two elements of the CKM matrix and go beyond that and put constraints on the "unitary triangle." This test is intrinsic to the Standard Model assumptions as to the structure of the CKM matrix.

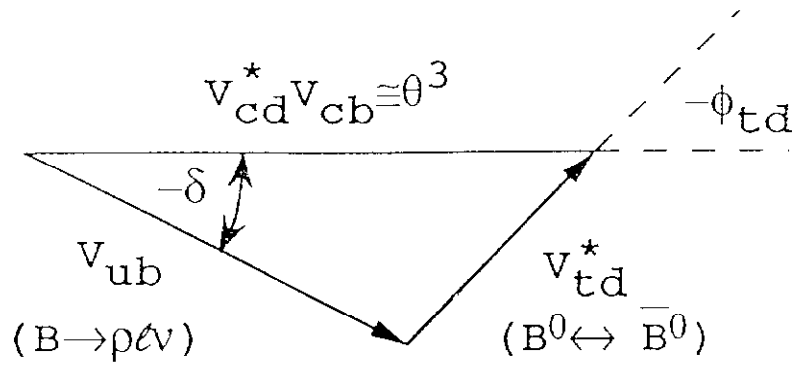

$$V_{ub}+V_{td}^{*} = -V_{cd}^{*}V_{cb} \sim \theta^3$$

Fig. 4.2.1 The "unitary triangle" relationship between V_{ub}, V_{td}^{*}, and $V_{cd}^{*}V_{cb}$.

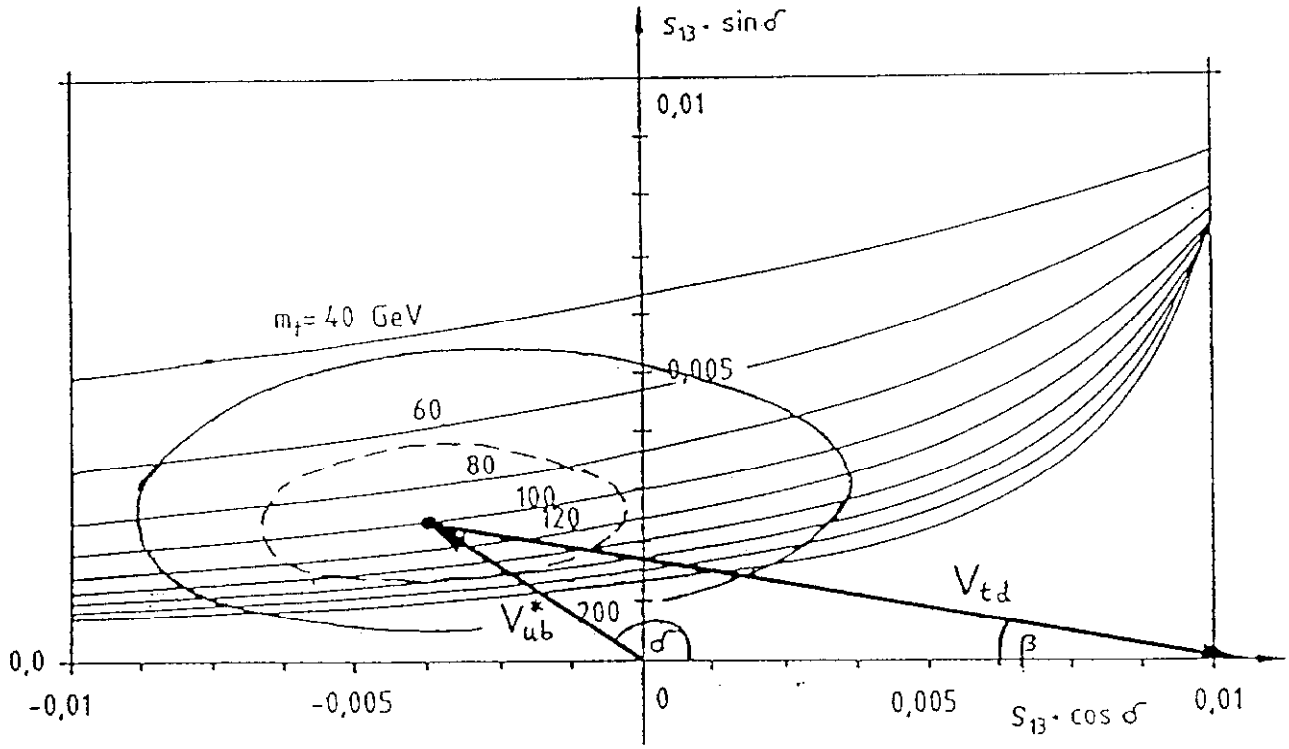

Fig. 4.2.2 Allowed topology of the "unitary triangle" as constrained by a variety of experimental data.

The allowed region of the "unitary triangle" is shown in Fig. 4.2.2. As we will discuss in Section 5, the input data, which constrains the allowed region of the CKM matrix elements, has to do with rare B decays which pin down the modulus of V_{bu}, and $B-\overline{B}$ mixing, which constrains the modulus of V_{td}. In addition, the ε parameter in the K^0 system is sensitive to the mass of the top quark and V_{td}.

As an example of conceptual experiments to measure elements in the "unitary triangle," consider the decay B_d goes to ψ Ks. The mass matrix contribution to the phase in the q/p ratio we've already seen is twice the phase of V_{td} whereas the allowed decay amplitude has no phase attached to it. Therefore, the asymmetry parameter has an imaginary part which is the product of those two factors, which is just 2 ϕ_{td}.

$$A_{B_d \to \Psi Ks}^{(t)} \sim \sin(2\phi_{td})\sin(\Delta M t) \qquad 4.2.5$$

One recalls that the expected CP asymmetry was asserted to be large, of the order of 10%. One can see from Fig. 4.2.2 that, indeed, the most likely value of the angle ϕ_{td} is of order 20°, which is the origin of the assertion that one can expect a large effect. Note that in the case of B_S, one needs a rare decay since the allowed decays for B_S have a phase of zero which means the CP asymmetry will be zero. However, that is not to say that measuring the phase of an allowed B_S decay asymmetry would not be useful. The measurement is in itself a constraint on the Standard Model. Therefore, observation of a non-zero asymmetry in a CKM favored B_S decay would be an indication of physics beyond the Standard Model.

4.3 K Decays and η

Let us briefly look at the time development of states in the case of the kaon system. There are characteristic differences between formulae for that system and the formulae we have already developed for the B system. It is certainly worth making this bypass because, in fact, the kaon system is the only one for which a CP violating effect has yet been measured. Recall that the CP eigenvalue for the 2π state is the negative of the CP eigenvalue for the 3π state. Given the low q value for kaon decays into 3 pions, this means that the lifetime difference between the CP eigenstates in the kaon system is very large. In fact, it is of order 580.

Suppose one makes a kaon in the state $|0>$ at $t = 0$. That state can then be decomposed into the CP eigenstates which we will again call $|1>$ and $|2>$. Those CP eigenstates evolve in time independently and orthogonally.

$$\Gamma_1 >> \Gamma_2$$
$$|0(t)> \sim \frac{1}{\sqrt{2}}\left[e^{-\lambda_1 t}|1(0)> + e^{-\lambda_2 t}|2(0)>\right] \qquad 4.3.1$$

Now consider a final state $|f>$. The probability amplitude for that final state as a function of time has oscillatory behavior.

$$< f|0(t)> \sim \frac{< f|1(0)>}{\sqrt{2}}\left[e^{-\lambda_1 t} + \eta e^{-\lambda_2 t}\right]$$
$$\eta \equiv \frac{< f|2>}{< f|1>} \qquad 4.3.2$$

One can then square the amplitude and find the decay rate as a function of time for the appearance of the final state $|f>$ having produced the state $|0>$ at t = 0.

$$\Gamma(t) \sim \frac{|< f|1(0)>|^2}{2}\left[e^{-\Gamma_1 t} + |\eta|^2 e^{-\Gamma_2 t} + 2|\eta| e^{-\frac{(\Gamma_1+\Gamma_2)t}{2}} \cos(\Delta M t + \phi)\right] \qquad 4.3.3$$
$$\eta \equiv |\eta| e^{i\phi}$$

In a very similar fashion one can find the rate for the appearance of the final state $|f>$ having produced the state $|\overline{0}>$ and t = 0 . One can then define a CP violating asymmetry between the appearance of the final state $|f>$ at time t for initial states prepared as $|0>$ and $|\overline{0}>$ at t = 0.

$$\frac{\Gamma(t) - \overline{\Gamma}(t)}{\Gamma(t) + \overline{\Gamma}(t)} \sim 2|\eta| e^{\Gamma_1 t/2}[\cos(\Delta M t + \phi)] \qquad 4.3.4$$

Clearly, the existence of this asymmetry depends on the parameter η being non-zero. Therefore η is a CP violating parameter. Given the definition of η in Eqs. 4.3.2, and the decomposition of the weak eigenstates in terms of the strong eigenstates, one can find an expression for η in terms of the q and p parameters and the amplitudes into the final state as we did previously for the B system.

$$\eta \sim \frac{< f|(p|0> - q|\bar{0}>)/\sqrt{2}}{< f|(p|0> + q|\bar{0}>)/\sqrt{2}}$$
$$\sim \frac{1 - q/p < f|\bar{0}> / < f|0>}{1 + q/p < f|\bar{0}> / < f|0>} \qquad 4.3.5$$
$$\eta \sim (p-q)/(p+q) = \varepsilon$$

At present, the data on CP violation in the kaon systems tells us that the magnitude of η is roughly 2 x 10^{-3}. If there were no CP violation in the final states, then all of the CP violation would be in the q/p ratio. In that case, it is easy to see that the η parameter is in fact the ε parameter which we defined previously. The current data on $K_L \to \pi^+\pi^-$ and $\pi^0\pi^0$ tells us that the modulus of η for decays into $\pi^+\pi^-$ is 2.3 x 10^{-3} and the phase of η for charged decays is 46°. For the $\pi^0\pi^0$ decays, the modulus is also 2.3 x 10^{-3} and the phase is 48°.

Within experimental errors the η parameters and the ε parameter are equal. The possible effects of CP violation in the final states are contained in the ε' parameter. The ratio of ε' to ε is presently measured to be no larger than something like 2 x 10^{-3}. Later we will discuss the ε and ε' parameters for the kaon system when we attempt to calculate them roughly using the Standard Model box diagram.

4.4 Time Integrated Information

In this Section, we will discuss the information which can be extracted using only measurements gained by integrating over all possible decay times. This is important experimentally because, given the lifetime of the B which we said is some hundreds of microns, it is difficult to construct a detector of sufficient resolution to accurately tag the decay time of the heavy flavors. Therefore, we expect that the experimental situation is such that if one can extract useful information in a time integrated fashion, it would be easier to do than to be forced to measure the decay time on an event by event basis for individual B decays.

4.4.1 Lepton Pairs

Consider the situation where one prepares a state of $|0>$ at t = 0 or a state of $|\bar{0}>$ at t = 0 and lets that state evolve. At the moment of decay let us assume that the state $|0>$ can be tagged by a lepton of one charge, whereas the state $|\bar{0}>$ can be tagged by the lepton of opposite charge. An obvious example of tagging is b goes to c transitions of B mesons. The B is tagged by a μ^- and the $\bar{B}$ is tagged by a μ^+. The time development of the states is given in Eqs. 3.4.6.

Consider the production of the state $|0>$ at t = 0 which evolves in time and is tagged at time t to be in a state $|0>$ also. The time integral of that condition gives you the integrated probability that the produced state $|0>$ decays into a state $|0>$ at any time.

$$\Gamma(0 \to 0 \to \ell^-) \equiv \int \Gamma\left[0(0) \to 0(t) \to \ell^- X\right] dt$$
$$P_{0/0} = \int_0^\infty e^{-\Gamma t} \cos^2(\Delta M t / 2) dt \qquad 4.4.1.1$$

The notation $P_{a/b}$ defines the probability for a state a produced at t = 0 to appear as the state b at some unmeasured later time t which is integrated over. As we said before, there is a competition between oscillation and decay. The parameter which measures that competition is x, which is defined to be the ratio of the mass difference to the decay width. One can use our previous expression for the time development of the states and integrate over all times. There are four possibilities. One produces the state $|0>$ which decays into $|0>$, or which decays into a state $|\bar{0}>$ or one makes a state $|\bar{0}>$ at t = 0 which decays into state $|0>$, or which decays into state $|0>$.

$$x \equiv \Delta M / \Gamma$$
$$P_{0/0} = (1 + x^2/2)/(1 + x^2)$$
$$P_{0/\bar{0}} = \left|\frac{p}{q}\right|^2 (x^2/2)/(1 + x^2) \qquad 4.4.1.2$$
$$P_{\bar{0}/\bar{0}} = P_{0/0}$$
$$P_{\bar{0}/0} = \left|\frac{q}{p}\right|^2 (x^2/2)/(1 + x^2) \sim P_{0/\bar{0}}$$

Some limits that one can think about are when x becomes very large (which means one oscillates before decaying) or the limit when x goes to 0 (which means you decay immediately before you have a chance to oscillate). In the case that x is large, the oscillation completely mixes the identity of the state, which means that the probabilities all go to one half. In the limit where x is very small, we have no mixing. That means the diagonally probabilities Po/o and $P\bar{o}/\bar{o}$ go to one, while the off diagonal probabilities $Po/\bar{o}$ and $P\bar{o}/o$ go to zero. Note that probability is conserved in that $Po/o + Po/\bar{o}$ sums to one. Similarly, the sum of the probabilities for an initial $|\bar{0}>$ state are also one, $P_{\bar{o}/\bar{o}} + P_{\bar{o}/o} = 1$.

In the literature one occasionally finds the parameter r, which is defined to be the ratio of decay rates for the observation of mixing to the observation without mixing. The ratio is just the ratio of the off diagonal probabilities to the diagonal probability.

$$\begin{aligned} r &\equiv \Gamma(0 \to \ell^+) / \Gamma(0 \to \ell^-) \\ &= P_{0/\bar{0}} / P_{0/0} \\ \bar{r} &= P_{\bar{0}/0} / P_{\bar{0}/\bar{0}} \end{aligned} \qquad 4.4.1.3$$

The relationship between x and the r and $\bar{r}$ parameters follows from Eqs. 4.4.1.2.

$$\begin{aligned} r &= \left|\frac{p}{q}\right|^2 (x^2)/(2+x^2), 0 \le r \le 1 \\ \bar{r} &= \left|\frac{q}{p}\right|^2 (x^2)/(2+x^2) \sim r \end{aligned} \qquad 4.4.1.4$$

Finally, there is yet a third set of parameters which appear in the literature which are the χ parameters. They define the off diagonal probability to the total probability for any decay.

$$\begin{aligned} \chi &\equiv \Gamma(0 \to \ell^+) / [\Gamma(0 \to \ell^+) + \Gamma(0 \to \ell^-)] \\ &\equiv r/(1+r) \end{aligned} \qquad 4.4.1.5$$

Using the previous results, it is easy to write down the χ parameter in terms of the x parameter which defines the ratio of oscillation to mixing.

$$\chi \equiv x^2 / \left[2(1+x^2)\right], 0 \le \mathrm{x} \le 1/2 \qquad 4.4.1.6$$

What about the situation for lepton pairs? In strong interactions one produces a pair of quarks and antiquarks (for example b and $\bar{b}$) and measures the time integrated probability of observing lepton pairs. For simplicity, one imagines an initial state of a $|0>$ and $|\bar{0}>$ and looks at the evolution of this state as a function of time, integrating over all times. One can get like sign and unlike sign pairs. For example, the probability of finding a $\mu^+\mu^-$ pair has a contribution from the probability of diagonal propagation without mixing. In order to have like sign pairs, one of the states $|0>$ or $|\bar{0}>$ needs to mix. Finally, to get the state $\mu^-\mu^+$ both the initial states must mix and reverse their identities.

$$
\begin{aligned}
&\psi(0)=|0\bar{0}>,\ \psi(t)\\
&\Gamma_{-+}=P_{0/0}\,P_{\bar{0}/\bar{0}}\\
&\Gamma_{--}=P_{0/0}\,P_{\bar{0}/0}\\
&\Gamma_{++}=P_{0/\bar{0}}\,P_{\bar{0}/\bar{0}}\\
&\Gamma_{+-}=P_{0/\bar{0}}\,P_{\bar{0}/0}
\end{aligned}
\qquad 4.4.1.7
$$

The asymmetry parameter for the lepton pairs is then the ratio of the probabilities for either of the initial particles to mix to the probability that neither mix or that both mix.

$$
\begin{aligned}
A(\ell\ell) &= \frac{\Gamma_{++}+\Gamma_{--}}{\Gamma_{-+}+\Gamma_{+-}}\\
&\simeq x^2\left(1+x^2/2\right)/\left(1+x^2+x^4/2\right)
\end{aligned}
\qquad 4.4.1.8
$$

Using our previous expressions for the probabilities, it is easy to see that the dilepton asymmetry vanishes as x^2 for small mixing. This means that there is no asymmetry in the absence of mixing, as is physically obvious. When x is very large the asymmetry becomes one, which means the states are entirely mixed before they decay. Therefore, any appearance of like sign dileptons means that there is mixing in the $|0>/|\bar{0}>$ two level quantum system.

One can also define a CP asymmetry which is the ratio of the difference in probabilities of $|0>$ mixing and $|\bar{0}>$ mixing over the sum of the probabilities of either no mixing or both the $|0>$ and $|\bar{0}>$ mixing.

$$
\begin{aligned}
A_{CP}(\ell\ell) &= \frac{\Gamma_{++}-\Gamma_{--}}{\Gamma_{++}+\Gamma_{--}}\\
&= \frac{|p/q|^2-|q/p|^2}{|p/q|^2+|q/p|^2} \sim [\mathrm{Im}(\Gamma_{12}/M_{12})\\
&\sim 4\,\mathrm{Re}\,\varepsilon
\end{aligned}
\qquad 4.4.1.9
$$

Note that one is measuring the CP violating parameter ε directly. There are no strong interaction effects in the final state as there were in our previous discussion of nonleptonic B decays. Therefore, a CP violating asymmetry measurement in the dilepton study would allow us to measure the ε parameter for the B system. Recall that ε is a small number which is in principle purely imaginary. Therefore, this is a very hard measurement which has yet to be accomplished.

4.4.2 $K \to \pi \ell \nu$ Asymmetry

A measurement that has already been made of a CP violating asymmetry arises in the kaon system. Suppose one has a K_L which in our present notation is the $|2>$ eigenstate of the $|0> / |\bar{0}>$ two level system. As one can see from Fig. 1.3.2, in a spectator model the strange quark decay is tagged by the appearance of a negative lepton, whereas the $\bar{s}$ quark decay is tagged by the appearance of a positive lepton. Therefore, one can tag the s and $\bar{s}$ content at any given time by looking at the sign of the lepton in the decay. Obviously, if CP were conserved, one would have equal numbers of negative and positive leptons from a neutral parent initial state. Using Eqs. 3.2.4 for the representation of the weak eigenstates in the $|0>$ and $|\bar{0}>$ basis, one can find the probability amplitude for the appearance of $|0>$ and $|\bar{0}>$ in the weak eigenstate $|2>$.

$$
\begin{aligned}
<0|2> &= \frac{p}{\sqrt{|p|^2+|q|^2}} \\
<\bar{0}|2> &= \frac{-q}{\sqrt{|p|^2+|q|^2}} \qquad\qquad 4.4.2.1 \\
A_{CP} &= \frac{\Gamma_+ - \Gamma_-}{\Gamma_+ + \Gamma_-} = 2\,\mathrm{Re}\,\varepsilon = <1|2>
\end{aligned}
$$

In analogy to the asymmetry in dileptons, one can look at the asymmetry in the appearance of positive and negative leptons in a weak eigenstate over the sum of the decay rates. Using our previous expressions for ε, it is again easy to see that there are no strong phases involved in the semileptonic decays. The CP violating asymmetry is proportional to the real part of ε. In fact, the result of this measurement is that the real part of ε is 1.4×10^{-3}. Note that this asymmetry measurement gives you a direct measurement of the CP violating parameter in the kaon system.

4.4.3 $\Delta M / \Gamma$ Data

Let us consider the data on dileptons in the B system. As we have already mentioned in the kaon system, very precise measurements have allowed us to measure the real part of the ε parameter for that system. This measurement is so far beyond the reach of experiment in the B system. However, the ratio of the like sign to unlike sign dileptons for the B system has been measured both at e^+e^- machines and $\bar{p}p$ machines. A glance at Eqs. 4.4.1.8 tells you that the measurement of like sign to unlike sign dileptons is a direct measurement of the mixing parameter x. Some of the recent data is shown in Table 4.1. For example, a recent CDF measurement is that χ is 0.176 which means that x for the B system is roughly 0.7.

TABLE 4.1

MIXING AND DILEPTON DATA

EXPERIMENT	BEAM	c.m. GeV	χ
UA1*	$\bar{p}p$	540	0.12 ± 0.047
JADE	e^+e^-	34	< 0.13 (90% c.l.)
Mark II	e^+e^-	29	< 0.12 (90% c.l.)
MAC	e^+e^-	29	$0.21^{+0.29}_{-0.15}$
ALEPH*	e^+e^-	91	$0.132^{+0.027}_{-0.026}$
L3*	e^+e^-	91	$0.178^{+0.049}_{-0.040}$
*average			0.142 ± 0.020

$$\begin{aligned} \chi &= 0.176 \\ \left(\frac{\Delta M}{\Gamma}\right)_{Bd} &\sim 0.7 \\ \Delta M &\sim 4x10^{-13} GeV \\ c\tau_B &\sim 350\mu m \end{aligned} \qquad 4.4.3.1$$

In contrast to the kaon system, there are two possible neutral B mesons, the B_d and the B_S. They have distinct mixing parameters x. We note that the controlling factors for the mixing can be read directly (in the Standard Model) from the box diagram as we asserted already in writing down Eq. 4.1.1. The mass difference has a contribution from the CKM factors at the four vertices of the box diagram. The decay, in the spectator model, has a factor which comes from the b to c transition at the vertex of the spectator diagram.

$$\begin{aligned} \frac{\Delta M}{\Gamma} &\sim \frac{(V_{tb}V_{tq}^*)^2}{(V_{bc})^2} \sim \frac{\left(V_{tq}^*\right)^2}{(V_{bc})^2} \\ \frac{x_{Bd}}{x_{Bs}} &\sim \left|\frac{V_{td}}{V_{ts}}\right|^2 \sim \theta^2 \end{aligned} \qquad 4.4.3.2$$

These vertex factors then imply immediately that the mixing parameter x for the neutral B_d meson is smaller than the B_S meson by roughly the ratio of the Cabbibo angle squared. Since we know that the mixing parameter is of order one for the B_d, the x value for the B_S must be very large.

$$x_{Bs} \sim 17 \qquad 4.4.3.3$$

Therefore, we expect that the B_S will mix before it decays whereas the B_d will have a competition between mixing and decay. Some of the constraints imposed by the data are shown in Fig. 4.4.1. For the e^+e^-machines, one is below threshold for the B_d and so the dilepton measurement is a pure measure of the B_d mixing, as one can see from Fig. 4.4.1. On the other hand, in the hadron collider experiments, UA1 and CDF, the data is a mixture of B_d and B_S so the effective measurement is a combination of the x parameters. Therefore, the hadron data is shown as a slope with narrow ranges in the two dimensional parameter space. Finally, the Standard Model relationship is shown as a curve. That curve is essentially a representation of the relationship given in Eq. 4.4.3.2. Note that χ is limited to the range, $0 < \chi < 1/2$.

What one can say is that B_d has a mixing parameter x of about 70% and that B_S probably, although there is no pure direct measurement, has a large mixing as is expected in the Standard

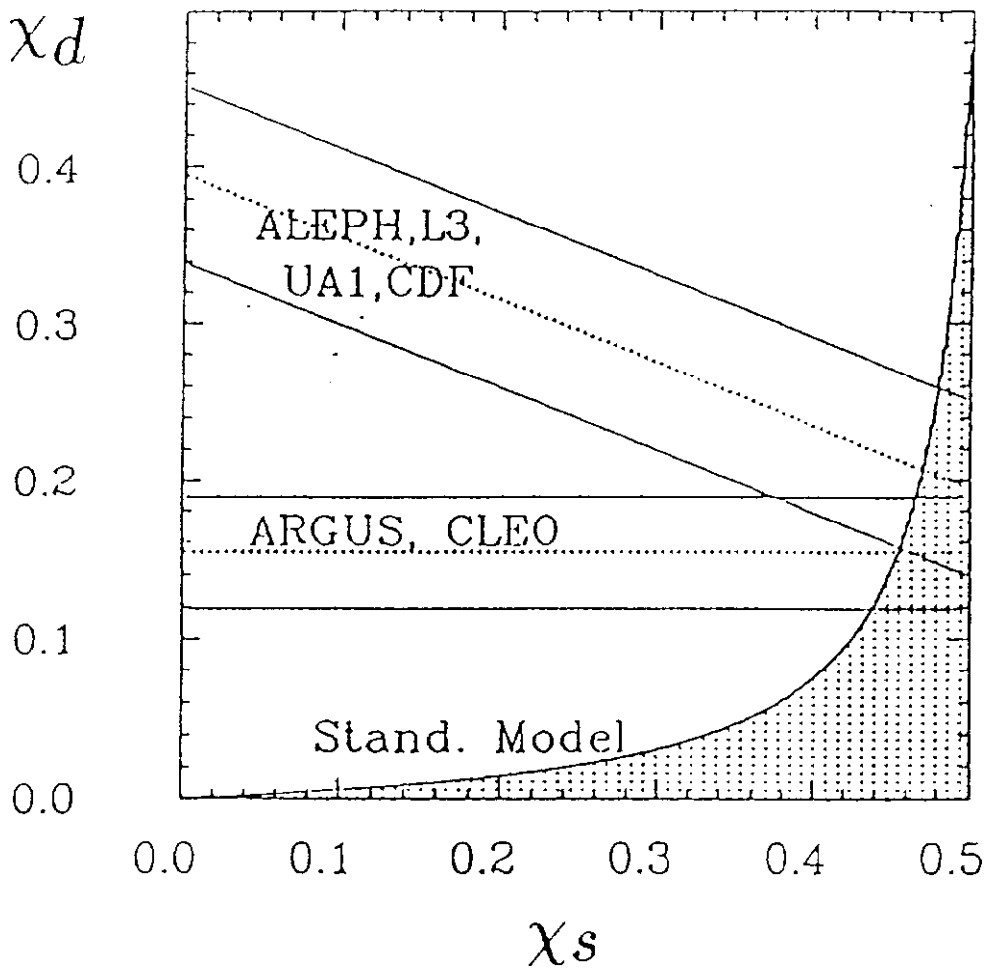

Fig. 4.4.1 Constraints on χ_s and χ_d from $\bar{p}p$ and e^+e^- collider data along with the allowed region in the CKM model.

Model. The data in its present state of accuracy certainly agrees with the Standard Model. Later in Section 5, we will attempt to make an estimate of the x parameter for the B_d meson. We will see that this data places useful constraints on the Standard Model parameters.

4.4.4 Integrated CP Violation Asymmetry

In Section 3, we discussed and derived the time distribution of the CP violating asymmetry for hadronic decays. Since there is, at present, no experimental data on proper time tagged decays of B systems, it is worthwhile to ask if there is any information that can be extracted from time integrated data. Let us define the CP violating parameter α which has potential contributions from the decay amplitudes and from the mass matrix.

$$\begin{aligned} \alpha &\equiv q/p\left(\frac{<f|\bar{0}>}{<f|0>}\right) \\ \bar{\alpha} &\equiv p/q\left(\frac{<\bar{f}|0>}{<\bar{f}|\bar{0}>}\right) \\ |\alpha| &= |\bar{\alpha}| = 1 \end{aligned} \qquad 4.4.4.1$$

The decay rate into a particular final state as a function of time is oscillatory in time. The amplitude of the oscillation is driven by the CP violating imaginary part of the amplitude α.

$$\begin{aligned} \mathrm{Im}(\alpha) &= -\mathrm{Im}(\bar{\alpha}) \\ \Gamma[0(t) \to f] &= e^{-\Gamma t}|<f|0>|^2[1 - \mathrm{Im}\,\alpha \sin(\Delta M t)] \end{aligned} \qquad 4.4.4.2$$

This latter equation is simply Eqs. 3.5.6. The integrated decay rates into the CP eigenstates $|f>$ and $|\bar{f}>$ are easily derived by integrating over time. The CP violating piece is,

$$\begin{aligned} \Gamma(0 \to f) &\sim \mathrm{Im}(\alpha)[x/(1+x^2)]|<f|0>|^2 \\ \Gamma(\bar{0} \to \bar{f}) &\sim \mathrm{Im}(\bar{\alpha})[x/(1+x^2)]|<\bar{f}|\bar{0}>|^2 \quad . \end{aligned} \qquad 4.4.4.3$$

The integrated asymmetry is then;

$$\int A(t)dt \equiv <A> \equiv \mathrm{Im}\,\alpha\left[\frac{x}{1+x^2}\right] \qquad 4.4.4.4$$

Clearly, this measurement requires that one has a tag to indicate the $|0>$ and $|\bar{0}>$ state. Obviously, as the mixing goes to zero, the asymmetry goes to zero. One needs both mixing and CP violation in order to get an integrated time asymmetry. One should also note the particular fact that in the integrated case, as x becomes very large, the asymmetry goes to zero. That means that the integrated asymmetry is washed out by mixing. Therefore in studying B_S, where x is expected to be rather large, one will be forced to measure the asymmetry at a tagged decay time in order to establish CP violation.

However, in the B_d system, with an x close to one, although one suffers some washing out of the asymmetry by doing the time integral, one still has a reasonably sensitive measurement. The integrated asymmetry as a function of the mixing parameter x is shown in Fig. 4.4.2. Also shown in the figure are the probabilities for a state $|0>$, to decay as a state $|0>$, and the probability of the state $|0>$ to decay as a state $|\bar{0}>$, $P_{0/0}$ and $P_{0/\bar{0}}$.

Recall that the "diagonal" probability is one for no mixing. With large mixing it approaches one half so that the states are completely mixed. The "off diagonal" mixing probability starts at zero for no mixing and also asymptotically reaches a value of 1/2. The CP time integrated asymmetry for small mixing vanishes because one needs both mixing and CP violation in order to have an asymmetry. In addition, as we have said, the asymmetry vanishes at large values of x because the time integrated measurement is washed out by oscillations. Therefore, there is a maximum in the time integrated asymmetry at x of 1. As we have said before, this means that the B_d system is nearly ideal for using time integrated information. The B_S measurement loses about a factor of 10 in sensitivity due to the oscillation and dilution. Therefore, in the case of B_S, one will need vertex detection.

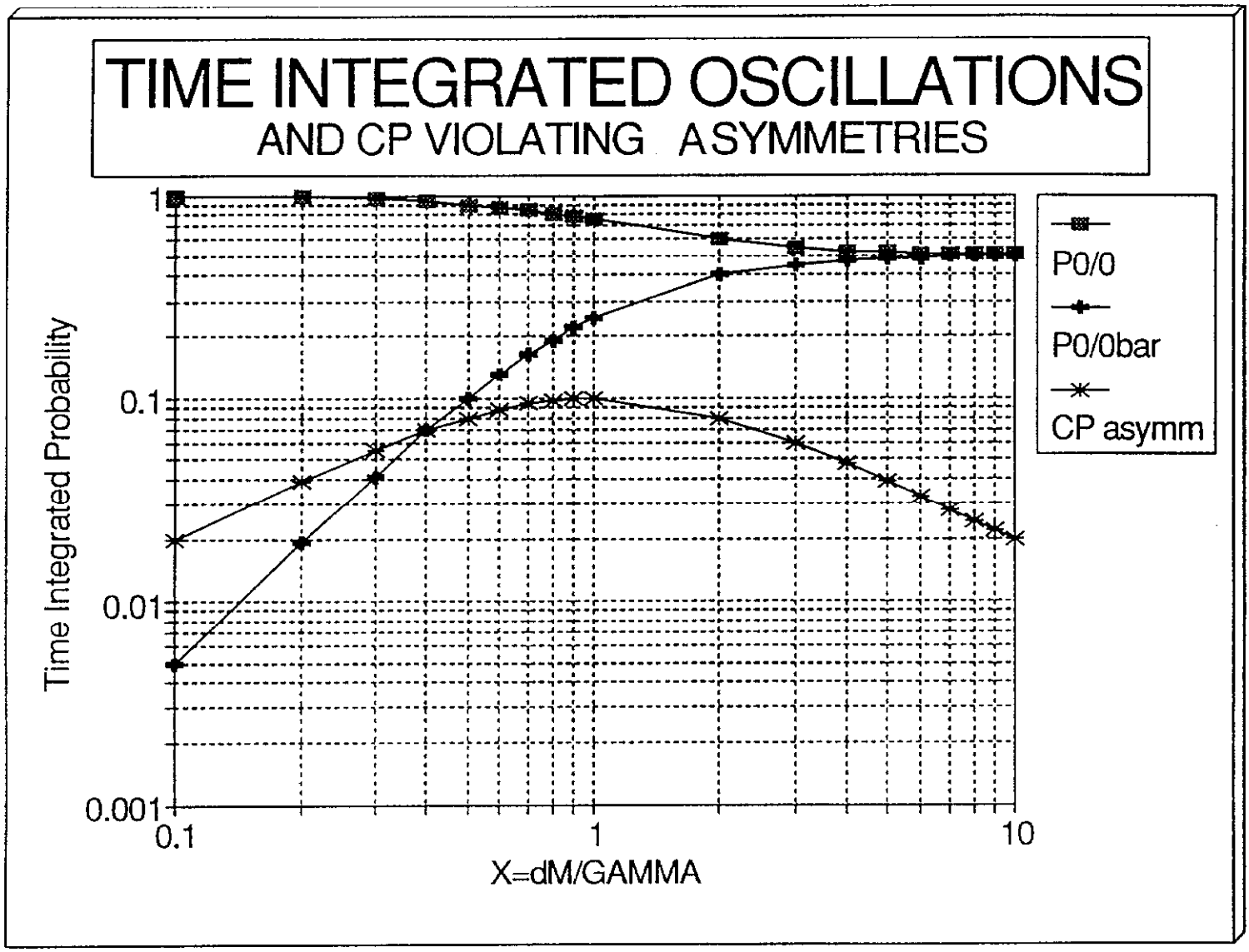

Fig. 4.4.2 Time integrated probabilities $P_{0/0}$ and $P_{0/\bar{0}}$ as a function of $x = \Delta M / \Gamma$. Also shown is the integrated CP violation asymmetry Eq. 4.4.4.4 for $\mathrm{Im}\alpha = 0.2$.

5. "BOX" DIAGRAMS AND SM CALCULATIONS

Until now we have treated the formalism which we have developed in Section 3 and expanded on in Section 4 in a purely phenomenological way. We have made little attempt to connect this to the Standard Model except where necessary to make some simple assertions referring to box diagram vertex factors. In this Section, we attempt to connect the measurements that we have discussed in Sections 3 and 4 with the elements of the CKM matrix using the Standard Model.

5.1 M_{12} and B_d, B_S

In Section 3, we discussed the general connection between the two level quantum systems with strong eigenstates $|0>$ and $|\bar{0}>$ via a complete set of intermediate states, $|n>$. In second order, there were on-shell elements of the decay matrix and off shell level shifts for the mass matrix.

$$M_{12} = \wp\sum_n \langle 0|H_W|n\rangle\langle n|H_W|\bar{0}\rangle / (M_0 - E_n)$$

$$M_{12} \sim \sum_{ij} \frac{G^2 f_B^2 M_B}{12\pi^2}\left[V_{ib}V_{iq}^*\right]\left[V_{jb}V_{jq}^*\right] \quad \text{(INT)} \qquad 5.1.1$$

Note that in the Standard Model there are no $\Delta B = 2$ transitions, so the first order piece of the off diagonal mass matrix elements are assumed to be zero. We will assume it to be true until there is evidence for something like a super weak theory. We will also make the assumptions that in the systems we are interested in, the spectator models dominate. We can then use the results which were developed in Section 2.

In particular, in looking at the box diagram, there is a connection between the physical B and $\overline{B}$ mesons and the quark and antiquark state at short distance. We will assume that, as in Section 2, this conversion probability is defined by the pseudoscalar coupling constant, f_B. We have experimental values for the pion and kaon coupling constant. It will be assumed that the D and B have similar values. Assumptions are necessary since the pseudoscalar coupling constant for B and D systems has yet to be measured.

Using the box diagram which we have already given in Fig. 3.1.1, one can write down the vertex factors and the exterior pseudoscalar couplings as in Eqs. 5.1.1. In Eq. 5.1.1 the term (INT) is a representation of the internal kinematics of the loops in the box diagram. A loop integral arises in integrating over the internal momentum of the interior legs of the box diagram. Let us define the vertex factors for the B system and write the amplitude for the box using the interior propagators.

$$\varepsilon_i \equiv V_{ib}V_{iq}^*$$

$$a_{Box} \sim \sum_{ij}\varepsilon_i\varepsilon_j\int \frac{dq^4\left(g_{\mu\nu}+\frac{q_\mu q_\nu}{M_W^2}\right)\left(g_{\lambda\rho}+\frac{q_\lambda q_\rho}{M_W^2}\right)(q+m_i)(q+m_j)}{\left(q^2-M_W^2\right)^2\left(q^2-m_i^2\right)\left(q^2-m_j^2\right)} \qquad 5.1.2$$

$$\sim \sum_{ij}\varepsilon_i\varepsilon_j \text{ (INT)}$$

One can expand as a power series in the interior fermion propagators and use the unitarity of the CKM matrix as it appears in the vertex factors. This means that in the expansion only the first term shown in Eqs. 5.1.3 survives in leading order.

$$\left(\frac{1}{q^2-m_i^2}\right)\left(\frac{1}{q^2-m_j^2}\right)=\frac{m_i^2m_j^2}{q^4\left(q^2-m_i^2\right)\left(q^2-m_j^2\right)}-\cdots$$

$$\sum_i \varepsilon_i = 0, V \textit{ unitarity} \qquad 5.1.3$$

$$a_{Box} \sim \sum_{i,j}\varepsilon_i\varepsilon_j\int \frac{dq^4q^6m_i^2m_j^2/\mathrm{M_W}^4}{q^4\left(q^2-M_W^2\right)^2\left(q^2-m_i^2\right)\left(q^2-m_j^2\right)}, q\to\infty$$

Thus, the leading power behavior in q^2 of the internal loop is dominated by the largest mass. Basically, this means that the propagator supports momenta up to a scale m_i so that the heaviest quark in the virtual loop dominates. As we will see later, a FCNC amplitude such as the box diagram is nonzero in higher order because of the propagator mismatch. An example of this behavior will be given in Section 5.5 (see Eq. 5.5.2). Therefore, under that assumption, ignoring the external momenta of the exterior legs of the box, and taking only the leading term in the integral for the loop, one finds that the loop integral is proportional to the square of the heaviest mass in the interior legs. Note that this is true for top masses less than M_W. Although we now know that this assumption is not true, we retain it for the sake of simplicity. The appropriate kinematic modifications are available in the references.

The off diagonal term in the mass matrix is a FCNC amplitude, which is second order in the electroweak coupling. Therefore, the ratio of M_{12} to the mass of the exterior particles is small for all allowed top masses.

$$(\mathrm{INT}) \sim \delta_{it}\delta_{jt}m_t^2$$

$$\mathrm{M}_{12} \sim \frac{G^2 f_{\mathrm{B}}^2 \mathrm{M}_{\mathrm{B}}}{12\pi^2}\varepsilon_t^2 m_t^2 = \frac{\left[\alpha_{\mathrm{W}}\left(f_B m_t \varepsilon_t / M_{\mathrm{W}}^2\right)\right]^2 \mathrm{M}_{\mathrm{B}}}{24} \qquad 5.1.4$$

$$\frac{\mathrm{M}_{12}}{\mathrm{M}_{\mathrm{B}}} \sim \frac{\alpha_W^2}{24}\left[\frac{f_{\mathrm{B}} m_t}{\mathrm{M}_W^2}\right]^2 \varepsilon_t^2$$

For the off diagonal elements of the decay matrix in the strong eigenstate basis, the calculation goes essentially exactly the same except, as we have said, the intermediate states must be real and on shell. Therefore, the loop integral is cut off earlier on a mass scale equal to the mass of the exterior particles which in this case we assume to be B mesons.

$$\Gamma_{12} \sim \frac{G^2 f_B^2 \mathrm{M}_{\mathrm{B}}}{8\pi}\varepsilon_t^2 \mathrm{M}_{\mathrm{B}}^2$$

$$\frac{\Gamma_{12}}{\mathrm{M}_{12}} \sim \left(\frac{\mathrm{M}_{\mathrm{B}}}{m_t}\right)^2 \qquad 5.1.5$$

$$\Rightarrow \Delta\Gamma \sim 0$$

Therefore, for large top quark masses, the elements of the decay matrix relative to the mass matrix are much less than one. This is the Standard Model justification for our previous explicitly stated assumption that the splitting in decay rates relative to the mass splitting was small for the B system.

5.2 $(\Delta \mathrm{M} / \mathrm{M})_K$

Data on the mass splitting exists to great precision for the kaon system. In fact, the x parameter for the K system is again a number of order one, indicating a roughly equal competition between oscillation and decay.

$$\left(\frac{\Delta \mathrm{M}}{\mathrm{M}}\right)_K^{\exp} = 7 \times 10^{-15}$$

$$x_K = 0.47 \qquad 5.2.1$$

$$(c\tau)_K = 2.7cm$$

Is this something that can be estimated in the Standard Model? One recalls from Section 3 that the mass splitting is proportional to the real part of the off diagonal elements of the mass

matrix. In a calculation very similar to that given in Eqs. 5.1.4, one gets the Standard Model estimate for the off diagonal mass matrix element given below (see Eq. 3.2.5).

$$\Delta M_K \sim 2\,\mathrm{Re}\,M_{12}$$
$$(M_{12})_K \sim \frac{G^2 f_K{}^2 M_K}{12\pi^2}(m_c{}^2)\left(V_{cs}{}^2 V_{cd}^{*\,2}\right) \qquad 5.2.2$$

The reason for the appearance of the charm quark in the loop, rather than the top quark, comes from a glance at the CKM matrix. The charm quark is coupled to the strange quark with unity strength, whereas the top quark coupling to the strange quark is very small, since one is far off the diagonal in the CKM matrix. Therefore, the charm quark is the one which dominates in the internal loop. It is not because of the kinematics of the mass of the internal loop, rather it is due to the unknown dynamics which is subsumed in the coupling given by the CKM matrix.

As an historical note, it was this sort of estimation which lead to an upper bound prediction on the charm-quark mass prior to its discovery. The constraint arose because if the charm quark became too heavy, the measured mass difference of the kaon would be exceeded in the Standard Model. Plugging in the numbers, one gets a fractional mass splitting of approximately 3 x 10^{-15}.

$$\left(\frac{\Delta M}{M}\right)_K \sim \frac{(G f_K m_c)^2}{6\pi^2}\theta^2 = \frac{\alpha_W{}^2\left(f_K m_c \theta / M_W{}^2\right)^2}{12} \qquad 5.2.3$$
$$\sim 3\times 10^{-15}$$

Comparing to the experimental data on the mass difference, it is clear that this quantity is roughly calculable for the kaon in the Standard Model. This estimate also makes clear the sensitivity of ΔM_K to the charm quark mass.

5.3 $\Delta M / \Gamma$ for K, D, B

One can continue the general treatment described in Section 5.1 into the D and B systems in the same vein as the treatment of the kaons given in Section 5.2. In order to get an estimate for the x parameter, one uses the mass splitting given by the Standard Model box diagram as outlined in Section 5.1. For the decay width the spectator diagram is used as was discussed in some detail in Section 2. For the B system, we assume that the internal box diagram is dominated by the top loop.

$$\begin{aligned}\frac{\Delta M}{\Gamma} &\equiv x \\ &\sim 2M_{12}/\Gamma \\ &\sim \frac{2G^2 f_B{}^2 M_B \varepsilon_t{}^2 m_t{}^2/12\pi^2}{3G^2 M_B{}^5 V_{bc}^2/192\pi^3}\end{aligned} \qquad 5.3.1$$

For the B system the vertex factors are straightforward to read off from the CKM matrix.

$$\begin{aligned}x_{Bd} &\sim \left(f_B m_t / M_b^2\right)^2 \left(\frac{V_{tb}V_{td}^*}{V_{bc}}\right)^2 \left(\frac{32\pi}{3}\right) \\ &\sim \left(\frac{f_B m_t \theta}{M_b{}^2}\right)^2 \left(\frac{32\pi}{3}\right)\end{aligned} \qquad 5.3.2$$

Numerically, if one assumes a pseudoscalar coupling constant equal to the pion coupling constant, a top mass of 120 GeV, a bottom mass of 5 GeV, and a Cabbibo angle of 1/5, one gets an x parameter for the B system of rougly 0.7. This is quite comparable to the observed B_d mixing parameter of 0.73.

$$\begin{aligned}x_{Bd}^{exp} &= 0.73 \pm 0.18 \\ f_B &\sim f_\pi \sim 0.14 GeV \\ x_{Bd} &\sim 0.7\end{aligned} \qquad 5.3.3$$

On an historical note, the first evidence for large mixing in the $B\bar{B}$ system was an early indication, albeit indirect, that the top quark mass would be quite large. Note from Eqs. 5.3.2 that the x parameter in the B_d system goes quadratically with the mass of the top quark. Therefore, as we have seen experimentally, mixing competes with decays for the B_d system. It is also quite obvious, as we have mentioned in Section 4, that the B_S system x parameter is related to the B_d system value simply by vertex factors. Therefore, we expect the x parameter for the B_S system to be roughly 17.

$$x_{B_s} \sim x_{B_d}/\theta^2 \sim 17 \qquad 5.3.4$$

Therefore, the Standard Model prediction is that mixing occurs at a much faster rate than decay for the B_S system. That expectation agrees with the measurements, such as they are, from hadron machines from which the x parameter for the B_S system is inferred.

Now what about the situation for the charm quark? The general expression for the mass splitting which we already derived implies internal s and b quark loops. The s quark internal loop is highly suppressed by the small value of the strange quark mass, whereas the b quark loop is strongly suppressed by the weakness of the coupling factors. This is the same small coupling, let us note, that leads to the slow decay rate of the b. Recall that the coupling is small enough to overcome the fifth power mass scaling in going from the c to the b system yielding comparable lifetimes for B and D mesons.

On the other hand, the decays are given, in the spectator context, by the $c \rightarrow s$ transition. Its strength is given by the V_{cs} CKM matrix element which occurs at full strength. The D decays are not slowed by coupling factors, whereas the internal loops are very highly reduced. In fact, they go as the tenth power of the Cabbibo angle. Therefore, one can expect that mixing in the D system, at least in the Standard Model, is extremely small. In fact, the experimental limit is that the mixing parameter x for the D system is less than 10%.

$$\begin{aligned} \Delta M_D &\sim \varepsilon_s^2 m_s^2 \sim \theta^2 m_s^2 \\ &\sim \varepsilon_b^2 m_b^2 \sim \theta^{10} m_b^2 \\ \Gamma_D &\sim V_{cs}^2 \sim 1 \\ x_D &<< 1, \left(x_D^{\exp}\right) < 0.085 \end{aligned} \qquad 5.3.5$$

Therefore, a high precision study of D mixing, with a nonzero result, would indicate physics beyond the Standard Model.

In the case of the kaon system, the situation is somewhat more complicated. In this case, the possible internal quarks connecting to the external s quarks, are the u, c, and t quarks. For internal c quarks the mass splitting is reasonably favorable, whereas top quarks, as we have said, are rather decoupled from the strange quarks because of the essentially diagonal nature of the CKM matrix. The ratio of the vertex and kinematic factors for the internal c and t quark loops is such that the c quark dominates the mass splitting by about a factor of 50.

$$\begin{aligned} \Delta M_K &\sim \varepsilon_c^2 m_c^2 \sim \theta^2 m_c^2 \\ &\sim \varepsilon_t^2 m_t^2 \sim \theta^{10} m_t^2, \left(\frac{\theta^4 m_t}{m_c}\right)^2 \sim 0.02 \\ \Gamma_K &\sim V_{sq}^2 \sim \theta^2 \\ x_K &\sim 1 \end{aligned} \qquad 5.3.6$$

However, a very heavy top would certainly upset the measurements of the mass splitting in the kaon system. Therefore, some modest constraints on the top mass arise. Recall that the kaon decay rate is slowed by Cabbibo suppression. Therefore, the kaon decay is somewhat slow as is the B decay. In both cases one has a suppressed decay and a heavy mass in the loop. Therefore, for both the B and the K system, one expects the x parameter to be of order one.

5.4 M_Z/M_W to $O(\alpha_W)$

Before going on to estimates of CP violating parameters in heavy quark systems in the Standard Model, we will look briefly at the effects of internal loops in various systems. First, one wants to look at the vacuum self energy contributions to the electroweak gauge bosons in lowest order due to virtual heavy quark loops.

The classical self energy for a charged system of mass M_O, can be visualized as being due to the electrical field of that charge which contains electromagnetic field energy and therefore, mass.

$$\begin{aligned} M_{CL} &= M_o + \frac{1}{2}\int |\vec{E}|^2 \, \vec{dr} \\ &= M_o + \frac{e^2}{8\pi a} + \frac{1}{2} \int_{r<a} |\vec{E}(r)|^2 \, \vec{dr} \end{aligned} \qquad 5.4.1$$

Smearing out the charge by a radius a, yields a self energy which diverges linearly with distance. This is quite familiar from classical electrodynamics. In quantum mechanics, one has a similar situation in that the self energy has a piece which diverges. However, the divergence is softened by the existence of virtual electron-positron pairs in the vacuum at small distance or at high momentum. This softening of the behavior due to the screening effects of the virtual pairs results in a logarithmic divergence of the self energy.

$$\begin{aligned} M_{QM} &= M_o + \frac{1}{2}\int f(r)\, dr \\ f(r) &\sim \left|\vec{E}(r)\right|^2 \quad for \;\; r > \lambda\!\!\!^{-} \end{aligned} \qquad 5.4.2$$

The size of this divergence can be estimated when one cuts off at a mass λ, which is complementary to the classical cutoff at size a.

$$M_{QM} \sim M_o\left[1 - \frac{3\alpha}{4\pi} \ell n\left(M_o / \lambda\right)^2\right] \qquad 5.4.3$$

A schematic representation of the classical and quantum mechanical self energy is given in Fig. 5.4.1. Quantum mechanical self energy is proportional to the fine structure constant and the divergence is logarithmic in the cutoff parameter. Note that this behavior is similar to the cutoff theory for the propagator in QED which was given in Eqs. 2.5.3 during the discussion of penguin diagrams and internal loops.

A similar sort of vacuum fluctuation graph is responsible for changes in the self energy of the gauge bosons. The graphs with internal heavy flavor loops for virtual intermediate states for both W and Z are shown in Fig. 5.4.2. In that Figure, only the heaviest flavors in the internal loops are shown, since we expect from our earlier discussions, those are the flavors which will dominate. The gauge boson self energy is then dominated for the Z by internal top pairs and for the W boson by internal CKM favored $t\bar{b}$ pairs. Since the top is so much heavier than the other quarks, a precise measurement of the gauge boson self energy will constrain the top quark mass. Note that the loop integrals are asymmetric in W and Z, which will change the W to Z mass ratio. To lowest order there is a relationship between W and Z which is given by the Weinberg angle. In higher order this relationship is broken by the top quark mass loops.

$$\begin{aligned} \rho &= \left(M_W / M_Z \cos\theta_W\right)^2 \equiv 1 \\ \Delta\rho &= \frac{3\alpha_W}{16\pi}\left(\frac{m_t}{M_W}\right)^2 \\ \alpha_W &\sim 1/30 \\ m_t &\sim 120\ GeV \\ \Delta\rho &\sim 0.4\% \end{aligned} \qquad 5.4.4$$

Note that this splitting of the W to Z mass is proportional to the quark mass squared and to the electroweak fine structure constant. Note also the similarity to Eq. 2.5.4 for internal loops in $b \to s\gamma$ decays. For photons, gauge invariance implies no fermion squared mass terms which leaves the soft logarithmic dependence of Eq. 5.4.3. Electroweak gauge invariance is broken, leading to fermion mass squared terms in radiative loops. Numerically, for 120 GeV top, the splitting is of the order of one percent. A precision electroweak measurement of the Z and W mass gives us constraints on the top. In particular, it gives us at present a limit on the top mass. Top cannot be so heavy as to cause a large splitting in the W to Z mass ratio. This is yet another Standard Model example of propagator mismatches in loop diagrams which give rise to splittings.

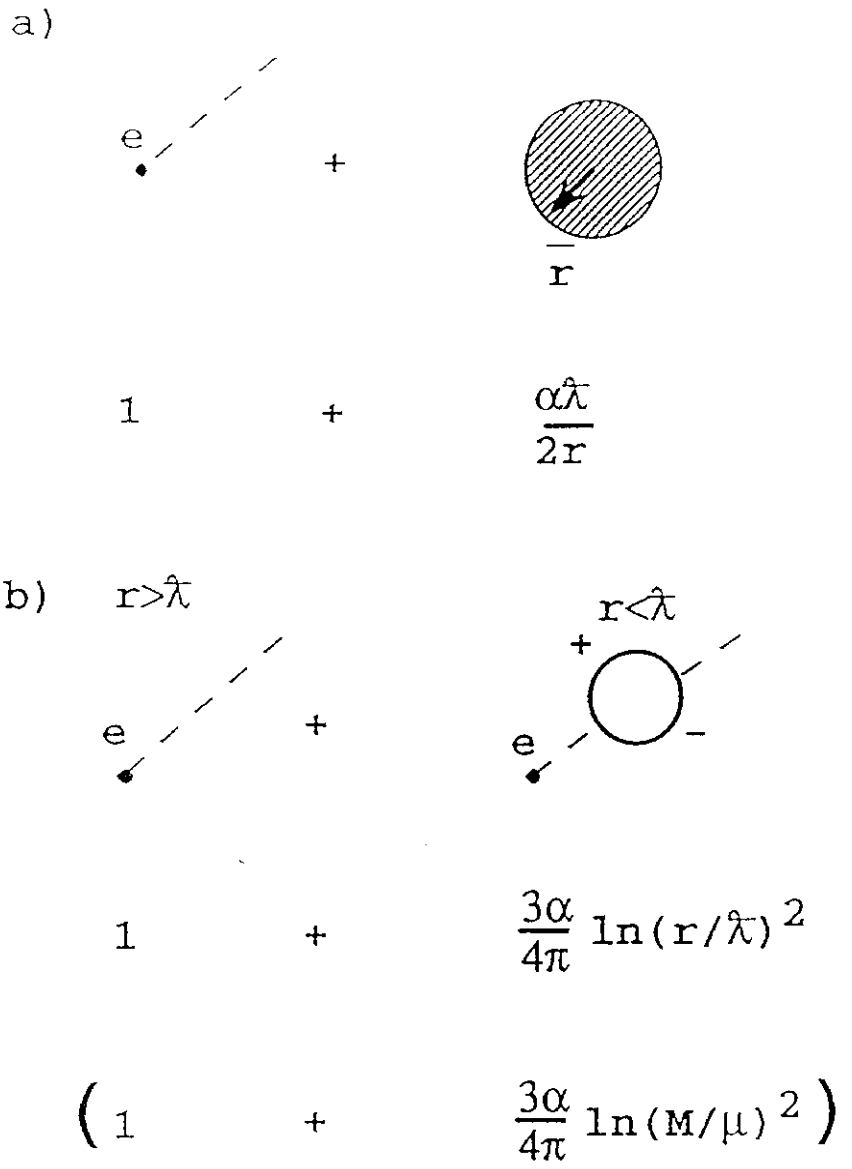

Fig. 5.4.1 a. Classical self energy of a charge distribution.
b. Quantum mechanical self energy in a diagrammatic representation.

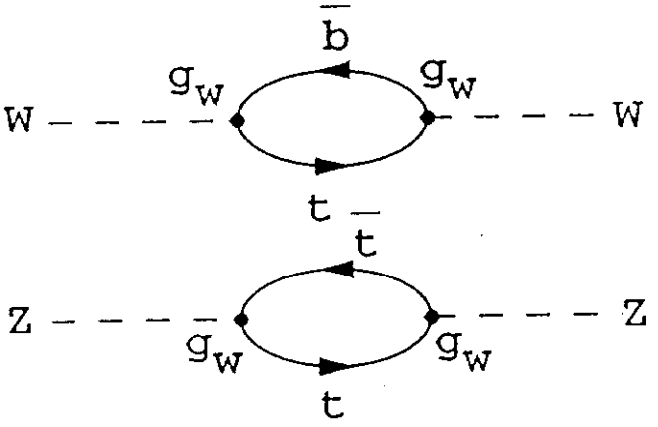

Fig. 5.4.2 Self energy diagrams for W and Z with heavy $Q\bar{Q}'$ intermediate states.

5.5 FCNC in $B \to \mu\mu, K \to \mu\mu$ and the GIM Mechanism

What about the potential existence of flavor changing neutral currents in the Standard Model? As noted in our previous discussion, the GIM mechanism cancels flavor changing neutral currents in lowest order. Of course, the question is then, what about higher diagrams? An example of box like higher order diagrams is given in Fig. 5.5.1 for B decays into dimuons. These are experimentally accessible signatures and they have been searched for. At present, there are only limits on the decay branching fractions. One expects that the heaviest flavor in the internal legs of the box will dominate. Can we estimate in the Standard Model the size of flavor changing neutral current effects? Note that experimentally the branching ratio for B_d into dimuons has a limit of 5×10^{-5}, whereas the branching ratio for K_L to dimuons has been positively measured and has a branching ratio of 6×10^{-9}.

Let us first look at the K_L decay and see if the Standard Model makes any plausible estimate for the flavor changing neutral current decay rate. A topologically similar diagram exists for purely leptonic decays of charged kaons to leptons and neutrinos as shown diagrammatically in Fig. 5.5.2. Recall the discussion in Section 2, wherein the purely leptonic decay rate for kaons was derived.

$$\Gamma(K \to \mu\nu) \sim \frac{G^2}{8\pi}\left[f_K \theta M_\mu\right]^2 \mathrm{M}_K \qquad 5.5.1$$

The box diagram contribution to the decay $K_L \to \mu\mu$ is suppressed by the GIM mechanism since it is a FCNC. However, the difference in internal propagators means that the suppression of FCNC is not complete. Looking at Fig. 5.5.2b one can write the vertex and propagator factors for the internal charm and up quarks in the box.

$$\begin{aligned} a_{Box} &\sim \frac{V_{us}V_{ud}^*}{q^2 - m_u{}^2} + \frac{V_{cs}V_{cd}^*}{q^2 - m_c{}^2} \\ &\sim \theta\left[\frac{1}{q^2 - m_u{}^2} - \frac{1}{q^2 - m_c{}^2}\right] \\ &\sim \theta m_c{}^2 \Big/ \left[q^2\left(q^2 - m_c{}^2\right)\right] \end{aligned} \qquad 5.5.2$$

Clearly, the amplitude is zero without the propagator difference which is a statement of two generation unitarity. This is in line with our previous discussion. Unitarity of the CKM matrix insures the vanishing of FCNC in lowest order. Looking at Eqs. 5.5.2, it is clear that the mass mismatch in the propagators makes for an incomplete GIM cancellation. The amplitude for the

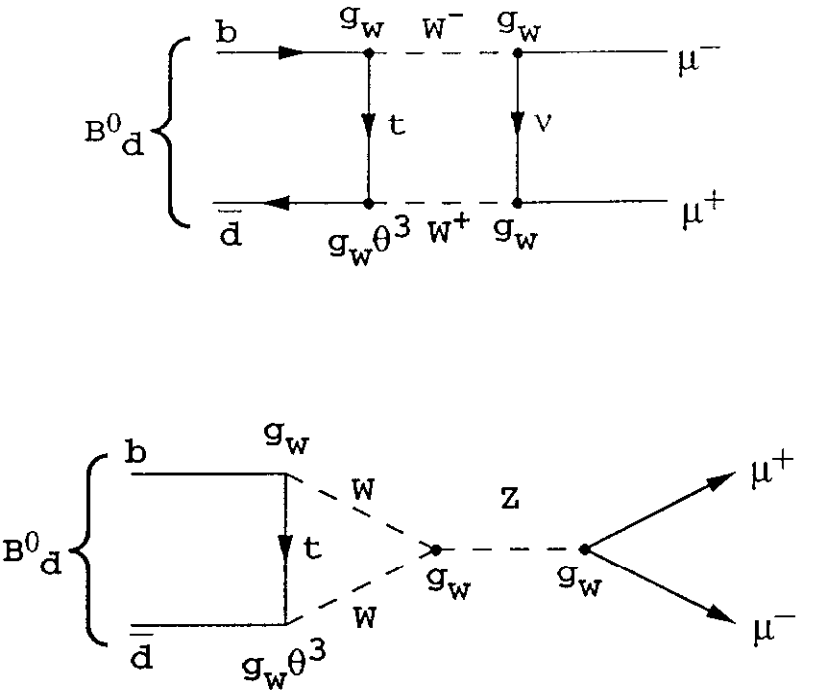

Fig. 5.5.1 FCNC diagrams for $B^0_d \rightarrow \mu^+\mu^-$ decays with intermediate

a. W States

b. Virtual $Z \rightarrow \mu\mu$ decay.

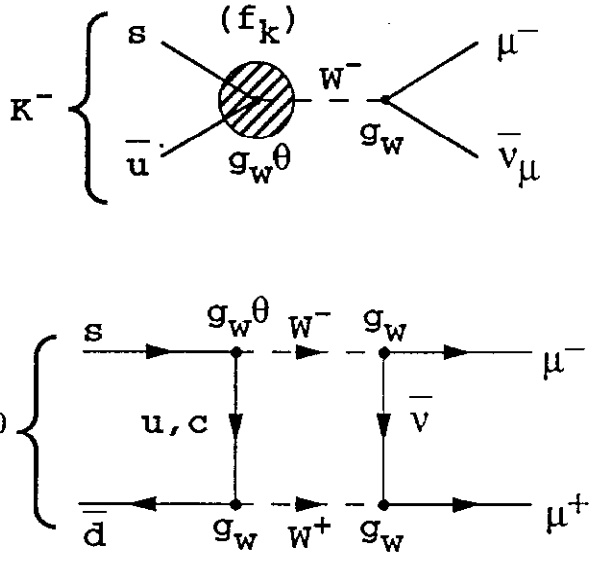

Fig. 5.5.2 Comparison of $P \rightarrow \mu\nu$ decay diagrams for

a. $K^- \rightarrow \mu^-\bar{\nu}_\mu$

and

b. FCNC, $K^0 \rightarrow \mu^+\mu^-$

showing vertex factors.

box is proportional to the vertex factors and the square of the heavy mass in the loop. This result is in complete agreement with the discussion of M_{12} in Section 5.1.

Comparing the two diagrams given in Fig. 5.5.2, counting vertices, and recalling the fact that the pseudoscalar kaon decay into two muons is still helicity suppressed (as is the purely leptonic decay for charged kaons), one is lead to an estimate of the ratio of the decay rates given below.

$$\frac{\Gamma\left(K_L \to \mu^+\mu^-\right)}{\Gamma\left(K^+ \to \mu^+\nu\right)} \sim \frac{G^2 m_c{}^4}{2\pi^4} \sim \frac{\alpha_W{}^2}{4\pi^2}\left(\frac{m_c}{M_W}\right)^4 \qquad 5.5.3$$

The dependence on the charm quark mass comes from the internal loop. The relative vertex factors for the two diagrams can be read off Fig. 5.5.2. Numerically, the ratio is about 2.6 x 10^{-12}. Therefore, using the measured decay rates, the branching ratio in the Standard Model for $K_L \to \mu^+\mu^-$ should be 7 x 10^{-12}. This is much less than the experimental value of 6 x 10^{-9}, which means that the Standard Model, at least at this level of understanding, is not responsible for this FCNC decay rate.

A possible reason for this disagreement is shown diagrammatically in Fig. 5.5.3. The question is whether the electromagnetic interaction swamps the Standard Model flavor changing neutral currents. Clearly, looking at Fig. 5.5.3a, one expects the branching fraction for K_S to $\gamma\gamma$ to be of order α^2 times the branching fraction of K_S to $\pi^0\pi^0$ which is of order one third. Since the observed branching fraction of K_S to $\gamma\gamma$ is 2.4 x 10^{-6}, as compared to α^2 which is 5.3 x 10^{-5}, the $\gamma\gamma$ branching ratio can be thought of as a higher order electromagnetic correction to the main $\pi^0\pi^0$ branching rate.

$$\begin{aligned} \mathrm{B}\left(K_S \to \gamma\gamma\right) &\sim \alpha^2 \\ \mathrm{B}\left(K_L \to \mu^+\mu^-\right) &\sim \alpha^2 \mathrm{B}\left(K_L \to \gamma\gamma\right) \\ &\sim 3\times 10^{-8} \end{aligned} \qquad 5.5.4$$

In yet higher order, the dimuon rate can be thought of as an electromagnetic higher order contribution to the $\gamma\gamma$ decay rate. The branching ratio of K_L to two photons is 5.7 x 10^{-4}. One expects a K_L to 2 muon rate roughly α^2 times smaller than that, or 3 x 10^{-8}. This is certainly of a comparable order of magnitude to the observed dimuon rate for K_L. Therefore, we expect that the K_L to two muon rate does not have too much to do with higher order standard box diagrams, but

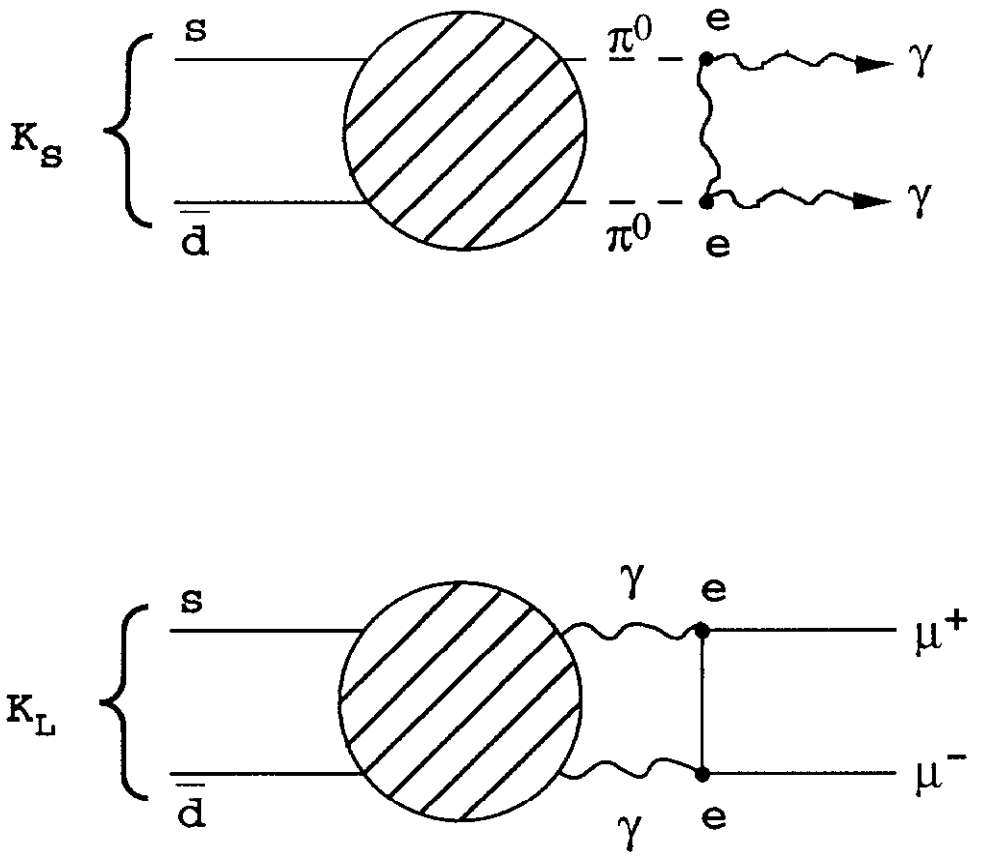

Fig. 5.5.3 FCNC and EM decays of kaons

a. Relationship of $K \to \pi^0\pi^0$ and $K \to \gamma\gamma$ decays.

b. Relationship of $K \to \gamma\gamma$ and $K \to \mu\mu$ decays.

rather with higher order electromagnetic corrections to the $2\pi^0$ rate of K_L. Thus, the expected flavor changing neutral current is probably masked by these electromagnetic effects.

5.6 Γ_{12} IN THE SM, ε FOR B_d, K

Let us, in this Section, look at the Standard Model calculation for the decay matrix, in particular, the off diagonal elements in the strong eigenstate basis. In Section 5.1, we argued that the decay matrix elements would be small relative to the mass matrix elements. At this time we will attempt to better quantify what we mean by small.

Recall that the decay matrix must be fed by real intermediate states which are on shell and which are common to, for example, the b and the $\bar{b}$ system. Note that, topologically, the mass and decay matrix elements share the same graph and therefore a common phase. In fact, the mass and decay matrices are the absorptive and dispersive parts of the same amplitude. Finally, one can note that the mass matrix does not go like the fifth power of the parent mass as the spectator decay rates have been shown to. That is because for the mass matrix, the momentum needs to be well aligned in order to go from B to intermediate state and back to $\bar{B}$. The spectator diagram does not have this property and therefore, is not kinematically favorable for $B \leftrightarrow \bar{B}$ transitions.

Let us write down the box diagram values for the decay and mass matrices. In this case, we will take the decay matrix to leading and next to leading order. The mass matrix will be kept only in leading order. The mass matrix expression then corresponds to a box diagram with two top quarks in the intermediate states, whereas, the decay matrix has a leading term corresponding to two top quarks in the intermediate state and a second term corresponding to a top and charm quark in the internal legs. Note that the decay matrix, in the case of internal tops, is proportional to the external B mass which cuts off the loop integral, whereas in the case of the charm quark intermediate state, the internal charm mass cuts off the loop integral.

$$\begin{aligned}
\Gamma_{12} &\sim \frac{G^2 f_B{}^2 M_B}{8\pi}\left[\varepsilon_t{}^2 M_b{}^2 + \frac{8}{3}\varepsilon_c \varepsilon_t m_c{}^2\right] \\
M_{12} &\sim \frac{G^2 f_B{}^2 M_B}{12\pi^2}\left[\varepsilon_t{}^2 m_t{}^2\right] \qquad 5.6.1 \\
\Gamma_{12}/M_{12} &\sim \frac{3\pi}{2}\left[\left(\frac{M_b}{m_t}\right)^2 + \frac{8}{3}\left(\frac{\varepsilon_c}{\varepsilon_t}\right)\left(\frac{m_c}{m_t}\right)^2\right]
\end{aligned}$$

Therefore, we have the higher order correction to the expression given in Eqs. 5.1.5. Recall also the expression for ε given in Eqs. 3.3.6. To lowest order, the mass and decay matrices are relatively real and therefore, the real part of ε is zero in that order. Basically, this happens

because we have a common lowest order diagram simply with different cutoffs. Therefore, they will have the same phase since the phases are associated with the vertex factors. Putting in values for the CKM vertex factors, one achieves a posteriori justification for the assumption that the real part of ε in the B system is small.

$$\begin{aligned} \mathrm{Re}\,\varepsilon &\sim \frac{1}{2}\left[\mathrm{Im}(\Gamma_{12}/2\mathrm{M}_{12})\right] \\ &\sim \mathrm{Im}\Gamma_{12}/4\mathrm{M}_{12} \end{aligned} \qquad 5.6.2$$

An estimate of the real part of ε in the B_d system follows as the ratio of the charm to top quark mass squared, which is of order 10^{-4}. Therefore, we recover the assumption that in the box diagram approximation for CP violation, ε is almost purely imaginary for the B system. This is the origin of the comment made with regard to dilepton asymmetries that it will be extremely difficult to measure CP violation using that method, because the asymmetry is proportional to the real part of ε.

$$\begin{aligned} \frac{1}{4}\mathrm{Im}(\Gamma_{12}/\mathrm{M}_{12}) &\sim \pi\left[\mathrm{Im}\left(\frac{\varepsilon_c}{\varepsilon_t}\right)\left(\frac{m_c}{m_t}\right)^2\right] \\ &\sim \pi\sin(\phi_{td})\left(\frac{m_c}{m_t}\right)^2 \\ \mathrm{Re}(\varepsilon_{Bd}) &\sim \pi\sin(\phi_{td})\left(\frac{m_c}{m_t}\right)^2 \end{aligned} \qquad 5.6.3$$

What about the situation for the ε parameter in the kaon system? It has been measured to be nonzero, as we said before, by measuring the lepton charge asymmetry in K_L semileptonic decays. We want to calculate it in the SM. First, one needs to look at unitarity of the CKM matrix. Recall that when we first looked at the GIM mechanism for two generations, the CKM matrix was real and corresponded to a rotation. Obviously, one needs at least three generations for the Standard Model to generate CP violation. In higher order within the CKM matrix, unitarity for the d and s columns leads to a small complex addition to the CKM elements which we have ignored so far. The unitarity relation for the d and s columns reads as follows.

$$
\begin{aligned}
&V_{ud}^{*}V_{us}+V_{cd}^{*}V_{cs}+V_{td}^{*}V_{ts}=0\\
&\theta+V_{cd}^{*}-\theta^{5}\left(1-re^{i\delta}\right)=0\\
&V_{cd}\sim-\theta\left[1-\theta^{4}\left(1-re^{-i\delta}\right)\right]
\end{aligned}
\qquad 5.6.4
$$

This means, specifically, that the cd element of the CKM matrix has a small complex part. By small we mean of order θ^4 with respect to the main part. Therefore, when one adds a third generation, one induces only a very small complex part in the 2 x 2 submatrix characterizing the first two generations. It's crucial that one needs three generations in order to generate CP violation and that the impact of the third generation on the reality of the 2 x 2 submatrix is very small.

For the kaon system, as we've said before, the splitting of decay rates is comparable to the K_S decay rate itself. This is an accident, in the sense that the mass difference for CP even and odd states, i.e., two pion and three pion systems, is comparable to the mass of the kaon itself.

$$
\begin{aligned}
&\Delta\Gamma_K=\Gamma_{K_S}-\Gamma_{K_L}\sim\Gamma_{K_S}\equiv\Gamma\\
&|K_S>\equiv|1>\\
&|K_L>\equiv|2>\\
&\varepsilon_K\sim-\mathrm{Im}\,M_{12}/(\lambda_1-\lambda_2)\\
&\quad\sim\mathrm{Im}\,M_{12}/(\Gamma+i\Delta M)
\end{aligned}
\qquad 5.6.5
$$

Without specializing to the B system, but under the assumption that the ε parameter is small, one can use Eqs. 3.3.2. Again, assuming the dominance of the mass matrix over the decay matrix, one gets the expression for ε for the kaon system given in Eqs. 5.6.6. Taking the measured value for the x parameter in the kaon system, one then gets a Standard Model estimate for ε_K.

$$
\begin{aligned}
|\varepsilon_K|&\sim\frac{G^2{f_K}^2M_K{m_c}^2\,\mathrm{Im}\left(V_{cd}^{*}V_{cs}\right)^2}{12\pi^2\Gamma|1+ix|}\\
&\sim\frac{\left[\alpha_W\left(f_Km_c/{M_W}^2\right)\right]^2}{24}\left[\frac{M_K\,\mathrm{Im}\left(V_{cd}^{*}V_{cs}\right)^2}{\Gamma|1+ix|}\right]
\end{aligned}
\qquad 5.6.6
$$

Recall that ε is a CP violating parameter. Therefore, one needs an imaginary part in the mass matrix in order to generate ε. Recall also that we have previously mentioned that the

weakness of the top quark coupling to kaons means that the off diagonal parts of the mass matrix are dominated by the charm quark interior loop.

For the kaon system M_{12} is approximately real, and therefore mixing depends on the real part of M_{12}. However, the CP violating parameter ε for the kaon system depends on the existence of an imaginary part. As we saw from Eqs. 5.6.4, this is quite a small part of the CKM matrix element if the vertex factor is to be associated with the internal charm quark. This is what is different with respect to the discussion of the mass splitting in the kaon system. For the mass splitting, due to the weakness of the coupling of the top quark, we were dominated by internal charm quark loops. In the case of CP violation, what is important is the existence of an imaginary part in the vertex factor. We have derived previously that the imaginary part of the vertex factor, for the charm quark, and top quark are both weak.

$$\begin{aligned} \mathrm{Im}(\varepsilon_c)^2 &\sim \left(r\theta^5 \sin\delta\right)^2 \\ \mathrm{Im}(\varepsilon_t)^2 &\sim \left(r\theta^5 \sin\delta\right)^2 \end{aligned} \qquad 5.6.7$$

In fact, the overall imaginary vertex factor for internal charm and top loops is essentially the same. Therefore, for CP violation in distinction to mass splitting, internal top loops are important. In fact, given the equal vertex factors, top loops dominate the estimate for the CP violation parameter in the kaon system.

$$\begin{aligned} |\varepsilon_K| &\sim \frac{\left[\alpha_W\left(f_K m_t / M_W{}^2\right)\right]^2}{24}\left(\frac{M_K}{\Gamma}\right)\frac{\left(r\theta^5 \sin\delta\right)^2}{|1+ix|} \\ &\sim 1.7 \times 10^{-3}(r\sin\delta)^2 \end{aligned} \qquad 5.6.8$$

Assuming a top mass of 120 GeV, the ε parameter is estimated to be 1.7×10^{-3} times phase factors squared which are of order 1. Experimentally, we know that the magnitude of ε for the kaon system is 2×10^{-3}. That means that m_t cannot be too large without exceeding the measured values of the ε parameter. Therefore, experimental limits on the top quark mass would put constraints on the unitary triangle because that triangle depends on the phase angles in the CKM matrix as does ε for the kaon system.

Another estimator can be obtained by, in addition, using the box diagram for the eigenvalue differences in the kaon system. Looking at Eqs. 5.6.8, one realizes that we have used the measured valued of the x and Γ parameters for the kaon system, assuming that the strange quark is too light for the box diagram to be reliable. If one blithely goes ahead and uses the Standard

Model box diagram estimator for the eigenvalues, the imaginary part of ε is driven (as we have said) by the internal top loop, whereas, the real part is dominated by the internal charm quark loop (see Eq. 5.2.3).

$$\varepsilon_K \sim \left(\frac{m_t}{m_c}\right)^2 \left(\frac{\mathrm{Im}\,\varepsilon_t}{\mathrm{Re}\,\varepsilon_c}\right)^2$$

$$\varepsilon_K \sim \left(\frac{m_t}{m_c}\right)^2 \left(r\theta^4 \sin\delta\right)^2 \qquad 5.6.9$$

$$\sim \left(1.6 \times 10^{-2}\right)(r\sin\delta)^2$$

Putting in values for 120 GeV top quark mass, 1.5 GeV charm quark mass, and 1/5 Cabbibo angle, one has again an estimate for ε in the kaon system which is small and of the same order as the measured value. Therefore, we conclude that ε is rougly calculable in the Standard Model for the kaon system and that its measured value constrains possible values for the phase of the V_{td} CKM matrix element and the top quark mass in concert. However, the fact that Eq. 5.6.9 and Eq. 5.6.8 are only in order of magnitude agreement argues for prudence.

5.7 ε'/ε and EM Penguins

Finally, one should mention CP violation in the kaon decay amplitudes in the Standard Model. The parameter ε refers to CP violation in the mass matrix. One needs two amplitudes which interfere for CP violation in decays. In the K_L system decaying two pions, we have the two pions in isotopic spin states of 0 and 2 which connect to the K_L via ΔI = 1/2 and 3/2 amplitudes. We know the ratio of those amplitudes from the measured 2 pion rates for K^+ and K_S.

$$a_2/a_0 \sim \sqrt{\frac{\Gamma\left(K^+ \to \pi^+\pi^0\right)}{\Gamma\left(K_S \to \pi\pi\right)}} \sim 0.04 \qquad 5.7.1$$

$$a_2/a_0 \sim \alpha$$

This small value for the ratio of the amplitudes means that ΔI = 3/2 transitions are suppressed with respect to ΔI = 1/2 transitions. A possible explanation for this fact is the existence of electromagnetic penguin diagrams. The photon carries isospin one and therefore, can be responsible for the ΔI = 3/2 amplitude. In the context of that explanation, one might expect the ratio of the amplitudes, counting diagrammatic vertex factors, to be simply the fine structure constant. Indeed, this is correct on an order of magnitude basis.

Now ε', being a CP violating parameter in the decay amplitudes, is the imaginary part of the $\Delta I = 3/2$ amplitude.

$$\varepsilon'_K \sim \mathrm{Im}(a_2 / a_o) \tag{5.7.2}$$

In the context of the electromagnetic penguin argument, ε' is shown diagrammatically in Fig. 5.7. Looking at Fig. 5.7.1, one can read off the coupling constant factors at the two electromagnetic and the two electroweak vertices and therefore, make some crude estimator of ε'. Note the similarity to Eq. 2.5.4 for $b \to s\gamma$ FCNC.

$$\begin{aligned}
\varepsilon' &\sim |a_2 / a_0| \mathrm{Im}(V_{ts} V_{td} / V_{su} V_{ud}) \left(\frac{m_t}{M_W}\right)^2 \\
&\sim |a_2 / a_0| \left(r\theta^4 \sin\delta\right) \left(\frac{m_t}{M_W}\right)^2 \\
&\sim \alpha\left(r\theta^4 \sin\delta\right) O(1)
\end{aligned} \tag{5.7.3}$$

Recall that a nonzero imaginary part of the isospin two amplitude requires the existence of a c, or t in the loop because the phase of an amplitude is defined by the vertex factors and the CKM matrix only has imaginary matrix elements for heavy flavors in the vertex. As mentioned previously for the kaon system, the top quark has an imaginary part comparable to the c quark as seen in Eq. 5.6.7. Using Eq. 5.6.9 to estimate ε for the kaon system, one can get an estimate for the ratio of $\varepsilon' / \varepsilon$ in the kaon system.

$$\begin{aligned}
\frac{\varepsilon'}{\varepsilon} &\sim |a_2 / a_0| \left(\frac{m_c}{M_W}\right)^2 / \left(r\theta^4 \sin\delta\right) \\
&\sim \alpha \left(\frac{m_c}{M_W}\right)^2 / \left(r\theta^4 \sin\delta\right) \\
&\sim 1.5 \times 10^{-3} / (r \sin\delta)
\end{aligned} \tag{5.7.4}$$

Obviously, this estimate for $\varepsilon' / \varepsilon$ is extremely crude. The main point is that the α factor comes from the electromagnetic penguin and hence the $\varepsilon' / \varepsilon$ parameter is "naturally" small in a "real" Standard Model. However, there are many many theoretical uncertainties and ambiguities in the calculation. The ultimate test is, of course, data. At the present time the ratio of $\varepsilon' / \varepsilon$ is experimentally less than 2×10^{-3}, although there is some disagreement experimentally between

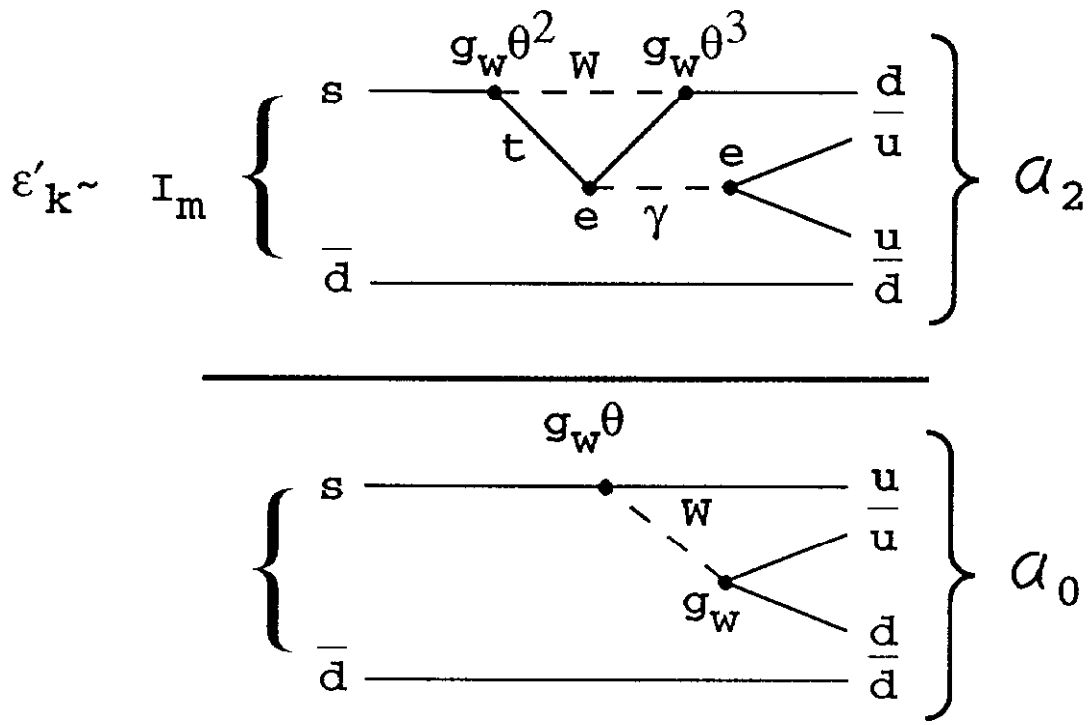

Fig. 5.7 ε' for K decays and the EM "Penquin" diagram.

Experiment 731 at Fermilab and CERN Experiment NA31. Note from Eq. 5.7.3 that ε'/ε places limits on electroweak parameters, e.g., imaginary elements in the CKM matrix and the top quark.

In summary, in order to observe CP violation, it is required that there be interference of two amplitudes with different phases. The experimental confirmation that the B and $\overline{B}$ system mixes and the realization that the B and $\overline{B}$ have common final states which are CP eigenstates, implies that CP violation is possible in the Standard Model for the B system. It is certainly allowed in the three generation Standard Model and, in fact, is predicted to exist. We've seen that CP violation can be measured in time independent integrated measurements and in time dependent asymmetry measurements. However, the sensitivity of those measurements is such that if the system mixes very rapidly, such as the B_S system, accurate determinations require time dependent asymmetry measurements.

6. SUMMARY

The result of all these proposed measurements of asymmetries, decay rates, and branching fractions would be data which directly determine the CKM matrix elements. There are Standard Model predictions for relationships between the CKM matrix elements such as unitarity. Therefore, measurements of the CKM matrix elements put pressure on the Standard Model in terms of consistency. A "complete set" of asymmetry measurements, for example, would put strong constraints on the Standard Model.

Now what does that, in fact, all mean? That is a much harder question to answer. One is basically taking experimental measurements and relating them to other parameters which one considers to be more fundamental. However, our understanding of the systematics and regularities found in the CKM matrix is minimal. Presumably, there is a "Balmer series" hiding somewhere in the CKM matrix. There is a regularity between the elements which is tantalizing; those regularities hint at more fundamental relationships between the generations.

What has been described in this set of lectures is simply the relationships between different sets of phenomenological parameters. A much more fundamental set of questions might be asked. How does one calculate the elements of the CKM matrix from first principles? Why is it almost diagonal? Why is the b quark decay so slow? Why does the coupling fall off rapidly the farther one gets off diagonal? What are the regularities in the masses between the three generations? Why are there three generations? What is the mechanism for inducing CP violation?

These are all extremely fundamental and interesting questions and one looks forward to finding answers to them. In order to get those answers, the first step on a long journey is to measure and constrain the matrix elements of this fundamental quantity, the CKM matrix. The use of B decays is universally seen within the high energy-physics community as a potential key to unlock some of the mysteries of the generation puzzle. We look forward to seeing what's behind the door.

> "In the plan of the Great Dance plans without number interlock, and each movement becomes in its season the breaking into flower of the whole design to which all else has been directed."
>
> Perelandra
> C.S. Lewis

REFERENCES

1. D. Green, "Particle Properties on an Abacus", Fermilab-FN-492 (1988).

2. K. Berkelman and S. Stone, "Decays of B Mesons", Ann. Rev. of Nucl. and Part. Sci. 41, 1, 1991.

3. M. Wirbel, B. Stech, and M. Bauer, Z. Phys. C. 29, 637, 1985.

   M. Bauer, B. Stech, M. Wirbel, Z. Phys. C. 34, 103, 1987.

4. J.S. Hagelin, Nuc. Phys. B193, 123, 1981.

5. Expression of Interest for a Bottom Collider Detector at the SSC, May 25, 1990.

6. I. Bigi and A.I. Sanda, Nuc. Phys. B193, 85, 1981.